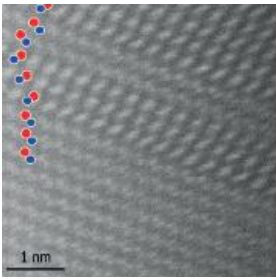


# Microscopy of Semiconducting Materials (MSM-XIX)

**29 March – 2 April 2015**  
**Murray Edwards College, Cambridge, UK**

Organised by the Institute of Physics Electron Microscopy and Analysis Group (EMAG)



# Microscopy of Semiconducting Materials (MSM-XIX)

## Programme

Sunday 29 March .....	2
Monday 30 March .....	3-4
Tuesday 31 March .....	4-5
Wednesday 1 April .....	6-7
Thursday 2 April .....	8-9
Poster programme .....	10-14
Abstracts .....	15-48
Poster abstracts .....	49-83

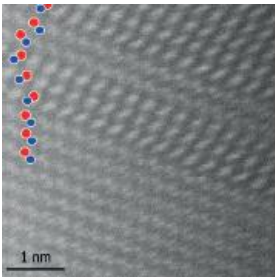
Dear Delegates,

We would like to welcome you to the 19th International Conference on Microscopy of Semiconducting Materials. This series of conferences was inaugurated by Prof AG Cullis in 1979 and has since been running in every odd year. With about 120 contributions from about as many participants from all over the world, the conference format without any parallel sessions allows every attendee to listen to all talks and to see all posters presented. May this again lead to stimulating discussions!

We would also like to thank all sponsors and exhibiting companies for their help in meeting the costs of the meeting - without their invaluable support the registration fees would be unacceptably high. As a *novum*, we have opted for an *app* instead of a printed abstract book, planned a punting tour, and replaced the standard printed proceedings volume by two special issues in well-known journals, the *Journal of Microscopy* and *Semiconductor Science and Technology*.

We wish all attendants, exhibitors and accompanying persons an interesting and exciting meeting here in Cambridge.

Ana Sanchez, Richard Beanland and Thomas Walther



# Microscopy of Semiconducting Materials (MSM-XIX)

## Programme

### Sunday 29 March

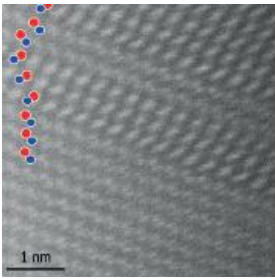
- 12.30      **Registration opens**  
**Location:** Buckingham House Foyer
- 13.00      Lunch  
**Location:** Buckingham House Foyer
- 14.15      **Presentations set-up**  
**Location:** Buckingham House Lecture Theatre
- 14.45      **Welcome by Chairs**

### Session 1: Analytical transmission electron microscopy

**Chair:** Dr Thomas Walther, University of Sheffield, UK

**Location:** Buckingham House Lecture

- 15.00      **(Invited) (S)TEM characterization of semiconductors - past, present and future**  
Dr Ondrej L Krivanek, Nion Co., USA and Arizona State University, USA
- 15.45      **(Invited) Time domain analysis of EELS in the STEM: nanoscale response from phonons to core excitations**  
Professor Philip E Batson, Rutgers University, New Jersey, USA
- 16.30      **(Invited) Analysis and manipulation of radiation sensitive 2-D materials, and recent developments on the Vienna UltraSTEM**  
Professor Jannik C Meyer, University of Vienna, Austria
- 17.15      **Distinguishing cubic and hexagonal phases within InGaN/GaN micro-structures using electron energy loss spectroscopy**  
Ian Griffiths, University of Bristol, UK
- 17.30      **(S)TEM analysis of segregation and CuPt atomic ordering in GaAsBi/GaAs layers**  
Daniel Fernández, Universidad de Cádiz, Spain
- 17.45      **Direct observation of indium segregation at dislocations in InGaN**  
Sneha Rhode, University of Cambridge, UK
- 18.00      **Session ends**
- 18.00      **Welcome drinks reception**  
**Location:** Buckingham House Foyer
- 19.00      **Dinner** – For residential delegates and those who have pre-booked.  
**Location:** Dome Dining Hall



# Microscopy of Semiconducting Materials (MSM-XIX)

## Monday 30 March

- 08.00      **Registration**  
              **Location:** Buckingham House Foyer
- 08.30      **Presentations set-up**  
              **Location:** Buckingham House Lecture theatre

### Session 2a: Cathodoluminescence and electron energy-loss spectroscopy

**Chair:** Dr Richard Beanland, University of Warwick, UK

**Location:** Buckingham House Lecture

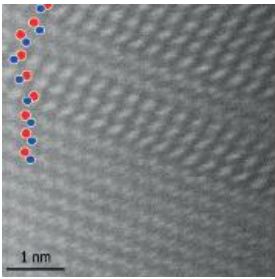
- 09.00      **(Invited) Nanowire-based structures for IR to UV emitters studied by cathodoluminescence**  
              Professor Anders Gustafsson, Lund University, Sweden
- 09.45      **(Invited) Electron energy loss spectroscopy on semiconductor heterostructures for optoelectronics and photonics applications**  
              Dr Francesca Peiró, University of Barcelona, Spain
- 10.30      **Analyses of defects in strained quantum wells grown on semipolar GaN plane by means of cathodoluminescence**  
              Lucja Marona, Institute of High Pressure Physics PAS, Poland
- 10.45      **Spatially- and time-resolved cathodoluminescence studies of InGaN/GaN multi-quantum wells grown on m-plane ammono bulk GaN**  
              Rachel Oliver, University of Cambridge, UK
- 11.00      **Refreshment break**  
              **Location:** Buckingham House Foyer

### Session 2b: Quantum dots and nanowires I

**Chair –** Dr Ana Sanchez, University of Warwick, UK

**Location:** Buckingham House Lecture

- 11.30      **(Invited) Silicon Nanowires: Synthesis, optical properties and photonic applications**  
              Dr Alessia Irrera, IPCF CNR, Messina, Italy
- 12.15      **Strain relaxation in InAs quantum dots and its suppression by indium flushing**  
              Fernando Ponce, Arizona State University, USA
- 12.30      **Structural characterization of Ga<sub>2</sub>O<sub>3</sub>/SnO<sub>2</sub> complex nanostructures by advanced transmission electron microscopy**  
              Bianchi Mendez, Universidad Complutense Madrid, Spain / University of Warwick UK
- 12.45      **Lunch, Exhibition, Poster Session P1 and refreshments**  
              **Location:** Fountain Court Walkway



# Microscopy of Semiconducting Materials (MSM-XIX)

15.30 **Presentations set-up**  
**Location:** Buckingham House Lecture Theatre

## Session 2c: Quantum dots and nanowires II

**Chair:** Dr Thomas Walther, University of Sheffield, UK

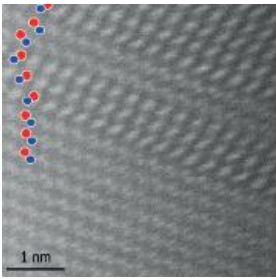
**Location:** Buckingham House Lecture Theatre

- 15.45 **(Invited) III-V nanowire-based heterostructures: surprises and challenges**  
Professor Anna Fontcuberta i Morral, EPFL Lausanne, Switzerland
- 16.30 **Building nanostructures in nanowires using sequential catalyst reactions**  
Stephan Hofmann, IBM TJ Watson Research Center, USA
- 16.45 **Microstructure of  $\text{In}_x\text{Ga}_{1-x}\text{N}$  nanorods grown by molecular beam epitaxy**  
David Cherns, University of Bristol, UK
- 17.00 **Understanding the true shape of GaAs nanowires grown by MOCVD**  
Jennifer Wong-Leung, The Australian National University, Australia
- 17.15 **Characterization of core-shell inversion domain boundaries in gallium nitride nanowires**  
Benedikt Haas, CEA / Univ. Grenoble Alpes, France
- 17.30 **Twinning and polymorphism in GaAs nanowires: a study using scanning precession electron diffraction (SPED)**  
Duncan Johnstone, University of Cambridge, UK
- 17.45 **Strain mapping accuracy improvement using Super-Resolution techniques**  
Guillermo Bárcena-González, University of Cádiz, Spain
- 18:00 **Sessions ends**
- 18:00 **Exhibition drinks reception**  
**Location:** Fountain Court Walkway
- 19:00 **Dinner** - For residential delegates and those who have pre-booked  
**Location:** Dome Dining Hall

## Tuesday 31 March

08.30 **Registration**  
**Location:** Buckingham House Lecture Theatre

08.45 **Presentations set-up**



# Microscopy of Semiconducting Materials (MSM-XIX)

## Session 3a: Scanning electron and ion beams

**Chair:** Dr Richard Beanland, University of Warwick, UK

**Location:** Buckingham House Lecture theatre

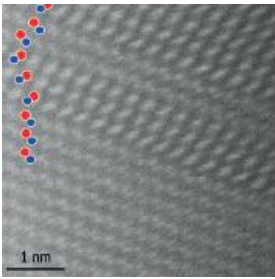
- 09.00 **(Invited) FIB analysis for advanced device technology**  
Dr Hugo Bender, imec, Leuven, Belgium
- 09.45 **SIMS-AFM-SEM combination for elemental mapping and 3D reconstruction**  
Lex Pillatsch, EMPA, Switzerland
- 10.00 **In-situ electronic probing of semiconducting nanowires in a FIB**  
Vidar T Fauske, Norwegian University of Science and Technology (NTNU), Norway
- 10.15 **Automated defect analysis with EBIC**  
Matthew Hiscock, Oxford Instruments NanoAnalysis, UK
- 10.30 **Post-ion beam induced degradation of Cu layers in TEM specimens**  
Felix Seidel, imec / Katholieke Universiteit Leuven, Belgium
- 10.45 **Refreshment break**  
**Location:** Fountain Court Walkway

## Session 3b: Scanning transmission electron beam techniques

**Chair:** Dr Thomas Walther, University of Sheffield, UK

**Location:** Buckingham House Lecture theatre

- 11.30 **Local TEM sample thickness determination via STEM defocal series**  
Andreas Beyer, Philipps-Universität Marburg, Germany
- 11.45 **Anomalous strain at interfaces in geometric phase analysis of Z-contrast images**  
Jonathan Peters, University of Warwick, UK
- 12.00 **Analysis and improvement of precision and accuracy of strain measurements by convergent nano-beam electron diffraction (SANBED)**  
Christoph Mahr, University of Bremen, Germany
- 12.15 **Quantifying indium content in semi-polar (11-22) InGa<sub>N</sub> quantum wells using precession electron diffraction**  
Yisong Han, University of Cambridge, UK
- 12.30 **Imaging STEM: A novel method for microscopy of semiconductors at ultra-high spatial resolution and precision**  
Andreas Rosenauer, University of Bremen, Germany
- 12.45 **Lunch, Exhibition, Poster Session 2 and Refreshments**  
**Location:** Fountain Court Walkway



# Microscopy of Semiconducting Materials (MSM-XIX)

- 15.15 **Social event**  
**Walk to Magdalen Bridge for Punt Tour - Please book your place when registering online. Then a complimentary drink to be served at The Anchor Pub (Drinks tickets will be provided)**
- 17.30 **Delegates are free to explore Cambridge town centre**

## Wednesday 1 April

- 08.30 **Registration**  
**Location:** Buckingham House Foyer
- 08.45 **Presentations set-up**  
**Location:** Buckingham House Lecture Theatre

### Session 4a: Nitride epitaxy I

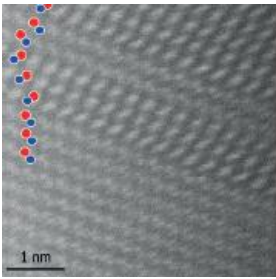
**Chair:** Dr Ana M Sanchez, University of Warwick, UK  
**Location:** Buckingham House Lecture Theatre

- 09.00 **(Invited) GaN heterostructures with diamond and graphene for high power applications**  
Professor Béla Pécz, Institute for Technical Physics and Materials Science, Research Centre for Natural Sciences, Hungary
- 09.45 **Transmission electron microscopy investigations of nucleation of AlN layers on sapphire substrates**  
Natalia Stolyarchuk, Leibniz-Institute for Crystal Growth, Germany
- 10.00 **Multi-microscopy techniques for the investigation of fully coalesced boundaries in GaN**  
Thomas O'Hanlon, University of Cambridge, UK
- 10.15 **GaN on SOI substrate: strain and defects**  
Nicolas Mante, CEA, France
- 10.30 **V-pit to truncated pyramid transition in AlGaIn-based heterostructures**  
Anna Mogilatenko, Ferdinand-Braun-Institut, Leibniz-Institut für Höchstfrequenztechnik, Germany
- 10.45 **TBC**
- 11.00 **Refreshments**  
**Location:** Fountain Court Walkway

### Session 4b: Nitride epitaxy II

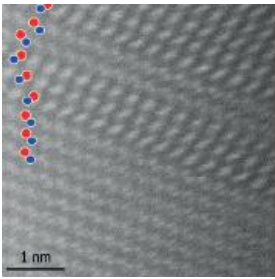
**Chair:** Dr Thomas Walther, University of Sheffield, UK  
**Location:** Buckingham House Lecture Theatre

- 11.30 **(Invited) Highly spatially resolved cathodoluminescence of III-nitride based nanostructures directly performed in a scanning transmission electron microscope**  
Professor Dr Jürgen Christen, Otto-von-Guericke-University Magdeburg, Germany



# Microscopy of Semiconducting Materials (MSM-XIX)

- 12.15 **Study of phases created due to thermal degradation of InGaN quantum wells**  
Julita Smalc-Koziorowska, Institute of High Pressure Physics, Poland
- 12.30 **Quantum mechanical interpretation of electron picodiffraction reveals atomic electric fields**  
Knut Müller, Universität Bremen, Germany
- 12.45 **Lunch, Exhibition, Poster session 3 and Refreshments**  
**Location:** Fountain Court Walkway
- 15.30 **Presentations set-up**  
**Location:** Buckingham House Lecture Theatre
- Session 4c: Thin films, multilayers and monolayers**  
**Chair:** Dr Richard Beanland, University of Sheffield, UK  
**Location:** Buckingham House Lecture Theatre
- 15.45 **(Invited) Heterostructured nanostructures in compound semiconductors**  
Professor Philomela Komninou, Aristotle University of Thessaloniki, Greece
- 16.30 **Investigation of antimonide-based materials grown on exactly oriented (001) silicon substrate**  
Andrea Ott, Philipps-Universität Marburg, Germany
- 16.45 **Effect of Sb content in the ordering of  $(\text{In}_{0.5}\text{Ga}_{0.5})\text{P}$  layers for tandem solar cells**  
Lluís López-Conesa, Laboratory of Electron Nanoscopies (LENS)-MIND/IN2UB, Spain
- 17.00 **Ga(NAsP)-layers in Si-based laser structures investigated by HRSTEM**  
Tatjana Wegele, Philipps-Universität Marburg, Germany
- 17.15 **Structure of  $\text{Fe}_3\text{Si}/\text{Al}/\text{Fe}_3\text{Si}$  metal thin film stacks on GaAs(001)**  
Bernd Jenichen, Paul-Drude Institute, Berlin, Germany
- 17.30  **$\text{SnS}_2$  – An emerging layered metal dichalcogenide semiconductor: Materials properties, device characteristics, and electron-induced structural transformation**  
Eli Sutter, Brookhaven National Laboratory, USA
- 17.45 **Controlling defects in topological insulator dichalcogenide thin films**  
Nadezda Tarakina, Queen Mary, University of London, UK
- 18.00 **Catalyst engineering for CVD of large single crystal hexagonal boron nitride monolayer domains**  
Sabina Caneva, University of Cambridge, UK
- 18.15 **End of sessions**
- 19.00 **Conference dinner**  
**Location:** Dome Dining Hall, Murray Edwards College



# Microscopy of Semiconducting Materials (MSM-XIX)

## Thursday 2 April

08.30 **Registration**  
**Location:** Buckingham House Foyer

08.45 **Presentations set-up**  
**Location:** Buckingham House Lecture Theatre

### Session 5a: Scanning probe and atom probe techniques

**Chair:** Dr Ana M Sanchez, University of Warwick, UK

**Location:** Buckingham House Lecture Theatre

09.00 **(Invited) Atomic scale analysis of semiconductor nanostructures and doping atoms by scanning tunnel microscopy and atom probe tomography**  
Professor Dr Paul Koenraad, Eindhoven University of Technology, The Netherlands

09.45 **(Invited) Atom probe tomography of semiconducting materials: Technology and applications**  
Peter H Clifton, CAMECA Instruments / Ametek Inc, USA

10.30 **Correlative investigation of II-VI heterostructures by atom probe tomography and transmission electron microscopy**  
Bastien Bonafant, CEA/INAC/SP2M/LEMMA, Grenoble, France

10.45 **Atom probe analysis of sub-surface phosphorus implantation profiles in single crystal silicon**  
James Douglas, University of Oxford, UK

11.00 **Refreshments**  
**Location:** Buckingham House Foyer

### Session 5b: Lattice defects in bulk materials

**Chair:** Dr Richard Beanland, University of Warwick, UK

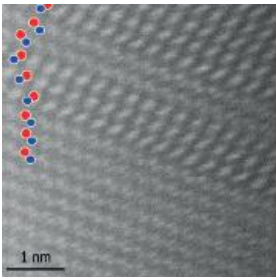
**Location:** Buckingham House Lecture Theatre

11.30 **(Invited) Structural characterization of semipolar GaN grown on Si(001)**  
Professor Lev Sorokin, Ioffe Physical technical Institute of the Russian Academy of Sciences, St Petersburg, Russia

12.15 **Epitaxial growth of GaN on polycrystalline diamond substrates**  
Richard Webster, University of Bristol, UK

12.30 **STEM optical sectioning for imaging screw displacements in dislocation core structures**  
Hao Yang, University of Oxford, UK

12.45 **Lunch**  
**Location:** Buckingham House Foyer



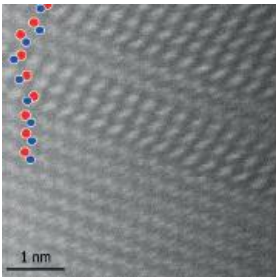
# Microscopy of Semiconducting Materials (MSM-XIX)

## Session 5c: Device studies

**Chair:** Dr Ana M Sanchez, University of Warwick, UK

**Location:** Buckingham House Lecture Theatre

- 13.30 **(Invited) The microstructure characterization of nitride laser diodes**  
Professor Piotr Perlin, Institute of High Pressure Physics "Unipress", Warsaw, Poland
- 14.15 **3D imaging of Si FinFET devices by combined HAADF-STEM and EDS tomography**  
Olivier Richard, imec FPS MCA, Leuven, Belgium
- 14.30 **Multi-microscopy analysis of inhomogeneous electroluminescence in InGaN/GaN quantum well LED structures**  
Christopher Ren, University of Cambridge, UK
- 14.45 **Spatial inhomogeneities in structural and optical properties of  $\text{Al}_x\text{Ga}_{1-x}\text{N}$  quantum wells induced by surface morphology of AlN/sapphire templates**  
Ute Zeimer, Ferdinand-Braun-Institut, Leibniz-Institut für Höchstfrequenztechnik, Berlin, Germany
- 15.00 **Refreshments**  
**Location:** Buckingham House Foyer
- 15:30 **End of conference**



# Microscopy of Semiconducting Materials (MSM-XIX)

## Posters

### Poster Session 1 – Monday 30 March

**P.1.1- In situ UHVEM study of {113}-defect formation in Si nanowires**

Hugo Bender, imec, FPS MCA, Belgium

**P.1.2- Influence of post-growth thermal annealing on InGaAs/GaAs quantum dot structures monolithically grown on silicon**

Wei Li, University of Sheffield, UK

**P.1.3 -Automated background subtraction for electron energy-loss spectroscopy and application to spectral imaging of semiconductor layers**

Veerendra C Angadi, University of Sheffield, UK

**P.1.4 - Cross-sectional cathodoluminescence investigations of GaN epitaxial grown on Si-based substrates**

Lucas Piot, CEA - LETI, France

**P.1.5 - Facetted growth of Fe<sub>3</sub>Si shells around GaAs nanowires on Si(111)**

Bernd Jenichen, PDI, Germany

**P.1.6 - A nanoscale cathodoluminescence study of nitride semiconductor nanowires**

David Stowe, Gatan UK

**P.1.7 - Epitaxial growth of wurtzite silicon on diamond silicon**

Hugo Bender, imec FPS MCA, Belgium

**P.1.8 - CL investigation of ZnO nanorods grown by ultra-fast hydrothermal process**

Bartłomiej Witkowski, Institute of Physics PAS, Poland

**P.1.9 - Quantitative characterization of composition and interface roughness of (Galn)As quantum wells**

Han Han, Philipps-Universität Marburg, Germany

**P.1.10 - Morphological and compositional STEM analysis of organic-inorganic hybrid Perovskites**

Florencia Wisnivesky Rocca Rivarola, University of Cambridge, UK

**P.1.11 - Construction and test of an annular aperture for novel Z-contrast imaging**

Thorsten Mehrtens, University of Bremen, Germany

**P.1.12 - Analysis of Sb and In distribution in GaAsSb-capped InAs quantum dots by advance transmission electron microscopy**

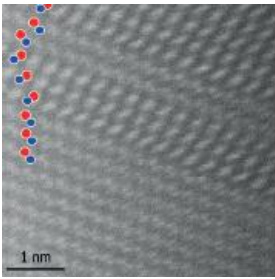
Daniel Fernández, Universidad de Cádiz, Spain

**P.1.13 - Composition analysis in SEM and STEM**

Meiken Falke, Bruker Nano GmbH, Germany

**P.1.14 - Structural properties of Si Nanowires**

Maria José Lo Faro, IPCF CNR MESSINA, Italy



# Microscopy of Semiconducting Materials (MSM-XIX)

## **P.1.15 - Strained heterostructures in III-Nitride nanowires**

Theodoros Karakostas, Aristotle University of Thessaloniki, Greece

## **P.1.16- Alloying variations in self-assembled InAs/GaAs (211)B quantum dot heterostructures**

Nikoletta Florini, Aristotle University of Thessaloniki, Greece

## **P.1.17 - Nanostructure and strain properties of core-shell GaAs/AlGaAs nanowires**

Philomela Komninou, Aristotle University of Thessaloniki, Greece

## **P.1.18 - Local optical properties of GaN/Al<sub>x</sub>Ga<sub>1-x</sub>N nanowires studied by cathodoluminescence**

Anna Reszka, Institute of Physics PAS, Poland

## **P.1.19 - Green luminescence band in ZnO microrods – a cathodoluminescence study**

Agnieszka Pieniżek, Institute of Physics PAS, Poland

## **P.1.20 - Polarity-driven compositional segregation in core-shell GaAsP nanowires**

Ana M Sanchez, University of Warwick, UK

## **P.1.21 - Approaches for quantifying X-ray spectra from thick semiconductor specimens in a transmission electron microscope**

Thomas Walther, University of Sheffield, UK

## **Poster Session 2 – Tuesday 31 March**

### **P.2.1 - Homogeneity and composition of MOVPE-grown AlInGaN: A multiprobe nanostructure study**

Florian F Krause, Institut für Festkörperphysik, Universität Bremen, Germany

### **P.2.2 - 3D investigation of gallium containing structures within silicon**

Katharina Gries, Philipps-Universität Marburg, Germany

### **P.2.3 - InGaN/GaN multiple quantum wells grown on m-plane bulk GaN**

Fengzai Tang, University of Cambridge, UK

### **P.2.4 - Electron energy-loss spectroscopy and energy dispersive X-ray spectroscopy studies of indium concentration in InGaN thin film structures**

Xiaoyi Wang, University of Sheffield, UK

### **P.2.5 - STEM strain measurement from a stream of diffraction patterns recorded on a pixel-free delay-line detector**

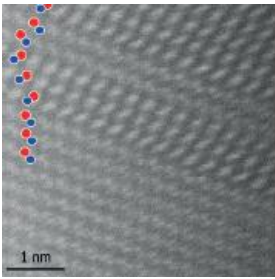
Knut Müller-Caspary, Universität Bremen, Germany

### **P.2.6 - Artifacts due to accidental single electrons in atom counting - Two different techniques for atom counting from HAADF-STEM imaging**

Marco Schowalter, University of Bremen, Germany

### **P.2.7- Hydrogen etching of InGaN/GaN quantum wells and epilayers**

An Bao, University of Cambridge, UK



# Microscopy of Semiconducting Materials (MSM-XIX)

**P.2.8 - Non-polar (11-20) InGaN nanostructures grown by modified droplet epitaxy**

Helen Springbett, University of Cambridge, UK

**P.2.9 - Investigation of defect formation during thermal annealing of Ga(NAs) and Ga(NP) using aberration corrected STEM**

Lennart Duschek, Philipps-Universität Marburg, Germany

**P.2.10 - Compositional analysis of non-polar (11-20) InGaN/GaN quantum well structures and the relation to the emission wavelength**

James Griffiths, University of Cambridge, UK

**P.2.11- Atomic structure of the GaN on Ge(111) interface**

Siyuan Zhang, University of Cambridge, UK

**P.2.12 - InN/GaN Superlattices – Resolving the discrepancies between theory and experiment**

Toni Markurt, Leibniz Institute for Crystal Growth, Germany

**P.2.13 - Determination of ion beam induced artifacts in TEM sample preparation of strained semiconductor heterostructures by means of FIB target preparation**

Jürgen Münzner, Philipps-Universität Marburg, Germany

**P.2.14 - Automated defect analysis with EBIC**

Matthew Hiscock, Oxford Instruments NanoAnalysis, UK

**P.2.15 - Structural and chemical studies of the GaN(0001)/GaAs (111)B Interface**

Suman-Lata Sahonta, University of Cambridge, UK

**P.2.16 - Microstructural analysis of cubic InGaN/GaN multiple quantum well structures grown on large-area 3C-SiC/Si (001)**

Suman-Lata Sahonta, University of Cambridge, UK

**P.2.17 - Strain accommodation and indium incorporation in  $\text{In}_x\text{Ga}_{1-x}\text{N}$  epilayers grown by molecular beam epitaxy**

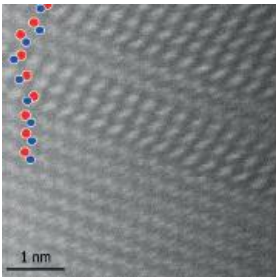
Calliope Bazioti, Aristotle University of Thessaloniki, Greece

**P.2.18 - Microstructure of  $\text{In}_x\text{Ga}_{1-x}\text{N}$  ( $x = 0.22$  to  $0.67$ ) films grown by metal-modulated epitaxy**

Fernando Ponce, Arizona State University, USA

**P.2.19 - High quality FIB lamella preparation for wide area atomic resolution TEM investigations**

Rainer Straubinger, Philipps-University Marburg, Germany



# Microscopy of Semiconducting Materials (MSM-XIX)

## Poster Session 3 - Wednesday 1 April

### **P.3.1 - The effects of Si-doping on dislocation core structures in GaN**

Sneha Rhode, University of Cambridge, UK

### **P.3.2 - Multi-microscopy investigation of the optical properties of dislocations in InGaN**

Fabien Massabuau, University of Cambridge, UK

### **P.3.3 - TEM Characterization of Perfluoropentacene grown on graphene**

Rocio Felix Angel, Philipps-Universität Marburg, Germany

### **P.3.4 - Multi-microscopy analysis of GaN-based microdisk lasers**

Rachel Oliver, University of Cambridge, UK

### **P.3.5 - Structure and morphology of para-sexiphenyl on polar and mixed-polar ZnO surfaces**

Holm Kirmse, Humboldt University of Berlin, Germany

### **P.3.6 - Magnetic and magneto-optical properties of doped and co-doped CdTe**

AIT RAISS Abderrahim, Med V University, Morocco

### **P.3.7 - Synthesis and some surface features of laminated ZnO/TiO<sub>2</sub> transparent bilayer by two growth techniques**

Bidini Taleatu, Obafemi Awolowo University, Nigeria

### **P.3.8 - Effects of deposition period on the optical properties of nano-crystallised Al/Pb- oxide and -sulphide films**

Mayowa Ojo, Federal University of Technology Akure, Nigeria

### **P.3.9 - Characterisation of vacancy-related point defects in Zn-doped CdTe**

David Keeble, University of Dundee, UK

### **P.3.10 - Microscopical characterization of 2D-film selenide heterostructures deposited on polar wurtzite AlN by molecular beam epitaxy**

C Bazioti, Aristotle University of Thessaloniki, Greece

### **P.3.11 - Origin of surface defects in RP-CVD grown Si<sub>1-y</sub>Cy epilayers by the oversaturation of carbon**

Gerard Colston, University of Warwick, UK

### **P.3.12 - Examination of polycrystalline growth caused by contaminations in epilayers by electron microscopy**

Phil Allred, University of Warwick, UK

### **P.3.13 - Challenges of growth and sample preparation of GeSn for electron microscopy**

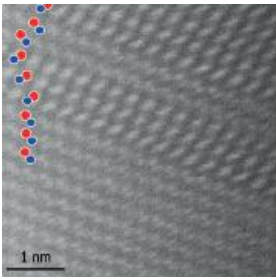
David Patchett, University of Warwick, UK

### **P.3.14 - Atom probe tomography analysis of defects in nitride semiconductors**

Rachel Oliver, University of Cambridge, UK

### **P.3.15 - Dislocation filters in GaAs on Si**

Richard Beanland, University of Warwick, UK



# Microscopy of Semiconducting Materials (MSM-XIX)

**P.3.16 - Structural characterisation of N-type SiGe/Ge superlattice structures for Terahertz emission**

John Halpin, University of Warwick, UK

**P.3.17 - Image processing approaches towards optical microscopic analysis of monolayers to thin films**

Shourjya Sanyal, University College Dublin, UK

**P.3.18 - Correlating atom probe tomography with high-resolution scanning transmission electron microscopy and micro-photoluminescence spectroscopy: the case of III-Nitride heterostructures**

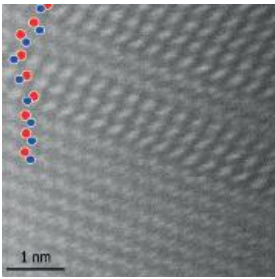
Lorenzo Rigutti, University and INSA of Rouen, France

**P.3.19 - Atom probe tomography visualizes elusive quantum dots in GaAs/AlGaAs core-multishell nanowires**

Lorenzo Rigutti, University and INSA of Rouen, France

**P.3.20 - Continuous changing of 1D  $TbBr_x$  stoichiometry inside the SWCNTs under the electron beam**

Nikolay Kiselev, The Shubnikov Institute of Crystallography of the Russian Academy of Sciences (IC RAS), Russian Federation



# Microscopy of Semiconducting Materials (MSM-XIX)

Sunday 29 March

## Session 1: Analytical transmission electron microscopy

### (Invited) (S)TEM characterization of semiconductors - past, present and future

O L Krivanek<sup>1,2</sup>

<sup>1</sup>Nion Co., USA, <sup>2</sup>Arizona State University, USA

Using electron microscopes to characterize semiconductor devices can trace one of its roots to the  $\sim 3$  Å resolution images of Si-SiO<sub>2</sub> interfaces in MOSFETs (metal-oxide semiconductor field-effect transistors) that I recorded at Cornell U. in the late 1970's, in collaboration with TT Sheng and Dan Tsui of Bell Labs. The images showed that this key interface was atomically abrupt with a roughness of a few Å, in good agreement with electrical measurements. Until our work, device physicists relied on techniques such as Rutherford back-scattering and Auger spectroscopy, which indicated a diffuse interface with a width of several tens of Å. The importance of electron microscopy for semiconductor characterization has very much increased since, due to the wide range of capabilities that TEM (transmission electron microscopy) now provides. In particular, scanning TEM (STEM) is able to image the structure and analyze the composition and other properties, at atomic resolution and often with single-atom sensitivity.

The resolution and current available in the electron probe of STEM instruments were improved substantially by the aberration corrector that Niklas Dellby, Mick Brown and I built in Cambridge UK in 1995-1997, and the many different correctors designed and built for STEM since. Another development that helped our field advance substantially was the UltraSTEM – a completely new STEM instrument introduced by Nion, a company started by Niklas and myself in 1997. Capabilities made available by the UltraSTEM include atomic-resolution elemental mapping by electron energy loss spectroscopy (EELS), EEL and X-ray spectroscopy studies of single atoms, and EELS fine structure studies of single atoms. More recently, Nion has introduced a monochromator that has improved the EELS energy resolution by about 30x compared to non-monochromated cold FEG microscopes. The monochromator is allowing vibrational properties of materials to be studied in the STEM, at energy/spatial resolution of about 10 meV/a few nm.

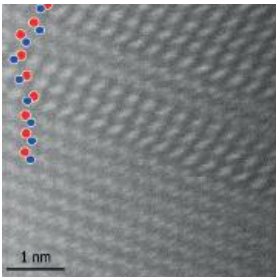
This talk will review the basic principles behind these developments, illustrate them with experimental results from a variety of samples, and discuss especially alluring future directions.

### (Invited) Time domain analysis of EELS in the STEM: nanoscale response from phonons to core excitations

P E Batson

Rutgers University, USA

During the past 60 years, Electron Energy Loss Spectroscopy has become a premier tool for characterization of the composition and behavior of nanoscale regions of heterogeneous materials. Useful spectral features have ranged from atomic core loss edges in the 100 eV range; bulk and surface plasmons at 1-10 eV energies; electronic transitions at optical energies, which couple strongly to external electromagnetic fields; and recently accessible vibrational and phonon modes in the 10-200 meV range, enabled by spectroscopic instrumental advances in the Nion Ultra-STEM. These spectral features show a strong propensity for interaction with each other, most obviously at optical energies where nanoscale structure can mediate coupled modes to produce new resonance energies, but also in the electronic fine structure on core edges, and recently observed plasmon-phonon coupling in graphene-SiO<sub>2</sub> structures. On a crude level, these interactions show up in spectra as variations in peak positions, intensities



# Microscopy of Semiconducting Materials (MSM-XIX)

and widths. In principle, however, EELS spectra contain not only as-measured intensity information, but amplitude-phase information separable from the spectra using a Kramers-Kroenig analysis. This process rests on the Principle of Causality, and for EELS it can be used to produce a time domain representation of charge density fluctuations within a structure. Using KeV electrons in an Angstrom-sized probe, this analysis can identify information down to a few atto-seconds resolution. Recently, we have been examining the time dependence of lateral forces in nano-scale metal particles, imposed by a passing KeV beam, finding rich, high spatial- and time- resolved structure, allowing us to better understand the movement of metal particles under the electron beam. This work is easily extendable to longitudinal forces, which are the primary drivers behind EELS spectra. Based on our experience with this work, we will discuss the time domain analysis of EELS results and comment on possible features of this information.

## **(Invited) Analysis and manipulation of radiation sensitive 2-D materials, and recent developments on the Vienna UltraSTEM**

J C Meyer

University of Vienna, Austria

The microscopic characterization of two-dimensional materials, and low-dimensional matter in general, poses unique challenges but also opens unique new avenues that are different from those for 3-D bulk structures or on the surfaces of 3D crystals. In a two-dimensional material, all atoms are located at the surface and therefore interact with the environment, while at the same time a single atomic layer produces only a small contrast and is very susceptible to radiation damage. On the other hand, individual atoms, rather than extended atomic columns, are readily accessible when studying 2-D samples. I will discuss insights to irradiation-induced modifications of graphene, which shed light onto the bonding mechanism in carbon [1] as well as on the knock-on damage mechanism [2]. Moreover, controlled amorphization of graphene provides insight to the transition from an ordered to a disordered material [3]. I will also discuss a new idea to circumvent radiation damage, based on low-dose imaging of repeatedly occurring atomic configurations [4].

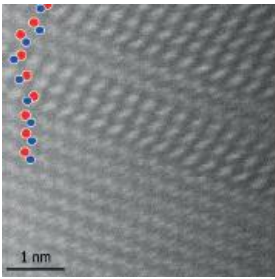
- [1] J. Kotakoski et al., Physical Review Letters **106**, 105505 (2011); Physical Review B **83**, 245420 (2011), and Nature communications 5, p. 3991 (2014).
- [2] J. C. Meyer et al., Physical Review Letters **108**, 196102 (2012).
- [3] F. Eder et al., Scientific Reports **4**, Art. No. 4060 (2014).
- [4] J. C. Meyer et al., Ultramicroscopy 145, p. 13 (2014).

## **Distinguishing cubic and hexagonal phases within InGaN/GaN micro-structures using electron energy loss spectroscopy**

I Griffiths

University of Bristol, UK

The growth of patterned InGaN/GaN micro-structures has increased in recent years due to their promise for high efficiency light emitting diodes (LEDs) [1-2]. The primary form in which InGaN grows is the hexagonal wurtzite phase; however under certain conditions the preferential form is cubic zinc blende. The chemical composition of both phases is identical, but the atom coordination differs, leading to changes in the fine structure of absorption edges.



# Microscopy of Semiconducting Materials (MSM-XIX)

These changes are investigated by electron energy loss spectroscopy (EELS) and mapping on micro-structures containing a mixture of cubic and hexagonal regions which were grown by molecular beam epitaxy (MBE) on GaN buffer layers for use as LEDs. The samples were prepared using a dual-beam Focussed Ion Beam (FIB) and studied using an aberration corrected JEOL ARM200F operating in STEM mode. EELS spectra showed differences between the hexagonal and cubic phases in the N K-edge and, to a lesser extent, in the Ga L-edges. Mapping of the cubic material was carried out using the fine structure within the N K-edge. The paper will outline these results and their use for studying regions of mixed phase where high densities of stacking faults are present.

- [1] Stat. Sol. C, 8, 2296(2011)
- [2] Adv. Mater, 23,3284(2011)

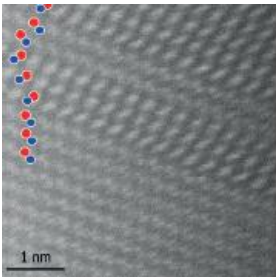
## (S)TEM analysis of segregation and CuPt atomic ordering in GaAsBi/GaAs layers

D Fernández<sup>1</sup>, F Bastiman<sup>2</sup>, A R Mohmad<sup>3</sup>, DL Sales<sup>1</sup>, R Beanland<sup>4</sup>, A M Sanchez<sup>4</sup>, J P R David<sup>2</sup> and D Gonzales<sup>1</sup>

<sup>1</sup>Universidad de Cadiz, Spain, <sup>2</sup>University of Sheffield, UK, <sup>3</sup>Universiti Kebangsaan, Malaysia, <sup>4</sup>University of Warwick, UK

The development of new semiconductor materials with diluted bismuth content has aroused great interest in recent years. Among other benefits, the strong bandgap reduction (of up to 90meV/%Bi in GaAsBi alloys), a strong enhancement of spin-orbit splitting and a temperature-insensitive bandgap make this materials useful for obtaining more efficient optoelectronic, thermoelectric and electronic devices. However, in the case of GaAsBi alloys, a high miscibility gap exists, typified in the low solubility of Bi in GaAs, which could result in a tendency for alloy clustering, phase separation and atomic ordering to occur during growth.

The present work analyses the structure and compositional distribution of bismuth in GaAsBi layers grown by molecular beam epitaxy by photoluminescence and transmission electron microscopy (TEM) techniques. The correlation between different techniques, such as energy dispersive X-ray analysis, analysis of diffraction contrast in 002-dark-field images and high resolution aberration-corrected scanning TEM images with resolved dumbbells, allow us draw bi-dimensional maps of the bismuth distribution. The maps reveal that bismuth content is not homogenous along the layer, presenting a gradient with an exponential decay from bottom to top. Moreover, the bismuth distribution does not follow a planar segregation front, but an uneven one as can be seen in the high Bi content region. High resolution TEM images and diffraction patterns evidence the formation of CuPt<sub>B</sub>-type atomic ordering of the As and Bi atoms in the {111}<sub>B</sub> planes, especially in the regions with a higher bismuth content. The long range ordering parameter was estimated along the GaAsBi layer by analysis the fast Fourier transform and the reconstruction of the phase maps extracted from HRTEM images. Finally a Bi incorporation mechanism is proposed correlating the degree of ordering and the bimodal Bi distribution which justified the PL behavior.



# Microscopy of Semiconducting Materials (MSM-XIX)

## Direct observation of indium segregation at dislocations in InGaN

S Rhode<sup>1</sup>, M K Horton<sup>1</sup>, S L Sahonta<sup>1</sup>, M J Kappers<sup>1</sup>, S J Haigh<sup>2</sup>, T J Pennycook<sup>3</sup>, C McAleese<sup>1</sup>, C J Humphreys<sup>1</sup>, R O Dusane<sup>4</sup> and M A Moram<sup>5</sup>

<sup>1</sup>University of Cambridge, UK, <sup>2</sup>University of Manchester, UK, <sup>3</sup>University of Oxford, UK, <sup>4</sup>Indian Institute of Technology Bombay, India, <sup>5</sup>Imperial College London, UK

The active region of GaN-based light-emitting diodes comprises of the ternary alloy InGaN. Threading dislocations which propagate into the active regions of these devices act as non-radiative recombination centres, thus reducing device efficiencies and lifetimes. However, GaN-devices can tolerate dislocation densities many orders of magnitude higher than in other III-V devices. We currently lack a clear understanding of how interactions between In atoms and dislocations may affect the optoelectronic properties of such devices.

160 nm  $\text{In}_x\text{Ga}_{1-x}\text{N}$  epilayers were grown by metalorganic vapour phase epitaxy on (0001) GaN-on-sapphire substrates and compared to undoped GaN to determine the effect of In alloying on dislocation core structures. Dislocation cores were observed using aberration-corrected scanning transmission electron microscopy (STEM) in the high-angle annular dark-field mode of imaging. Energy dispersive X-ray spectroscopy in the STEM-mode was performed to observe segregation of In around TDs.

All a-threading dislocation cores formed double 5/7-atom ring structures, independent of growth conditions or alloying. In contrast, (a+c)-core structures were affected by alloying with In, where more cores dissociated with shorter dissociation-lengths when compared with the studies performed on GaN. We attribute this to the segregation of In near (a+c)-cores in  $\text{In}_x\text{Ga}_{1-x}\text{N}$ .

**Monday 30 March**

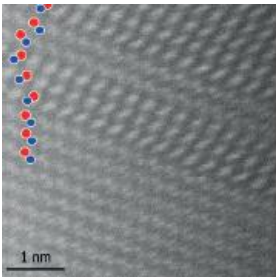
## Session 2a: Cathodoluminescence and electron energy-loss spectroscopy

### (Invited) Nanowire-based structures for IR to UV emitters studied by cathodoluminescence

A Gustafsson

Lund University, Sweden

Nanowires have shown potential for use in future optoelectronic devices. The small footprint means that it is possible to combine materials that cannot be done in bulk material due to lattice mismatch. The crystal structure can be zincblende or wurtzite, which does not occur in bulk growth. Nanowires give the opportunity to study the properties of wurtzite material. The nanowires can be grown in different geometries, from a homogeneous core, core-shell, radial quantum well(s) to axial heterostructures. The diameter and length of nanowires make them very suitable for studies using cathodoluminescence. We have used a conventional scanning electron microscope to study the spatial and spectral variation along the nanowires. All the structures presented here are intended for use as light emitters, varying from near infrared to deep ultraviolet. We will demonstrate thickness variations in radial quantum wells of InAs/InP and GaAs/AlGaAs, where we observe thickness variations on a scale of one monolayer. The intentional introduction of an irregular stacking of the core can lead to local thickness variations in the radial layers, forming quantum dots in these areas. The AlGaAs barriers can show some interesting features, as the corners where the side facets meet have different compositions. In some cases, these corners can form either quantum dots or quantum wires, revealed by CL imaging. We will also present investigations of nanowire-based III-Nitride structures. GaN nanowires have the ability to split along the length when the substrate is cleaved, giving access to



# Microscopy of Semiconducting Materials (MSM-XIX)

the interior of the layers in a radial structure. In radial device structures, we can distinguish between the radial quantum-well and the p- and n-type GaN layers by their emission energies. Finally, we will present data on flat micro substrates of micron-sized hexagons seeded by nanowires, for red (InGaN) to ultraviolet (AlGaIn) devices.

## **(Invited) Electron energy loss spectroscopy on semiconductor heterostructures for optoelectronics and photonics applications**

F Peiró<sup>1</sup>, A Eljarrat<sup>1</sup>, L López-Conesa<sup>1</sup>, J López-Vidrier<sup>1</sup>, S Hernández<sup>1</sup>, B Garrido<sup>1</sup>, Ž Gačević<sup>2</sup>, E Calleja<sup>2</sup> and S Estradé<sup>1</sup>

<sup>1</sup>Universitat de Barcelona, Spain, <sup>2</sup>Universidad Politécnica de Madrid, Spain

Nowadays the characterization of nanoscale semiconductor devices is routinely achieved through the combination of electron microscopy tools as STEM-HAADF and EELS. The examination of the low-loss region of the EELS spectra can provide invaluable localized information to disentangle valence properties through the analysis of the spectral features related to transitions from occupied to unoccupied states above the Fermi level, and about the dielectric behavior of the material through the analysis of the loss function.

This work deals with the advanced processing of EELS data obtained in an aberration corrected and monochromated microscope for the elucidation of the structural and electronic properties of semiconducting nanostructures for optoelectronics and photonics.

In a first part multilayers of nitride compounds grown by MBE onto sapphire substrates will be the object of interest to test the validity of the generation of maps from properties derived of the low-loss EELS-SI, such as plasmon energy, and relative thickness to mean free path ratios. Measurements of positions and FWHM of the plasmon peak, combined with geometrical phase analysis, will help us to identify inhomogeneous composition and strain distribution in strained  $\text{In}_x\text{Ga}_{1-x}\text{N}$  multiquantum wells.

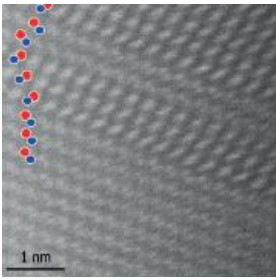
In a second part, we will focus on the characterization of silicon nanocrystals embedded in multilayer stacks for tandem solar cells, where  $\text{SiO}_2$ , SiC and  $\text{Si}_3\text{N}_4$  are used as dielectric barriers. A collection of fast and powerful computational tools have been developed enabling nanometric spatial resolution imaging of the Si-NCs using sub-eV energy resolution EELS. MVA factorization has been also applied to EELS data using decomposition by principal component analysis, followed by blind source separation by independent component analysis. We have also used non-negative matrix factorization and the Bayesian linear unmixing methods. The possibility of extracting electro-optical properties by Kramers-Kronig analysis of the average spectra and MVA factors has also been explored.

## **Analyses of defects in strained quantum wells grown on semipolar GaN plane by means of cathodoluminescence**

L Marona<sup>1</sup>, M Sarzynski<sup>1</sup>, E Grzanka<sup>1</sup>, T Suski<sup>1</sup>, R Czernecki<sup>2</sup> and P Perlin<sup>1</sup>

<sup>1</sup>Institute of High Pressure Physics PAS, Poland, <sup>2</sup>TopGaN, Poland

Semipolar GaN planes are used in the construction of light emitting devices with the purpose of decreasing the influence of quantum confinement Stark effect on the quantum wells efficiency. Reduction of electron-hole wavefunction separation leads to the increase of recombination efficiency in QWs. However, the epitaxial growth on semipolar GaN in case of laser diodes structure poses many challenges. We have to cope with smaller incorporation of indium on semipolar planes and smaller critical thickness for defect generation than in standard c-plane structures. InGaIn and AlGaIn layers grown on semipolar GaN tend to have a faster relaxation and defects formation.



# Microscopy of Semiconducting Materials (MSM-XIX)

In this work we analyse quantum wells structures grown on semipolar (20-21) GaN plane by means of cathodoluminescence. We focused on defects created in InGaN and AlGaIn layers. We observed two types of relaxation defects - one characteristic for InGaIn layers and the second one for AlGaIn layers. Both kinds of defects are dislocations and act as a nonradiative recombination centers. To avoid relaxation defects formation we fabricated specially patterned substrate. We used silicon nitride stripe-shaped mask to stop the dislocation propagation. We compared cathodoluminescence maps for samples with and without relaxation stripes.

## **Spatially- and time-resolved cathodoluminescence studies of InGaIn/GaN multi-quantum wells grown on *m*-plane ammono bulk GaN**

T Zhu<sup>1</sup>, D Gachet<sup>2</sup>, F Tang<sup>1</sup>, J T Griffiths<sup>1</sup>, F Oehler<sup>1</sup>, D Sutherland<sup>3</sup>, P Dawson<sup>3</sup>, M J Kappers<sup>1</sup> and R A Oliver<sup>1</sup>

<sup>1</sup>University of Cambridge, UK, <sup>2</sup>Attolight AG, Switzerland, <sup>3</sup>University of Manchester, UK

Growth of InGaIn/GaN quantum wells in non-polar orientations is of interest not only due to the potential of improving the recombination efficiencies over conventional *c*-plane, but also due to the possibility of highly linearly polarised light emission. Heteroepitaxial films grown in non-polar orientations often suffer from very high defect densities in comparison to conventional *c*-plane GaN: basal plane stacking fault and partial dislocation densities in excess of  $10^5 \text{ cm}^{-1}$  and  $10^{10} \text{ cm}^{-2}$ , respectively. Therefore, the use of low-defect density free-standing bulk GaN would improve our understanding of the physics of the QW emission and ultimately lead to better device performances.

We report on microstructural and optical characterisation of InGaIn/GaN multiple QWs grown on *m*-plane bulk Ammono GaN. Atomic force microscopy analysis reveals step bunches on the sample surface, which were formed as a result of the 2° GaN substrate miscut. Cross-sectional transmission electron microscopy analyses suggest that in addition to the non-polar QWs on the *m*-plane surface, semi-polar QWs had formed at the step bunches during the QW growth, at which a higher Indium concentration was detected than that of the planar *m*-plane surface.

Spatial and spectral mapping performed on an Attolight quantitative cathodoluminescence (CL) system reveal that there is a single broad QW emission peak with a distinct low energy tail, which were originated from the semi-polar QW emission at the step-bunches. Spatially resolved streak camera maps indicate that the *m*-plane emission has a typical CL decay time ~300 ps, whilst the regions across the step-bunches also exhibit a slower decay component, as expected for semi-polar QWs. Therefore, combining a range of characterisation techniques, the low energy emission features and slower CL decays have been assigned to the formation of QWs on the semi-polar facet across the step bunches associated with the miscut of the GaN substrate.

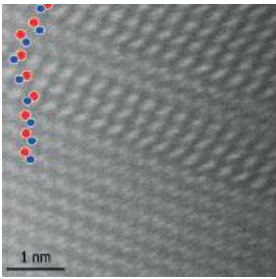
## **Session 2b: Quantum dots and nanowires I**

### **(Invited) Silicon Nanowires: Synthesis, optical properties and photonic applications**

A Irrera

IPCF CNR Messina, Italy

Semiconductor nanowires (NWs) are attracting the interest of a large scientific community as building blocks for a wide range of future nanoscaled devices. In this work we show that metal-assisted chemical etching of Si substrates is a powerful technique to obtain nanometer-size, high density and low-cost Si NWs with high and controllable



# Microscopy of Semiconducting Materials (MSM-XIX)

aspect ratio. NWs obtained by this technique maintain the same structure and doping of the starting substrate and exhibit a very bright room temperature PL, which is tunable with NWs size, in agreement with the occurrence of quantum confinement effects. Light emitting devices based on Si NWs, showing an efficient room temperature EL emission at low voltage, have also been realized. We demonstrate that the design of new textures of NWs and the optimization of their size and spatial arrangement may play a key role for the improvement of the optical properties, such as light trapping and multiple scattering phenomena. We also realized a room temperature operating hybrid light source by coupling Si NWs and carbon nanotubes (CNT). This system exhibits an emission in the visible range from Si NWs and in the IR from CNT; a detailed study of the PL properties has been performed, and the conditions leading to the prevalence of the visible or of the IR signal have been identified. Finally, we report the structural and optical properties of Si NWs decorated with metallic clusters, a system which has great potentialities for biosensing applications.

## Strain relaxation in InAs quantum dots and its suppression by indium flushing

F Ponce<sup>1</sup>, H Xie<sup>1</sup>, R Yakomin<sup>2</sup>, M Pires<sup>2</sup>, R Prioli<sup>2</sup> and P Lustoza<sup>2</sup>

<sup>1</sup>Arizona State University, USA, <sup>2</sup>PUC-Rio, Brazil

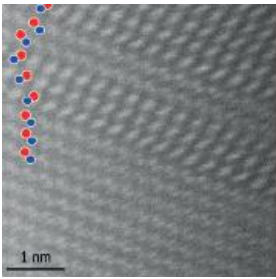
InAs quantum dots (QDs), grown on and encapsulated by Al<sub>0.3</sub>Ga<sub>0.7</sub>As for optimized intermediate band solar cells, have been studied using transmission electron microscopy. In QDs with a 20 nm GaAs capping layer, strain relaxation is observed as moiré fringes in two-beam diffraction images, and as dislocation lines with an edge component in lattice images. The addition of an indium flush step after deposition of a 5 nm GaAs capping layer results in bend-contour contrast, indicating fully strained QDs. The absence of strain relaxation is explained by a proposed model in terms of the critical diameter of QDs required to form dislocations.

## Structural characterization of Ga<sub>2</sub>O<sub>3</sub>/SnO<sub>2</sub> complex nanostructures by advanced transmission electron microscopy

B Mendez<sup>1,2</sup>, I Lopez<sup>1</sup>, E Nogales<sup>1</sup>, A M Sanchez<sup>2</sup> and J Piqueras<sup>1</sup>

<sup>1</sup>Universidad Complutense Madrid, Spain, <sup>2</sup>University of Warwick, UK

Complex nanowires architectures have a great interest to upgrade functions of nanomaterials. For example, crossing wires of p and n type semiconductors may lead to 1D heterojunctions of interest in novel nanodevices. The growth mechanism of complex nanostructures based on Ga<sub>2</sub>O<sub>3</sub> and SnO<sub>2</sub> was investigated. Advanced transmission electron microscope (TEM) provided novel information on structural, chemical and morphological properties of these nanostructures. Samples were obtained by a thermal evaporation process in an open furnace without the aid of any catalyst. Gallium oxide compacted pellets with small amounts of pure Ga and tin oxide were used as source materials. After the thermal treatment, different complex nanostructures were accomplished, i.e. crossing Ga<sub>2</sub>O<sub>3</sub>/SnO<sub>2</sub> nanowires, skewer-like structures formed by a main Ga<sub>2</sub>O<sub>3</sub> trunk and decorated with SnO<sub>2</sub> islands, *tens of microns* in length Ga<sub>2</sub>O<sub>3</sub> nanowires emerging from ultra-thin belts. The structure and morphology of the nanostructures were analysed using a JEOL 2100 TEM and a JEOL ARM200F TEM working at 200kV. Luminescence properties were measured in a Leica Steroscan SEM equipped with Catholuminescence mode and a FEI Inspec SEM with EBSD mode. We mainly focused on the local structure of the crossing point in Ga<sub>2</sub>O<sub>3</sub>/SnO<sub>2</sub> nanowires with EBSD, and found no significant structural changes at the crossing point. The origin of long nanowires emerging from thin belts is related to planar defects in the primary structures. Additional chemical information using Energy-dispersive X-ray spectroscopy and high angle annular dark field imaging showed a non-uniform Sn and Ga distribution in the belts, probably related to the defective regions.



# Microscopy of Semiconducting Materials (MSM-XIX)

## Session 2c: Quantum dots and nanowires II

### (Invited) III-V nanowire-based heterostructures: surprises and challenges

A Fontcuberta i Morral

EPFL Lausanne, Switzerland

Nanowires are filamentary crystals with a tailored diameter. Thanks to this particular morphology and size, they enable new kinds of heterostructures and materials combinations. As a consequence, nanowires have been proposed as building blocks for the improvement of existing and as well as new applications.

In this talk we will review our work on the synthesis and characterization of GaAs nanowire-based heterostructures obtained by molecular beam epitaxy. Starting with the well-known axial and radial -prismatic- quantum wells, we move to even more sophisticated structures by lowering their dimensionality. We show how ternary alloys are challenging in the nanowire form. Segregation phenomena at the nanoscale result in the formation of quantum dots with exciting optical properties. This opens up even more challenges for their characterization. We show our recent structural and compositional characterizations using state-of-the-art aberration corrected scanning transmission electron microscopy, high resolution Energy-dispersive X-ray spectroscopy (EDX) and atom probe tomography. This work can be extended to other materials systems and kinds of nanostructures.

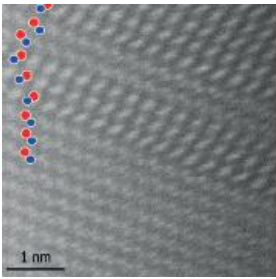
### Building nanostructures in nanowires using sequential catalyst reactions

F M Ross<sup>1</sup>, F Panciera<sup>2</sup>, Y C Chou<sup>3</sup>, M C Reuter<sup>1</sup>, D Zacharov<sup>4</sup>, E A Stach<sup>4</sup> and S Hofmann<sup>2</sup>

<sup>1</sup>IBM TJ Watson Research Center, USA, <sup>2</sup>University of Cambridge, UK, <sup>3</sup>National Chiao Tung University, Taiwan,

<sup>4</sup>Brookhaven National Laboratory, USA

Semiconductor nanowires can be grown with excellent control over length, diameter, crystal structure and composition by making use of the vapor-liquid-solid growth mechanism. Here we show how this growth mechanism can be augmented to form a different type of structure, in which individual nanocrystals are incorporated within nanowires. In conventional vapor-liquid-solid growth, nanowires are grown by exposing catalytic liquid droplets to source gases that supply the semiconductor. Instead, if we supply other species such as metals, we can trigger the nucleation of new phases in the liquid droplets that form as floating, faceted nanoparticles and become incorporated into the nanowires during further growth. We view this process with in situ transmission electron microscopy, using both conventional dark field imaging at video rate in an ultra high vacuum TEM and high speed aberration-corrected imaging in an environmental TEM. Movies obtained during growth allow us to observe the nucleation of the nanocrystal, identify the sequence of phases, and measure the kinetics of the incorporation of the nanocrystal into the growing nanowire. We will demonstrate this “sequential catalyst reaction” process by forming nickel disilicide nanocrystals in Si nanowires. We will then show how the concept can be extended to other materials and structures. Nanocrystals can in principle be placed at specific locations within nanowires such as at p-n junctions or compositional changes. We therefore anticipate a range of electronic and optoelectronic applications. “Programming” a sequence of reactions in the catalyst provides exciting opportunities for the growth of complex nanostructures in which quantum dots can be combined with quantum wells of precise dimensions in single nanowires.



# Microscopy of Semiconducting Materials (MSM-XIX)

## Microstructure of $\text{In}_x\text{Ga}_{1-x}\text{N}$ nanorods grown by molecular beam epitaxy

D Cherns<sup>1</sup>, R Webster<sup>1</sup>, Q Soundrarajah<sup>1</sup>, I Griffiths<sup>1</sup>, S Novikov<sup>2</sup> and T Foxon<sup>2</sup>

<sup>1</sup>University of Bristol, UK, <sup>2</sup>University of Nottingham, UK

InGaN alloys with high In content are of great interest for solar cells and light emitting diodes operating at longer wavelengths. However, the efficiency of these devices falls as the In content increases, owing partly to mismatch defects and stress, and material instabilities. In this paper we examine the structure of  $\text{In}_x\text{Ga}_{1-x}\text{N}$  nanorods grown on Si substrates by molecular beam epitaxy over the whole composition range  $0 < x < 1$ . Such nanorods are of great interest, as they can, in principle, be grown free of extrinsic defects (dislocations and planar faults), and the geometry allows elastic relaxation of misfit stresses.

Transmission electron microscopy (TEM) studies show that  $\text{In}_x\text{Ga}_{1-x}\text{N}$  nanorods can be grown free of extrinsic defects for all fixed compositions in the range  $0 < x < 1$ , and for samples in which the In composition was graded from  $x=0.5$  both to pure GaN or InN. However, detailed studies of  $\text{In}_{0.5}\text{Ga}_{0.5}\text{N}$  nanorods have shown fine scale variations in composition leading to a core-shell structure with a Ga-rich shell, and a generally In-rich core which itself is separated into In-rich and Ga-rich regions [1]. Recent studies using atomic resolution EDX mapping and high angle annular dark field (HAADF) imaging have shown that both the core-shell structure and the material decomposition are functions of the In content. These results lead to a new and detailed understanding of mechanism of InGaN nanorod growth. This model will be explained, along with the implications of the results for future device applications.

[1] D. Cherns et al, *Nanotechnology* **25** 215705 (2014)

## Understanding the true shape of GaAs nanowires grown by MOCVD

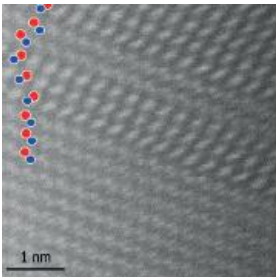
J Wong-Leung<sup>1</sup>, N Jiang<sup>1</sup>, H Joyce<sup>2</sup>, Q Gao<sup>1</sup>, H Tan<sup>1</sup> and C Jagadish<sup>1</sup>

<sup>1</sup>The Australian National University, Australia, <sup>2</sup>University of Cambridge, UK

Semiconductor nanowires offer the potential for large scale integration with the successful growth of axial and radial heterostructures. Recent work on AlGaAs/GaAs radial heterostructures has shown that the uniformity of the core-shell structure is influenced by polarity effects [1]. In addition, GaAs has a high surface recombination velocity and the effectiveness of the AlGaAs layer for surface passivation depends on the quality of the GaAs/AlGaAs interface [2]. From this perspective, it is essential to understand key factors determining the nanowire morphology.

In this presentation, we study the morphology of Au-catalyzed GaAs nanowires grown by metal organic chemical vapour deposition. These GaAs nanowires have a zinc blende structure. Different growth temperatures and annealing are used to separate the effects of radial growth and surface diffusion on the morphological transformation of the GaAs core nanowire. The cross-section of our GaAs nanowires during the vapour-liquid-solid (VLS) growth is revealed to be a Reuleaux triangle [3]. While this is consistent with the three-fold symmetry expected from the polarity of the zinc blende crystal, this contrasts with the nanowire shape assumed in the nucleation theory for VLS growth. The polarity of the curved surfaces is revealed to be  $\{112\}A$  and these curved surfaces transform into  $\{112\}B$  facets during radial growth. The facet transformation during nucleation, radial growth and annealing is determined by the minimisation of surface energies of the nanowire facets.

[1] Changlin Zheng, Jennifer Wong-Leung, Qiang Gao, Hark Hoe Tan, Chennupati Jagadish, and Joanne Etheridge, *Nano Letters* **2013** 13 (8), 3742-3748.



# Microscopy of Semiconducting Materials (MSM-XIX)

- [2] N. Jiang, Q. Gao, P. Parkinson, J. Wong-Leung, S. Mokkaapati, S. Breuer, H. H. Tan, C. L. Zheng, J. Etheridge, and C. Jagadish, *Nano Letters* **2013**, 13 (11), pp 5135–5140.
- [3] Nian Jiang, Jennifer Wong-Leung, Hannah Joyce, Qiang Gao, Hark Hoe Tan, Chennupati Jagadish, *Nano Letters* **2014** 14 (10), 5865-5872.

## Characterization of core-shell inversion domain boundaries in gallium nitride nanowires

B Haas<sup>1,2</sup>, T Auzelle<sup>1,2</sup>, X Zhang<sup>1,2</sup>, M D Hertog<sup>2,3</sup>, B Daudin<sup>1,2</sup> and J L Rouvière<sup>1,2</sup>

<sup>1</sup>CEA, France, <sup>2</sup>Université Grenoble Alpes, France, <sup>3</sup>Institut Néel, France

Semiconductor nanowires (NWs) are promising candidates for more efficient photo-voltaic or light-emitting devices. The interest in this class of materials, especially in the case of nitrides, stems from their superior crystalline quality compared to bulk materials. One of the reasons for that is the possibility to relieve strain through surface relaxation [1].

In this study, many gallium nitride (GaN) NWs grown either directly on Si (111) substrate or on a 3nm AlN layer by molecular beam epitaxy have been investigated by (S)TEM (mostly high-resolution HAADF and ABF). Two kinds of NWs have been observed: pure N-polar wires and ones with a core/shell type inversion domain boundary (IDB). In the latter case the core is always Ga-polar. The IDB could be identified by high-resolution ABF as the IDB\* structure already found by Liu et al. in bulk GaN [2].

This situation seems to be prototypical for the material system as not only the change of substrate but also variations of the buffer growth conditions always lead to the two types of NWs.

In addition, a few NWs were specially prepared to be individually measured by photo-luminescence before being observed by TEM. By comparing the photo-luminescence spectra of single NWs to their respective structure a signature at 3.45eV (already linked to IDBs in bulk material [3]) could be directly attributed to the core/shell IDB structure.

In another growth experiment indium was added after an initial growth of the NWs and only the pure N-polar wires incorporate it, while the core/shell IDB wires exhibit no evidence of indium incorporation.

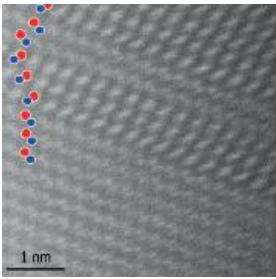
- [1] F. Glas, *Phys. Rev. B*, 74 (2006), 121302.
- [2] F. Liu et al., *Adv. Mater*, 20 (2008), 2162.
- [3] P.J. Schuck, *Appl. Phys. Lett.*, 79 (2001), 925.

## Twinning and polymorphism in GaAs nanowires: a study using scanning precession electron diffraction (SPED)

D Johnstone<sup>1</sup>, A Eggerman<sup>1</sup>, A van Helvoort<sup>2</sup> and P Midgley<sup>1</sup>

<sup>1</sup>University of Cambridge, UK, <sup>2</sup>Norwegian University of Science and Technology, Norway

Semiconducting III-V nanowires are promising materials for future optoelectronics and in particular, GaAs nanowires with homogeneous composition or incorporating axial or radial heterostructures have attracted much attention. Crystal structure variations, particularly twinning and the presence of wurtzite regions in zinc blende nanowires, are nearly always observed and affect optical performance. However, specific structure-property relationships are



# Microscopy of Semiconducting Materials (MSM-XIX)

currently unclear and systematic structural studies of individual nanowires with known optical properties are required. High-resolution lattice imaging and dark-field TEM have been used previously but the small field of view in the former and contrast variations due to bending in the latter, may limit the length and number of nanowires that can be analysed.

Here we use scanning precession electron diffraction (SPED) to overcome these limitations and to quantify structural variations over relatively large areas. SPED involves scanning a convergent electron beam across the region of interest and recording PED patterns in an automated fashion at each point using a double conical rocking beam system. The 4-dimensional data set can then be analysed in a number of ways. The simplest is to create “virtual” dark-field images by plotting the intensity of a diffracted beam (pixel or set of pixels) as a function of beam position. To determine the crystallography, each acquired PED pattern can be matched to a library of simulated patterns, producing orientation images, typically in the form of Euler angle maps. For improved and automated quantification of the nanowire structure, we have explored the optimum precession angle (to minimize “bending artifacts” but maintain spatial resolution) and applied multivariate statistical analyses to determine the important independent components (or phases) and achieve much improved structural analysis. Results are presented that provide a clear quantitative analysis of the GaAs nanowires and an improved basis for structural studies of similar nanostructures in the future.

## Strain mapping accuracy improvement using Super-Resolution techniques

G Bárcena-González, M D L P Guerrero-Lebrero, D F Reyes, D González, A Mayoral, E Guerrero and P Galindo

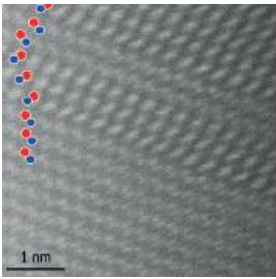
University of Cádiz, Spain

Super-resolution (SR) [1] allows the reconstruction of a high resolution image from several noisy low-resolution (LR) images. SR can be applied to overcome the inherent resolution limitation of the microscope and improve the performance of most digital image processing applications such as Geometrical Phase Analysis (GPA) [2] and Peak Pairs Analysis (PPA)[3,4]. Different works have been devoted to show how higher signal-to-noise ratio improves GPA precision [5]. In this work we applied GPA to LR and SR images and compare their results showing how GPA accuracy is improved using SR.

For that purpose, a set of low resolution images of several GaAs/InAs quantum dots oriented along the horizontal and vertical directions obtained in an X-FEG FEI Titan microscope at 300 kV have been analysed. Images have been low-pass filtered using a Gaussian filter and subsequently a Vandewalle’s algorithm [6] modification has been used for alignment. A variant of the Non Local Means algorithm [7, 8, 9] has been applied to obtain a final reconstructed image, that provides far more detail (in spite of having the same pixel density) than any individual low resolution image.

Experimental strain maps from LR images and the corresponding SR image have been generated. To quantitatively compare strain mapping measurements, the distribution of strain values in the substrate have been compared using GPA, following in both cases a gaussian distribution. While mean strain values are closely clustered around zero in both cases, its standard deviation is significantly reduced in the SR case.

These results indicate that SR arises as a remarkable tool to increase the signal-to-noise ratio in High-resolution Scanning Transmission Electron Microscopy images, therefore improving the accuracy made by strain mapping algorithms.



# Microscopy of Semiconducting Materials (MSM-XIX)

Tuesday 31 March

## Session 3a: Scanning electron and ion beams

### (Invited) FIB analysis for advanced device technology

H Bender

IMEC, Leuven, Belgium

For sub-14 nm device technologies the resolution of even the most advanced scanning electron microscopes, in dual-beam FIB as well as stand-alone systems, is often insufficient to analyze all details with sufficient accuracy. Therefore the demand for fast and high volume TEM/STEM analysis is booming strongly. This is facilitated by e.g. increased automation for specimen preparation and analysis, compatibility of sample holders for easy transfer between systems, or in-situ STEM in FIB systems.

As site specificity is crucial for the investigation of the 3D device structures, focused ion beam is the major route followed for sample preparation. A high quality SEM image is then crucial to control the position and thickness of the final lamella. Substrate side milling combined with final low energy ion milling allows to improve specimen uniformity and reduces the beam damage considerably. Typical applications of such workflow for advanced device structures will be reviewed. Also less common preparation procedures for plan-view specimens and pillars with different shapes for 3D analysis will be discussed.

Contrary to top down SEM analysis in full wafer systems, FIB analysis has a major impact on the wafers by milling/deposition of structures and possible redeposition or surface damage on the wafer. "Wafer return" is a possible workflow for the microelectronics manufacturing that allows to continue wafer processing after FIB analysis for local cross-sectional imaging or extraction of lamella for TEM/STEM. The feasibility of such procedure is explored by investigation with TOFSIMS and micro-sheet resistance of the surface contamination and damage induced by the FIB process around typical FIB craters and deposits. Results will be discussed for milling with different doses in silicon and Cu layers, or deposition of Pt pads. The results indicate that these effects are generally limited to an area corresponding to only few dies and acceptable contamination levels.

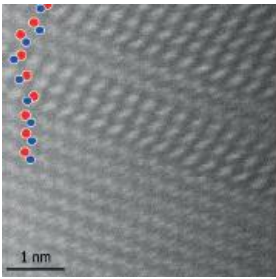
### SIMS-AFM-SEM combination for elemental mapping and 3D reconstruction

L Pillatsch, J Whitby, L van Werra and J Michler

EMPA, Switzerland

The complexity of semiconductor structures often requires a combination of different analysis methods to fully characterise the elemental distribution of semiconductor samples.

Within the frame work of the European FP7 UnivSEM project, a tool for multiple correlated chemical analyses at nanometer scales has been developed, based upon a FIB-SEM instrument from TESCAN. One of the measurement, a time-of-flight (TOF)- mass spectrometer [1,2] which detects all elements simultaneously, is optimal for small sample volumes (since FIB-SIMS measurements are locally destructive). The lateral distribution of the elements can be recorded with a resolution <50 nm. Limits of detection are many orders of magnitude lower than for EDX measurements. To ease data analysis and visualisation, we have developed an open source software to apply several clustering algorithms to the four-dimensional datasets. The integration of an *insitu (in vacuo)* atomic force microscope (AFM), opens up the possibility for 3D reconstruction of the sputtered volume.



# Microscopy of Semiconducting Materials (MSM-XIX)

Imaging of the sputtered crater and the induced surface topography may be done by SEM, or by using secondary electrons induced by the Ga<sup>+</sup>-FIB

The capabilities of combined analysis techniques will be demonstrated for a semiconductor Vertical Cavity Surface Emitting Laser (VCSEL). The elemental layer composition is recorded by TOF-SIMS. The layer thickness and crater dimensions are measured by AFM. The shape of the crater recorded by SEM helps to confirm the AFM results.

## Acknowledgements:

Mr Fredrik Oestlund and Mr Tobias Spetzler of Tofwerk AG and Mr Gerhard Bürki of Empa. This research project has been funded by the European Union's FP7 Program (no. 280566 for FIBLYS, 214042 for UnivSEM) and financial supported by the Swiss Commission for Technology and Innovation.

- [1] J.A. Whitby et al, Advances in Materials Science and Engineering, 2012, article ID 180437
- [2] D. Alberts et al, Instrumentation Science & Technology 2014 DOI:10.1080/10739149.2013.878843.

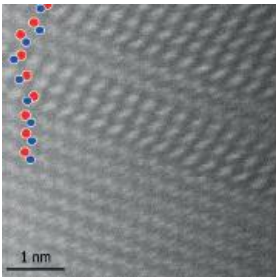
## In-situ electronic probing of semiconducting nanowires in a FIB

V T Fauske<sup>1</sup>, M B Erlbeck<sup>1</sup>, J Huh<sup>1</sup>, D C Kim<sup>2</sup>, M A Munshi<sup>2</sup>, D L Dasa<sup>1</sup>, H Weman<sup>1</sup>, B O Fimland<sup>1</sup> and A T J van Helvoort<sup>1</sup>

<sup>1</sup>Norwegian University of Science and Technology, Norway, <sup>2</sup>CrayoNano AS, Norway

Semiconducting nanowires are seen as promising building blocks in future optoelectronic devices. Due to their limited size, ca. 10-300 nm diameter and a few micrometres long, electronic characterisation of them can be challenging. Here, we present the results of electronically probing p-doped GaAs nanowires within a DualBeam focused ion beam (FIB) system. The FIB is equipped with a gas-injection system and four micromanipulators. Current-voltage (I-V) characteristics of single nanowires can be obtained in a relatively short time via different approaches, and analysed with the commonly used metal-semiconductor and/or metal-semiconductor-metal models. These alternative routes based on nanoprobng inside a FIB could prove advantageous for one-dimensional nanostructures compared to downscaling conventional techniques developed for bulk and planar structures.

First, as-grown, freestanding nanowires are probed by contacting the catalytic metal particle on the top of the nanowire and through the substrate, in a so called "1-probe" set-up. The same nanowire batch was also characterised in a 2-probe and a 4-probe set-up. For these configurations, common metal contacts were made by electron beam lithography as well as by directly contacting the nanowires in the FIB using electron beam induced deposition (EBID) of Pt. The resulting electronic characteristics deduced via these four different contacting methods are compared. For EBID-based contacting in a FIB, stray deposition causing shunting, and the reduced conductivity of the metal have to be considered in the design and analysis of the metal-semiconductor-metal configuration. Finally, for the 2-probe set-up electron beam induced current (EBIC) mapping was performed. This allows the extraction of minority carrier diffusion lengths and imaging of the Schottky depletion layer. The study demonstrates that there are different ways to deduce the electronic characteristics of doped GaAs nanowires by using a FIB combined with *in-situ* microprobing.



# Microscopy of Semiconducting Materials (MSM-XIX)

## Automated defect analysis with EBIC

M Hiscock<sup>1</sup>, G Moldovan<sup>1</sup>, S Lotharukpong<sup>2</sup> and P Wilshaw<sup>2</sup>

<sup>1</sup>Oxford Instruments NanoAnalysis, UK, <sup>2</sup>University of Oxford, UK

Electron Beam Induced Current (EBIC) characterization is unique in its ability to provide quantitative high-resolution imaging of electrical defects in solar cells. In particular, EBIC makes it possible to image electrical activity of single dislocations in a Dual-Beam Focused Ion Beam (FIB) Scanning Electron Microscope (SEM), to cut and lift out a micro-specimen containing a particular dislocation, and then transfer it for further structural or chemical analysis. As typical solar cell material presents a complex array of defects, it is important to observe statistical variations within a sample and select key sites for analysis.

This work describes a method for automated defect identification and characterization, and shows an application to multi-crystalline silicon (mc-Si) solar cell wafers selected from different heights along a manufactured ingot. Information presented here includes the experimental setup for data acquisition, as well as the analysis algorithms used for identification and extraction of dislocation contrast.

Application to this solar cell material revealed that the average contrast of dislocations is shifting from 0.12 at the bottom of the ingot to 0.08 at the top of the ingot. This shift may be assigned to the different total times available for collecting impurities, where dislocations at the bottom of the ingot have more time compared with those at the top, or to the different densities of dislocations along the height of the ingot, where impurities at the bottom are spread between a reduced number of dislocations, as compared with those at the top.

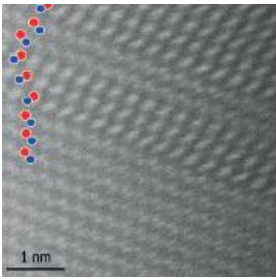
## Post-ion beam induced degradation of Cu layers in TEM specimens

F Seide<sup>1,2</sup>, O Richard<sup>1</sup>, H Bender<sup>1</sup> and W Vandervorst<sup>1</sup>

<sup>1</sup>IMEC, Belgium, <sup>2</sup>Katholieke Universiteit Leuven, Belgium

FIB has become the standard preparation procedure for TEM specimens in the semiconductor and nanotechnology domain. Specimen quality is crucial for obtaining excellent TEM results. Therefore there is particular interest in possible ion beam induced material alterations. In this work we study the corrosion process from Cu containing specimens after FIB preparation and storage in laboratory ambient, the mechanism behind this process and procedures to prevent the corrosion.

We observe that TEM specimens containing Cu structures show frequently, but quite arbitrarily severe, a tarnish layer consisting of Cu and S on the specimen surface. The layer grows within minutes after the specimen is taken out of the FIB and transferred to the TEM. It causes voids in the Cu and diffusion of the corrosion material over the specimen surface so that it overlays with regions of interest in TEM and STEM imaging and hampers the TEM chemical analysis. The growth of the tarnish is triggered by the ion beam, as the Cu surface is chemically reactive after ion beam milling. Possibly also charge which is retained in very thin specimen and implanted gallium from milling can contribute to the corrosion process. The ambient laboratory air is most likely the main source of S, as compared to other possible sources, and therefore cannot be avoided easily. Nevertheless, one can protect the specimen by sealing it with a thin oxide. Preventive measurements include a long storage of the sample in the FIB vacuum chamber and an O-plasma cleaning in-situ in the FIB or as soon as possible after unloading. These actions lead to a thin protective oxide on the surface. The oxide thickness, tarnish layer properties and other beam induced damages are compared and discussed by TEM, STEM and chemical analysis on specially prepared cone shaped specimen from Cu containing layer stacks



# Microscopy of Semiconducting Materials (MSM-XIX)

## Session 3b: Scanning transmission electron beam techniques

### Local TEM sample thickness determination via STEM defocal series

A Beyer, R Straubinger and K Volz

Philipps-Universität Marburg, Germany

Defocal series in transmission electron microscopy (TEM) mode are well known and applied regularly for a variety of materials. However, changing the defocus in scanning TEM (STEM) mode deliberately is rather new. Nevertheless, due to the large condenser apertures usable in  $C_s$ -corrected microscopes and the resulting reduction of depth of focus one can obtain valuable information on the 3d structure of a sample.

To investigate the dependence of the high-angle annular dark-field (HAADF) intensities on the defocus we choose silicon as a model system as it is one of the most commonly used materials in the semiconductor industry. A JEOL 4610F FIB/SEM was used to prepare plan parallel electron transparent samples with defined thicknesses. The samples were characterized in a double aberration corrected JEOL 2200FS. Complementary image simulations were carried out using the frozen phonon approximation of the STEMSIM code.

Changing the defocus qualitatively results in the loss of resolution. A good measure to quantify this behavior is the standard deviation of the intensity of an experimental or simulated HAADF-image. Simulated defocal series for different sample thicknesses show that the standard deviation in dependence on the defocal values exhibits a pronounced maximum at the optimum defocus and drops to a background value for higher or lower values. The FWHM of the curve is equal to the sample thickness above a minimum thickness given by the size of the used aperture. The thicknesses derived from experimental series are in good agreement with the values derived from other established techniques like position averaged convergent beam electron diffraction or the comparison of the measured intensity with simulations.

This contribution shows the benefit of defocal series in STEM via the example of thickness determination.

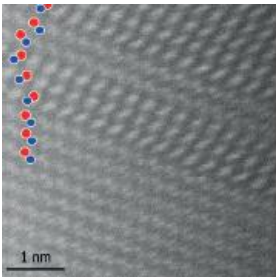
### Anomalous strain at interfaces in geometric phase analysis of Z-contrast images

J Peters<sup>1</sup>, R Beanland<sup>1</sup>, J Cockburn<sup>2</sup>, D Revin<sup>2</sup>, S Zhang<sup>2</sup> and A Sanchez<sup>1</sup>

<sup>1</sup>University of Warwick, UK, <sup>2</sup>University of Sheffield, UK

Strain fields, common at heterointerfaces, can have a large influence on the functional properties of a heterostructure. For example, in InAs/GaSb quantum cascade lasers, strain due to different layer compositions and different interface structures are predicted to have a significant impact on heterojunction band alignments, band structure and carrier mobility. To analyse the strain field at such interfaces in TEM images, different algorithms have previously been developed [1,2] Geometric phase analysis (GPA), based on a Fourier analysis, has become one of the more popular strain mapping techniques due to its tolerance of noise and ease of use. Additionally, GPA is more frequently being combined with atomic resolution, Z-contrast scanning transmission electron microscopy (STEM) images that contain additional elemental information. However, this additional information can present complications to the GPA algorithm and must be fully considered.

Here, we analyse the anomalous strain that appears in an analysis of an InAs/GaSb multilayer by applying GPA to Z-contrast images. In these type of images, consisting of multiple sublattices, both sublattices contribute to the same Bragg spots in the Fourier transform with their contribution dictated by the intensity of the sublattice. Across



# Microscopy of Semiconducting Materials (MSM-XIX)

interfaces where the intensity of the sublattices change, the measured strain field depends on the selection of the lattice planes, particularly if there is an intensity inversion between the sublattices. This causes artificial features in the GPA strain maps that can be mistakenly attributed to interface structure.

Annular dark field STEM images have been used in conjunction with multislice simulation, where the strain can be controlled precisely, to demonstrate the presence of anomalous strain and take steps towards avoiding it.

- [1] Hýtch M.J. et al. *Ultramicroscopy* **87** (2001) 199
- [2] Galindo P.L. et al. *Ultramicroscopy* **107** (2007) 1186

## Analysis and improvement of precision and accuracy of strain measurements by convergent nano-beam electron diffraction (SANBED)

C Mahr, K Müller, T Mehrtens, T Grieb, F F Krause, D Erben and A Rosenauer

University of Bremen, Germany

The measurement of lattice strain is an important aspect in the characterisation of semiconductor nanostructures. As strain has large influence on the electronic band structure, methods for strain measurements with high precision, accuracy and spatial resolution are mandatory. In this contribution we present a study of precision and accuracy of the SANBED method proposed by Müller et al. [1]. With this method we measure strain from distances between diffraction discs in convergent beam electron diffraction (CBED) patterns. As these distances depend on the local lattice parameters, according to Bragg's law information about strain can be achieved simply by comparing the disc distances at different positions of the scanning electron probe.

Rouviere et al. [2] demonstrated that using a precessing electron beam the precision of strain measurements from CBED patterns can reach  $2 \times 10^{-4}$  [2]. We show that this precision is also reached by our method. Nevertheless close to interfaces between parts of the specimen with different strain, the accuracy suffers from an effect that occurs in the recorded CBED patterns: In the scanning mode of a transmission electron microscope the incident electron wave can approximately be described as the Fourier transform of the condenser aperture. As a consequence the electron beam is not only focussed in one point and high spatial frequencies of the Fourier transformed aperture can pass through parts of the specimen with different strain, affecting the appearance of diffraction discs in the CBED patterns. In our contribution the influence of this effect on the accuracy of strain measurements will be discussed for the first time by evaluation of simulations. Furthermore we show how this interface effect can be minimised.

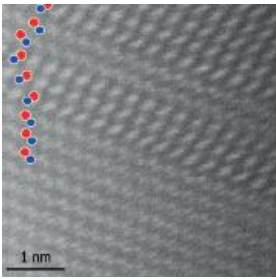
- [1] K. Müller and A. Rosenauer et al., *Microsc. Microanal.* **18** (2012), p. 995.
- [2] J.-L. Rouviere et al., *Appl. Phys. Lett.* **103** (2013), p. 241913.

## Quantifying indium content in semi-polar (11-22) InGaN quantum wells using precession electron diffraction

Y Han, A Eggeman, W Y Fu, M Pristovsek and C Humphreys

University of Cambridge, UK

Precession electron diffraction (PED) has been shown to be a powerful technique for structure solution and refinement, symmetry determination, texture analysis and measurements of bonding charge densities. The precession of the electron beam leads to many more reflections becoming visible and makes the intensities in the



# Microscopy of Semiconducting Materials (MSM-XIX)

diffraction discs more uniform and free of the complex contrast commonly shown in conventional CBED patterns. Therefore, the positions of the diffraction discs can be located according to their edges rather than to their intensity maxima, allowing for a more precise measurement of lattice strain in crystals.

In this challenging work, we map lattice strain at a nanometer scale in semi-polar InGaN quantum wells (QWs) by PED. The QWs are grown on the (11-22) plane by metalorganic vapour phase epitaxy (MOVPE) on pre-structured sapphire substrates. The QWs are less than 5 nm thick, having a nominal In content in the range between 15 to 20%. PED patterns are recorded along the [1-100] zone axis on a Philips CM300 FEG transmission electron microscope, operated at 300 kV. To maximize the number of visible reflections and to minimize the effect of lens aberrations being significant at high angles, a compromised precession angle close to  $1^\circ$  is used. The spot size of the electron beam on the samples is estimated to be 1.5 nm. The centre of the diffraction discs on the diffraction patterns is found by a program written in MATLAB. A strain map is then generated with reference to the GaN substrate, which is converted to an In content map based on the fact that the QWs are biaxially strained to the GaN substrate as confirmed by XRD reciprocal lattice mapping.

## **Imaging STEM: A novel method for microscopy of semiconductors at ultra-high spatial resolution and precision**

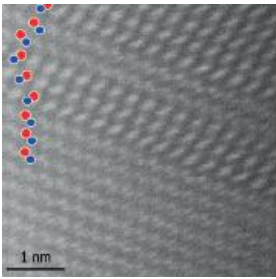
A Rosenauer, F F Krause, K Müller, M Schowalter and T Mehrtens

University of Bremen, Germany

In our contribution we introduce ISTEM (imaging STEM), a new TEM imaging mode [Phys.Rev.Lett. 113(2014)096101] which combines STEM illumination with CTEM imaging. We use a CCD camera to acquire images formed with the focused electron beam scanning over the specimen. As the acquisition time of the CCD-camera is equal to the area scan time, the images corresponding to all the probe positions are summed up. The wave functions for different electron beam positions occur at different times, so that they cannot interfere and corresponding images are summed up incoherently. Thus, ISTEM exploits an improvement in resolution obtained by switching the spatially coherent illumination to highly incoherent illumination. The gain in resolution can easily be understood for the case of a completely incoherent illumination where the transfer function is given by the autocorrelation of the coherent transfer function, whereby the maximum spatial frequency transferred by the system is increased.

In our contribution we will present a simulation study showing that ISTEM generally allows extending the point resolution of CTEM imaging beyond the diffraction limit. We will also reveal by image simulation that this new TEM mode is more robust against chromatic aberration, which allows overcoming the conventional information limit of a microscope. These calculations are confirmed by experimental data for GaN along the [1-100] and [11-20] directions taken on our TITAN80/300 microscope with a conventional information limit of 80pm, where we resolved gallium and nitrogen at a distance of 63pm.

Thus, ISTEM combines advantages of STEM imaging with advantages of the CTEM imaging mode while avoiding disadvantages of STEM. ISTEM images do neither suffer from scan noise nor is the image resolution influenced by the finite source size. Due to the principle of reciprocity, ISTEM can be made equivalent to annular bright field STEM promising ultra-high resolution imaging of light elements.



# Microscopy of Semiconducting Materials (MSM-XIX)

Wednesday 1 April

## Session 4a: Nitride epitaxy I

### (Invited) GaN heterostructures with diamond and graphene for high power applications

B Pécz

Institute for Technical Physics and Materials Science, Research Centre for Natural Sciences, Hungary

Self-heating of high power devices is a major problem in GaN high electron mobility transistors (HEMT), in which the power reached the values of 10 W/mm (the length of the gate in mm). Therefore the heat dissipation became one of the major issues and substrates with high heat conductivity are needed. Apparently there are two kinds of materials with excellent thermal conductivity which can be used as a heat sink: diamond and graphene.

Two examples using diamond are shown. In the first one GaN layers (device structures) were grown on diamond substrates by molecular beam epitaxy and the deposition process was optimised using transmission electron microscopy (TEM). The grown GaN layers are free of inversion domains and are of high quality.

The second example is a polycrystalline diamond coating layer which covers the grown HEMT transistor and provides a heat sink for the high power devices close to the active region. This method is more general, than the former one and can be applied on various semiconductors.

The third example shows how one can grow GaN over a graphene/SiC substrate. TEM investigations are used to determine the dislocation density in grown GaN and to explore the nanoscale details of the grown structure.

### Transmission electron microscopy investigations of nucleation of AlN layers on sapphire substrates

N Stolyarchuk<sup>1</sup>, S Mohn<sup>1</sup>, A Courville<sup>2</sup>, R Kirste<sup>3</sup>, MP Hoffman<sup>3</sup>, R Colazzo<sup>3</sup>, Z Sitar<sup>3</sup>, R DeFelice<sup>4</sup>, J Northrup<sup>4</sup>, O Tottereau<sup>2</sup>, S Vézian<sup>2</sup>, P Vennéguès<sup>2</sup> and M Albrecht<sup>1</sup>

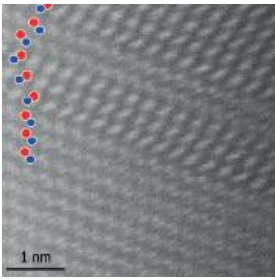
<sup>1</sup>Leibniz-Institute for Crystal Growth, Germany, <sup>2</sup>Centre National de la Recherche Scientifique, France, <sup>3</sup>North Carolina State University, USA, <sup>4</sup>Palo Alto Research Center, USA

The important characteristic of the wurtzite structure of GaN and AlN grown along the [0001]-direction is the polarity that essentially influences its physical properties. The most commonly used substrate for the growth of GaN is sapphire (Al<sub>2</sub>O<sub>3</sub>) which is nonpolar. Thus controlling the properties governing the selection of the polarity of the deposited films is the one of the main problems in growth GaN on c-sapphire.

Despite of a number of theoretical and experimental studies, little is known on the atomic structure of the III-nitride/Al<sub>2</sub>O<sub>3</sub> interfaces and the processes that govern the polarity. This is mainly due to the fact that conventional transmission electron microscopes were not capable to resolve single oxygen and nitrogen atoms with high spatial resolution.

The classical GaN and AlN MOVPE-growth leads to films with a metal polarity. In the present work we study the initial stages of MOVPE growth of GaN and AlN on sapphire by conventional (JEOL2010F) and aberration corrected (TITAN) transmission electron microscopes, i.e:

- nitridation of sapphire surface in NH<sub>3</sub> flux at 1080 °C



# Microscopy of Semiconducting Materials (MSM-XIX)

- growth of a thin nucleation layer of AlN at low temperatures (LT) around 650°C with subsequent annealing in NH<sub>3</sub> ambience at 1050°C

The cross-section analysis of nitridation layer reveals the presence of Al-polar domains together with a continuous N-polar (Al,O)N layer over so-called “voids” in Al<sub>2</sub>O<sub>3</sub>. The interface structure mostly fits well with the theoretical predictions of AlN grown under N-rich growth conditions.

The LT AlN buffer layer causes a switch of the polarity from mainly N-polar to Al-polar. The polarity of the interface is not influenced by the growth of the buffer layer. After several N-polar bilayers we see a transition to Al-polarity within two layers of up to now unknown structure. The crystalline structure of the transition resembles the model for the polarity inversion which was found in GaN:Mg.

## Multi-microscopy techniques for the investigation of fully coalesced boundaries in GaN

T O'Hanlon and R Oliver

University of Cambridge, UK

The prevalence of threading dislocations (TDs) in nitride semiconductors is well known, but their generation mechanism is not fully understood. Early models suggested TDs formed at GaN island coalescence boundaries (CBs) with slightly differing misorientations. However, later work using partially coalesced films to directly correlate CBs with dislocation distributions found no evidence of increased TD density at CBs: most dislocations seemed to be carried through from the initial nucleation layer.

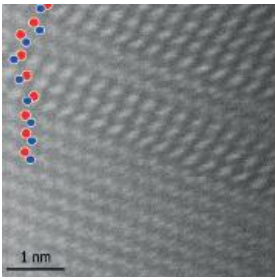
As these studies were restricted to partially coalesced films, to allow CB identification, the impact of complex late-coalescing boundaries could not be investigated. Here, the development of a multi-microscopy technique allowing comparisons of CB and TD locations in fully coalesced films is presented.

A c-plane 3D-2D growth GaN-on-sapphire sample was grown with 100 nm thick highly *n*-type silicon-doped GaN marker layers every 750 nm. Mapping of carrier types and concentrations on cleaved cross-sections with Scanning Capacitance Microscopy (SCM) allowed these layers to be seen, showing the surface evolution over time and allowed CB location after full coalescence.

Lithographic markers and topographic cleavage steps were used to allow the exact areas characterized in SCM to be located in the Focused Ion Beam / Scanning Electron Microscope. The previously characterized cross-sections were then lifted out as lamellae from the cleaved edge by milling from only the back side, with careful preparation and choice of milling angles to avoid exposure of the characterized surface to the ion beam.

Transmission Electron Microscopy defect analysis could then be used to correlate observed TDs with known CB locations to shed further light on the controversial issue of dislocation origins in the nitrides.

These techniques could also be applied to numerous other problems where direct correlation of observed cross-sectional features between techniques would yield a greater understanding of the behavior observed.



# Microscopy of Semiconducting Materials (MSM-XIX)

## GaN on SOI substrate: strain and defects

N Mante<sup>1</sup>, G Feuillet<sup>1</sup>, N Bernier<sup>1</sup>, V Delaye<sup>1</sup>, F Semond<sup>2</sup>, E Frayssinet<sup>2</sup> and P Vennéguès

<sup>1</sup>CEA, France, <sup>2</sup>CRHEA-CNRS, France

Gallium nitride is a widely used material in optoelectronic devices like LEDs which are epitaxially grown mostly onto sapphire substrates. For cost reasons, silicon is studied as a possible contender. In order to cope with issues related to lattice and thermal mismatch between the nitrides and silicon, strain engineering during growth is necessary. This is usually carried out through the insertion of strain compensating layers before the growth of the active regions. A possible alternative consists in using compliant substrates such as Silicon-on-Insulator substrates (SOI) for strain accommodation during growth and/or upon cooling down.

GaN epilayers were grown by MBE or MOVPE on SOI substrates having different thicknesses for the top silicon layer (from 16nm to 2 $\mu$ m) and the oxide layer (from 150nm to 1 $\mu$ m). Reference samples were grown onto bulk silicon. Moreover, to investigate the influence of the misfit on the compliance effect, the nitride layers were grown onto  $\langle 110 \rangle$  oriented silicon: for this particular c-GaN /  $\langle 110 \rangle$ -Si interface, the misfit is high in one direction (18% when  $\langle 10-10 \rangle$ -GaN //  $\langle 001 \rangle$ -Si) and low in the perpendicular direction (below 1% when  $\langle 11-20 \rangle$ -GaN //  $\langle -110 \rangle$ -Si).

In order to assess a possible elastic compliant effect, the distribution of strain was measured in the nitride layers and the top silicon layer of the SOI. Since compliance can also be plastic, the possible presence of defects was checked in each layer. This was carried out by using complementary TEM techniques performed on a FEI Titan<sup>3</sup> Microscope: diffraction contrast, HR(S)TEM, EELS and nanobeam electron diffraction in precession mode. We could demonstrate the presence of strain in the top silicon layer depending on its thickness and the misfit. These measurements are attributable to stress transfer from the layer to the substrate, meaningful in case of thin silicon and for the low misfit interface.

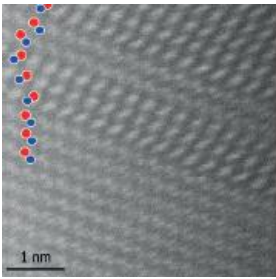
## V-pit to truncated pyramid transition in AlGaN-based heterostructures

A Mogilatenko<sup>1</sup>, J Enslin<sup>2</sup>, A Knauer<sup>1</sup>, F Mehnke<sup>2</sup>, K Bellman<sup>2</sup>, T Wernicke<sup>2</sup>, M Weyers<sup>1</sup> and M Kneissl<sup>2</sup>

<sup>1</sup>Leibniz-Institut für Höchstfrequenztechnik, Germany, <sup>2</sup>Technische Universität Berlin, Germany

AlGaN base layers with smooth surfaces and low dislocation densities are required for high-efficiency AlGaN quantum well light emitters in the ultra-violet spectral range. However, growth of  $\text{Al}_x\text{Ga}_{1-x}\text{N}$  with Al content  $x$  below 0.6 on (0001) AlN often results in poor surface morphologies due to formation of three-dimensional (3D) structures. The shape of these structures resembles truncated pyramids. Their height can reach a few hundreds of nanometers, and their base extends over several micrometers. Commonly, the formation of these 3D surface structures is described as surface roughening, which is believed to occur as a consequence of strain relaxation process.

In this study we have analysed the formation of truncated pyramids after deposition of AlN/GaN superlattices on AlN layers grown on (0001) sapphire substrates. Using cross-sectional STEM analysis we will show that the truncated pyramids are formed on top of v-pit defects, which are present within the AlN template layer. We suggest that a preferential Ga accumulation on the v-pit sidewalls and a higher growth rate on these semipolar v-pit surfaces lead to a rapid change from the concavely shaped v-pit defect to a convex pyramidal shape of the 3D-pyramid. This behaviour is only observed above a critical GaN layer thickness and a critical strain energy level in the AlN/GaN superlattice.



# Microscopy of Semiconducting Materials (MSM-XIX)

We will show that despite the high surface roughness of the superlattice due to formation of truncated pyramids, smooth AlGaIn base layers can be achieved by overgrowth of these 3D structures. However, the presence of the inclined sidewalls of the 3D pyramids leads to an inhomogeneous composition, strain and defect distribution in subsequently grown AlGaIn layers. A local reduction of compressive strain above the truncated pyramids is confirmed by different propagation directions of dislocation lines observed in AlGaIn grown on smooth template surface and on template layers containing pyramidal structures.

## Session 4b: Nitride epitaxy II

### **(Invited) Highly spatially resolved cathodoluminescence of III-nitride based nanostructures directly performed in a scanning transmission electron microscope**

J Christen, G Schmidt, F Bertram, M Müller and P Veit

Otto-von-Guericke-University Magdeburg, Germany

For a detailed understanding of complex semiconductor heterostructures and the physics of devices based on them, a systematic determination and correlation of the structural, chemical, electronic, and optical properties on a nanometer scale is essential. Luminescence techniques belong to the most sensitive, non-destructive methods of semiconductor research. The combination of luminescence spectroscopy – in particular at liquid He temperatures – with the high spatial resolution of a scanning transmission electron microscope (STEM) ( $dx < 5$  nm at 10 K), as realized by the technique of low temperature scanning transmission electron microscopy cathodoluminescence microscopy (STEM-CL), provides a unique, extremely powerful tool for the optical nano-characterization of semiconductors, their heterostructures as well as their interfaces.

Our CL-detection unit is integrated in a FEI STEM Tecnai F20 equipped with a liquid helium stage ( $T = 10$  K / 300 K) and a light collecting mirror. The emitted CL light is collected by a parabolically-shaped mirror above the sample and focused onto the entrance slit of a grating monochromator. In STEM mode the electron beam is convergent and either kept at a single position for local spectra or scanned over the region of interest in imaging mode. Panchromatic as well as spectrally resolved CL imaging is used. The CL-intensity is collected simultaneously to the STEM signal at each pixel. The TEM acceleration voltage is optimized to minimize sample damage and prevent luminescence degradation under electron beam excitation.

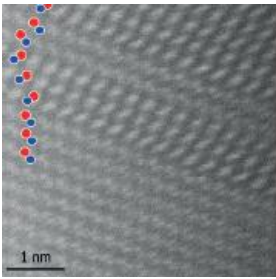
Typical results, which will be presented, include nm-scale correlation of the optical properties with the crystalline real structure of GaN/AlN quantum dots. In particular, we will show the preferential nucleation of GaN/AlN quantum dots at threading dislocation without inhibition of very sharp emission lines with line width below 500  $\mu\text{e}$ .

### **Study of phases created due to thermal degradation of InGaIn quantum wells**

J Smalc-Koziorowska, S Kret, E Grzanka, R Czernecki, M Leszczyński, P Perlin and T Suski

Institute of High Pressure Physics PAS, Poland

Growth of nitride structures with controlled indium composition is one of the hot topics related to development of blue-green light emitting diodes and laser diodes. The realization of green InGaIn laser diodes requires preparation of InGaIn layers with In content higher than 30%. However such high In content layer are unstable and tend to



# Microscopy of Semiconducting Materials (MSM-XIX)

degrade during the growth of p-type layers, which are typically grown at higher temperatures than the growth of InGaN layers. In these studies we describe the phases created due to thermal degradation of InGaN quantum wells and we propose the mechanism leading to the formation of these various phases. Typically the phases observed in the degraded areas of quantum wells contain voids partially filled with crystalline In, and partially filled with amorphous material, as well as the areas with In content higher than 70% of In. The degraded areas contain also basal stacking faults attached to the voids and extended in the structure. Preserved sections of the InGaN quantum well remain between the degraded areas. The voids and high In content areas embrace the quantum well and in many cases also include the preceding GaN quantum barrier. We observe quite often that in case of two InGaN quantum wells layers separated by few-nanometer-thickness GaN layer, only one of them decomposes. Possibly the degradation of the InGaN quantum wells starts as the spinodal decomposition to lower and higher In content areas. Less stable high In content areas further decompose to liquid solution of indium, gallium and nitrogen. When the whole structure is cooled down, the recrystallization takes place and various phases are created.

Acknowledgement: Research is co-financed by the BRIDGE project founded by the Foundation for Polish Science in the frame of the operating programme Innovative Economy.

## Quantum mechanical interpretation of electron picodiffraction reveals atomic electric fields

K Müller<sup>1</sup>, F F Krause<sup>1</sup>, A Béché<sup>2</sup>, M Schowalter<sup>1</sup>, V Galioit<sup>3</sup>, S Löffler<sup>4</sup>, J Verbeeck<sup>2</sup>, J Zweck<sup>3</sup>, P Schattschneider<sup>4</sup> and A Rosenauer<sup>1</sup>

<sup>1</sup>Universität Bremen, Germany, <sup>2</sup>EMAT Antwerpen, Belgium, <sup>3</sup>Universität Regensburg, Germany, <sup>4</sup>Vienna University of Technology, Austria

A prominent scanning TEM (STEM) technique for studying atomic-scale electric fields is differential phase contrast (DPC) microscopy. Conventionally, segmented ring detectors are utilised to record portions of the ronchigram [1], which is assumed to be homogeneously filled and shifted as a whole in presence of electric fields in the specimen.

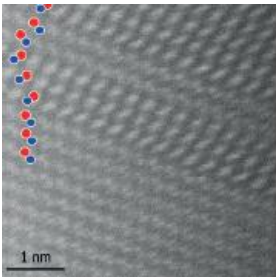
We firstly investigate the reliability of these assumptions by showing that electron ronchigrams exhibit rich intensity variations already for thinnest specimens (1-2nm), and that the dominant effect of atomic electric fields on aberration-corrected probes is a complex redistribution of intensity inside ronchigrams. This explains why segmented DPC detectors yield high contrast at atomic sites whereby a quantification of electric fields in terms of ronchigram shifts is prone to errors.

Then we give a quantum mechanical interpretation of DPC: The ronchigram is recorded in the diffraction plane, showing the Fourier transform of the specimen exit wave. According the axioms of quantum mechanics, the local ronchigram intensity  $I(\mathbf{p})$  is thus proportional to the probability for the lateral momentum vector  $\mathbf{p}$  to occur. Hence the expectation value for the momentum is calculated by a centre-of-gravity-type summation, relating the rich details of the ronchigram to a single vector with fundamental physical meaning in a direct and simple manner. To put this into practice, we use a pixelated detector in experiment.

Finally, Ehrenfest's theorem is applied to relate the electric field to the momentum transfer via a proportionality factor. In a comprehensive simulation study of GaN, we demonstrate the capability of our method by calculating momentum transfer, electric field and charge-/electron densities from simulated ronchigrams. We then prove the experimental applicability by mapping the electric field in an SrTiO<sub>3</sub> unit cell quantitatively and verify these results by simulations [2].

[1] Shibata et al., Nat.Phys. 8, 611 (2012)

[2] Müller et al., Nat.Comm. 5, 5653, (2014)



# Microscopy of Semiconducting Materials (MSM-XIX)

## Session 4c: Thin films, multilayers and monolayers

### (Invited) Heterostructured nanostructures in compound semiconductors

P Komninou

Aristotle University of Thessaloniki, Greece

Nanostructures of compound semiconductors are mainly fabricated in non-equilibrium conditions forming one, two and three-dimensional systems. Combining binary and ternary alloys of III-V semiconductors, complex architectures of nanowires (NWs), multiple quantum wells (MQWs) and quantum dots (MQDs) comprise the building blocks of novel photonic and electronic devices. Microstructure, interfacial structure, defect content, compositional fluctuations of the alloys in the active region and strain state of the heterostructures play a crucial role for interfacial and bandgap engineering. In addition, they are the key factors in the mechanisms responsible for new phenomena observed and new properties measured. A series of results on heterostructures in single and complex NWs and systems containing QDs in III-Nitrides and III-Arsenides, derived by employing analytical and quantitative transmission and scanning electron microscopy techniques, will be presented. Quantitative high resolution transmission electron microscopy (qHRTEM) methods, including geometric phase analysis (GPA), were applied to quantify local strains and compositions around defected structures and interfaces. Empirical interatomic potential simulations and density functional theory calculations were used for computational design and modeling of dimensions, structures, defects, compositions and strains

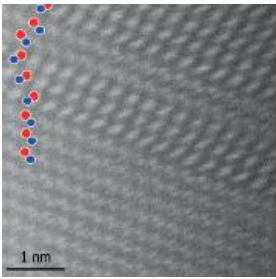
### Investigation of antimonide-based materials grown on exactly oriented (001) silicon substrate

A Ott<sup>1</sup>, A Beyer<sup>1</sup>, K Jandieri<sup>1</sup>, P Ludewig<sup>2</sup>, A Ruiz Perez<sup>2</sup>, W Stolz<sup>1</sup> and K Volz<sup>1</sup>

<sup>1</sup>Philipps-Universität Marburg, Germany, <sup>2</sup>NAsP III/V GmbH, Germany

Antimonide-based materials, such as gallium antimonide (GaSb), that are grown highly mismatched on silicon substrates, have interesting applications in high electron mobility III/V channel layers. As there are no III/V semiconductors with high electron mobility that can be grown lattice matched on silicon, different buffer layers have to be studied and the defect formation within these layers has to be understood in detail to optimize the layer structures for later device applications. In our approach, a gallium phosphide (GaP) layer is grown between the exact (001) Si substrate and the buffer so that the antiphase boundaries created by the growth of a polar material on the non-polar Si annihilate within the GaP. The buffer layers have been grown by metal organic vapor phase epitaxy (MOVPE) and were investigated in detail by several transmission electron microscopy (TEM) techniques. High resolution TEM and high-angle annual dark-field (HAADF) scanning TEM (STEM) investigations of the interface using a double C<sub>s</sub>-corrected JEOL 2200FS (S)TEM have revealed that the misfit dislocations mainly are Lomer

dislocations and 60° dislocation pairs. The strain induced by the high mismatch should be relaxed by misfit dislocations at the interface. However, dark-field and high resolution TEM have shown that the bulk contains other defects like stacking faults, twins and threading dislocations. Molecular dynamics simulations with Stillinger-Weber potentials have been used to model the structure of the dislocations theoretically. The crystal model has been used as input to simulate the HAADF images with the multislice algorithm. This contribution shows that HAADF imaging in combination with molecular dynamics simulation is very suitable for defect characterization at the interface of strained materials. TEM is very useful to gain insight on the crystal structure of GaSb and other metamorphic buffer layers so that their growth can be optimized.



# Microscopy of Semiconducting Materials (MSM-XIX)

## Effect of Sb content in the ordering of $(\text{In}_{0.5}\text{Ga}_{0.5})\text{P}$ layers for tandem solar cells

L López-Conesa<sup>1</sup>, C Coll<sup>1</sup>, J M Rebled<sup>1</sup>, E Barrigon<sup>2</sup>, L Barrutia<sup>2</sup>, I Rey-Stolle<sup>2</sup>, S Estradé<sup>1</sup> and F Peiró<sup>1</sup>

<sup>1</sup>Universitat de Barcelona, Spain, <sup>2</sup>Universidad Politécnica de Madrid, Spain

We use TEM for a detailed structural characterization of  $\text{Ga}_{0.5}\text{In}_{0.5}\text{P}$  layers grown by MOVPE onto (001) Ge substrates misoriented  $6^\circ$  to [111].  $\text{Ga}_{0.5}\text{In}_{0.5}\text{P}$  is a III-V compound frequently used in multijunction solar cells, and developing epitaxial routines that yield highly disordered material is key to attain high efficiency. This alloy might show  $\text{CuPt}_b$  ordering, which consists of an alternation of In and Ga atoms on {111} planes. Conventional and aberration corrected TEM techniques enable the elucidation of the type of ordering and the assessment of the degree of order in the layers as a function of Sb content.

Conventional bright field TEM confirmed the high quality of all epitaxial samples. No layer decomposition was observed. For cross-section samples along [110], satellite spots observed in SAED at positions  $(h+1/2, k-1/2, l+1/2)$  revealed the existence of  $\text{CuPt}_b$  ordering. Dark field imaging mode using the satellites was used to highlight the ordered domains. The domain size as a function of Sb content will be discussed in correlation with the photoluminescence properties.

The samples were also examined in an aberration corrected instrument in STEM-HAADF to assess the polarity in the direction of ordering using the HAADF sensitivity to Z number. An alternation of bright {111} planes at a distance double of  $d_{111}$ , reveals the alternation of the indium-rich ( $Z_{\text{In}} = 49$ ) and gallium-rich planes ( $Z_{\text{Ga}} = 31$ ) respectively, in agreement with the presence of satellite spots in SAED. HAADF image at atomic resolution confirmed the expected polarity.

In summary, dark field and STEM-HAADF modes have been applied to assess the type and degree of order in  $\text{Ga}_{0.5}\text{In}_{0.5}\text{P}$  layers. Through this analysis we will be able to correlate MOVPE growth conditions and surfactant action with the microstructure in order to optimize the growth of disordered  $\text{Ga}_{0.5}\text{In}_{0.5}\text{P}$  to be used in highly efficient multijunction solar cells.

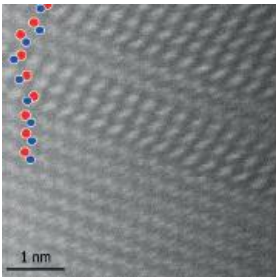
## Ga(NAsP)-layers in Si-based laser structures investigated by HRSTEM

T Wegele<sup>1</sup>, P Ludewig<sup>2</sup>, A Beyer<sup>1</sup> and K Volz<sup>1</sup>

<sup>1</sup>Philipps-Universität Marburg, Germany, <sup>2</sup>NAsPIII/V GmbH, Germany

Quaternary semiconductor materials such as Ga(NAsP) are very promising as active layers in laser devices [1]. On the one hand the combination of many elements with different physical properties allows to modify the band structure in a desired way, reduces the lattice mismatch and consequently enables the improvement of the electronic and optical properties of the semiconductor devices. On the other hand the materials consisting of many components are very complex systems. There is still not much knowledge about the driving forces for structure formation or phase separation during the growth process of such crystalline materials. Therefore a choice of suitable growth parameters to produce layers of high quality with a reproducible and predictable composition is not trivial.

We investigated Ga(NAsP)-quantum wells in laser structures grown on silicon-substrates using metal organic vapour phase epitaxy (MOVPE). The investigations were performed at a double Cs-corrected JEM 2200 FS microscope in scanning mode using the annular dark field technique, also at different angular ranges. The micrographs were evaluated quantitatively by means of a home-written software to extract composition homogeneity as well as interface roughness.



# Microscopy of Semiconducting Materials (MSM-XIX)

According to our results there is a strong correlation between the interface roughness of the Ga(NAsP)- quantum wells and the change of the growth temperature. In addition, there is an influence of the growth procedure on the element distribution in the samples.

[1] S. Liebich et al., Appl. Phys. Lett. 99, 071109 (2011)

## Structure of $\text{Fe}_3\text{Si}/\text{Al}/\text{Fe}_3\text{Si}$ metal thin film stacks on GaAs(001)

B Jenichen, U Jahn, A Nikulin and J Herfort

Paul-Drude Institute, Berlin, Germany

The integration of spin transfer torque (STT) elements into semiconductor structures should allow for a new type of electrically controlled spin manipulation in the semiconductor transport channel, utilizing the magnetic stray field of STT elements. High-quality epitaxial growth of thin film stacks consisting of ferromagnetic (FM) and non-FM metal layers on top of a semiconductor is a prerequisite. Here, we report about the epitaxial growth of  $\text{Fe}_3\text{Si}/\text{Al}/\text{Fe}_3\text{Si}$  metal thin film stacks on GaAs(001) by molecular beam epitaxy. Samples were characterized by x-ray diffraction (XRD), transmission electron microscopy (TEM), and electron backscattered diffraction. The first 4.5-nm-thick  $\text{Fe}_3\text{Si}$  layer deposited on top of a 300-nm-thick GaAs buffer layer at 200 °C grows single-crystalline with a (001) orientation as visible from high resolution (HR) TEM and XRD. The subsequent 23-nm-thick Al film deposited at 0 °C grows almost (111) oriented as shown by selected area diffraction (SAD). In HRTEM only the Al(111) fringes parallel to the interface are detected. Al(111) is more favorable energetically due to the fact that the unstrained (111) plane is more densely packed than the (001) plane. However, the final structural properties of the whole stack depend on the substrate temperature  $T_s$  during deposition of the second  $\text{Fe}_3\text{Si}$  layer. SAD shows that the upper  $\text{Fe}_3\text{Si}$  layer is (110) oriented within the whole substrate temperature range, i.e.  $0\text{ °C} \leq T_s \leq 200\text{ °C}$ . At low  $T_s < 50\text{ °C}$ , all layers retain their original structural properties. Crystalline  $\text{Fe}_3\text{Si}/\text{Al}/\text{Fe}_3\text{Si}$  metal thin film stacks can be achieved on GaAs(001) substrates with smooth and abrupt interfaces and an overall rms roughness of about 1 nm when growing the uppermost layers at low  $T_s$ . Hence, such stacks could be well suited for the integration of STT elements into semiconductor structures.

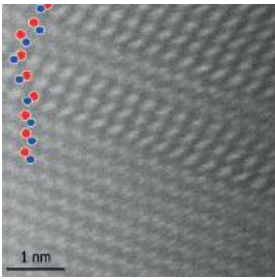
## $\text{SnS}_2$ – An emerging layered metal dichalcogenide semiconductor: Materials properties, device characteristics, and electron-induced structural transformation

E Sutter, Y Huang and P Sutter

Brookhaven National Laboratory, USA

Layered metal dichalcogenides have received attention as 2D materials beyond graphene. Semiconducting dichalcogenides are particularly attractive since they may enable next-generation low-dimensional electronics benefiting from carrier confinement and other attractive characteristics, such as flexibility and bendability. While transition metal dichalcogenides – particularly  $\text{MoS}_2$  – have been studied as prototype systems, other materials, especially those incorporating normal metals, have received much less attention.

Here we discuss the structure, electronic properties, and device characteristics of tin disulfide ( $\text{SnS}_2$ ), a semiconducting non-transition metal dichalcogenide. We demonstrate the isolation of few-layer and single-layer  $\text{SnS}_2$ . Using aberration-corrected transmission electron microscopy (AC HR-TEM) and other microscopy methods, we establish the characteristics of single- and few-layer  $\text{SnS}_2$ . Band structure measurements in conjunction with photoluminescence and TEM-cathodoluminescence spectroscopy allow us to determine the electronic structure of semiconducting  $\text{SnS}_2$  and its evolution from the bulk to a single layer [1]. By fabricating field-effect transistors, we



# Microscopy of Semiconducting Materials (MSM-XIX)

explore the achievable carrier mobility and the characteristics of photodetectors, and we identify the factors that govern the performance of SnS<sub>2</sub> (opto-) electronic devices.

Electron irradiation in the TEM is used to assess the stability of few-layer SnS<sub>2</sub> and study possible electron-beam driven transformations. Electron irradiation has been used to evaluate the radiation response and defect production of 2D materials, and to develop beam-mediated processing techniques. We establish that electron irradiation between 80 and 300 keV invariably affects the structure of few-layer SnS<sub>2</sub>. Using real time AC HR-TEM, we follow these structural transformations and show that the associated loss of the chalcogen species (S) accompanies a controlled conversion from Sn(IV) to Sn(II) sulfide. Driving this conversion locally with the electron beam creates in-plane 2D heterostructures between different layered sulfides.

- [1] Y. Huang, E. Sutter, et al., ACS Nano 8, 10743 (2014).
- [2] E. Sutter, Y. Huang and P. Sutter, submitted (2014).

## Controlling defects in topological insulator dichalcogenide thin films

N Tarakina<sup>1</sup>, S Schreyeck<sup>2</sup>, M Luysberg<sup>3</sup>, M Duchamp<sup>3</sup>, C Schumacher<sup>2</sup>, K Brunner<sup>2</sup>, C Gould<sup>2</sup>, H Buhmann<sup>2</sup>, G Karczewski<sup>4</sup>, R Duninborkowski<sup>3</sup> and L Molenkamp<sup>2</sup>

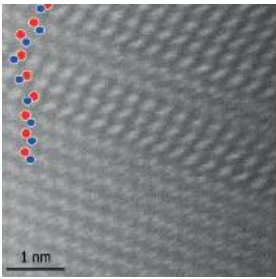
<sup>1</sup>Queen Mary, University of London, UK, <sup>2</sup>Universität Würzburg, Germany, <sup>3</sup>Ernst RuskaCentre for Microscopy and Spectroscopy with Electrons and Peter Grünberg Institute, Germany, <sup>4</sup>Polish Academy of Sciences, Poland

Topological-insulator Bi<sub>2</sub>Se<sub>3</sub> and Cr-doped (Bi<sub>x</sub>Sb<sub>1-x</sub>)<sub>2</sub>Te<sub>3</sub> thin films are promising compounds for spintronics applications. These dichalcogenide thin films bind to substrates through weak van der Waals interactions (quasi-van der Waals epitaxy) and can thus be grown on a broad variety of substrate materials. Although conditions for realizing high-quality thin films are considered to be less strict compared to standard epitaxial growth, defects like twinning, antiphase boundaries, anion vacancies, mosaicity twist and tilt still form and influence transport properties. In this work, we present a detailed study of the origins of different structural defects in such films and show how some of these defects can be eliminated.

Films grown by molecular beam epitaxy on Si(111), InP(111)B, rough InP(111)B and InP(111)A substrates have been compared. A combination of X-ray diffraction, X-ray reflectivity, reflection high-energy electron diffraction, atomic force microscopy and particularly probe-corrected scanning transmission electron microscopy data enabled us not only to describe the microstructure of these films in great detail but also to control the formation of twins. Using a rough Fe-doped InP(111)B substrate, complete suppression of twins in Bi<sub>2</sub>Se<sub>3</sub> thin films has been achieved. The mechanism of twin suppression is understood on the atomic scale. We showed that the substrate surface termination determines which family of twin domains dominates [1].

We believe that our study is relevant not only for Bi<sub>2</sub>Se<sub>3</sub> and Cr-doped (Bi<sub>x</sub>Sb<sub>1-x</sub>)<sub>2</sub>Te<sub>3</sub> growth but that it also provides essential insights for obtaining monocrystalline A<sub>2</sub>B<sub>3</sub> (A = Bi, Sb; B = S, Se, Te) chalcogenide thin films and for realizing desirable electronic properties within this class of materials.

- [1] N.V. Tarakina, S. Schreyeck, M. Luysberg, S. Grauer, C. Schumacher, G. Karczewski, C. Gould, K. Brunner, H. Buhmann, R.E. Dunin-Borkowski, L.W. Molenkamp, Advanced Materials Interfaces (2014) pp. 201400134(1)



# Microscopy of Semiconducting Materials (MSM-XIX)

## Catalyst engineering for CVD of large single crystal hexagonal boron nitride monolayer domains

S Caneva<sup>1</sup>, R Weatherup<sup>1</sup>, B Bayer<sup>2</sup>, B Brennan<sup>3</sup>, S Spencer<sup>3</sup>, K Mingard<sup>3</sup>, A Cabrer-Vilatela<sup>1</sup>, C Baehtz<sup>4</sup>, A Pollard<sup>3</sup> and S Hoffman<sup>1</sup>

<sup>1</sup>University of Cambridge, UK, <sup>2</sup>University of Vienna, Austria, <sup>3</sup>NPL, UK, <sup>4</sup>Helmholtz-Zentrum Dresden-Rossendorf, Germany

Large-area monolayers of insulating hexagonal boron nitride (h-BN) are highly sought in nanoelectronics due to the range of attractive electronic, chemical and mechanical properties they display, as well as their design compatibility with other 2D layered materials such as graphene (semi-metal) and WS<sub>2</sub> (semiconductor).

One of the main challenges to their integration in novel device architectures is the scalable growth of high quality films, which requires control over the domain size and thickness. The use of catalytic growth techniques has become the preferred route towards tailored synthesis.

We demonstrate the growth of large (~0.3 mm side length) h-BN domains via low pressure chemical vapor deposition (LPCVD) on Fe films [1]. Using complementary selected area electron diffraction (SAED), transmission electron microscopy (TEM) and atomic force microscopy (AFM) we show that the large h-BN domains are monolayers and single crystals. We also demonstrate that an increase in precursor flux leads to a rise in the nucleation density, which can be exploited to achieve full coverage of the Fe catalyst with a uniform and continuous h-BN film. We perform a combination of *in-situ* X-ray diffraction (XRD) and *ex-situ* secondary ion mass spectrometry (SIMS) to elucidate the role of the catalyst on the growth of h-BN thin films, and illustrate that interlayer diffusion during annealing plays a central role in controlling the material's morphology.

We report an example of rational catalyst engineering based on previous work on graphene growth [2,3] and aim to show that optimization of the catalytic process hinges on the understanding of the chemical and structural state of the catalyst during all CVD stages.

- [1] Caneva *et al.*, Nano Lett. (under review)
- [2] Weatherup *et al.*, Nano Lett. (2013)
- [3] Weatherup *et al.*, Nano Lett. (2011)

Thursday 2 April

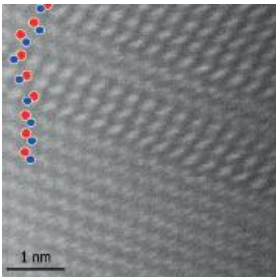
## Session 5a: Scanning probe and atom probe techniques

### (Invited) Atomic scale analysis of semiconductor nanostructures and doping atoms by scanning tunnel microscopy and atom probe tomography

P Koenraad

Eindhoven University of Technology, The Netherlands

Present day semiconductor nanoscience depends heavily on the precise construction of nanostructures in which atomic scale details determine their opto-electronic properties. It is thus of key importance to have techniques that allow such details to be assessed by novel microscopy techniques that can obtain atomic resolution, preferable in 3D. In this presentation I will show recent results that we have obtained by two exciting microscopy techniques that allow for an atomic scale resolution. We have used cross-sectional Scanning Tunneling Microscopy (X-STM) and



# Microscopy of Semiconducting Materials (MSM-XIX)

Atom Probe Tomography (APT) on a range of semiconductor nanostructures such as quantum dots and rings. The X-STM technique offers a superb 2D true atomic resolution in a single atomic plane intersecting the nanostructure. Atom Probe Tomography is a technique that only recently has become available for the analysis of semiconductor nanostructures. Laser induced field emission is used to get a full, atomically resolved, 3D map of the composition of the semiconductor nanostructure. In the presentation I will apply and compare these techniques on quantum dots and rings that have been obtained by various growth procedures such as the traditional Stransky-Krastanow process, droplet epitaxy or by applying Sb during the dot formation process. I will also show a few examples of the study and manipulation of (individual) doping atoms in a semiconductor.

## (Invited) Atom probe tomography of semiconducting materials: Technology and applications

P Clifton, T Prosa, D Olson, D Lawrence, I Martin, H Saint-Cry, P Clifton and R Ulfing

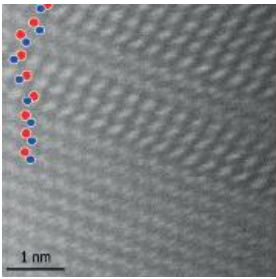
Cameca Instruments / Ametek Inc, USA

Atom probe tomography (APT) offers unique capabilities for 3D semiconductor characterisation including compositional mapping (volume  $>10^6 \text{ nm}^3$ ), detection efficiency approaching 80%, and sensitivity allowing detection of features as small as a few atoms [1-3]. With the recent release of the LEAP<sup>®</sup> 5000, advances such as flexible data acquisition control, signal-to-noise improvement, and improved compositional accuracy enable new prospective areas of analysis with respect to semiconducting materials.

Analysis yield is often a critical limitation of APT, especially for devices as opposed to bulk materials. Advanced control algorithms have been developed to allow stable data collection at lower collection rates to promote higher specimen yield. In addition, adaptive laser scan and focus algorithms with specimen voltage control have been developed to keep the field evaporation-promoting laser pulses to be optimally aligned with specimen apex. This improvement may result in increases in both yield and data quality, especially at low data collection rate. Examples of these advances will be shown.

For single semiconductor device, APT characterization is often limited by the capability to isolate a given region within the sample. Preparation techniques which allow for re-orientation and isolation of discrete regions of interest (ROI) have been developed. These techniques use a focused ion beam system to create markers which delineate specific regions that may be subsequently positioned in a specimen apex in a reversed orientation. An example based on a commercially available device will be shown.

- [1] T.J. Prosa, *et al.*, *Proc. SPIE* 9173, 917307 (2014).
- [2] M.K. Miller, *et al.*, "Detection and Quantification of Solute Clusters in a Nanostructured Ferritic Alloy", *Journal of Nuclear Materials*, in press (2015).
- [3] D.J. Larson, *et al.*, *Local Electrode Atom Probe Tomography* (Springer 2013).
- [4] D.F. Lawrence, *et al.*, "Routine Device-level Atom Probe Analysis", *Proceedings 40<sup>th</sup> ISTFA*, Houston, TX, 19 (2014).



# Microscopy of Semiconducting Materials (MSM-XIX)

## Correlative investigation of II-VI heterostructures by atom probe tomography and transmission electron microscopy

B Bonafé<sup>1</sup>, R André<sup>2</sup>, C Bourgerol<sup>2</sup>, H Boukari<sup>2</sup>, L Gérard<sup>2</sup>, A Grenier<sup>3</sup>, P-H Jouneau<sup>1</sup> and S Kuroda<sup>4</sup>

<sup>1</sup>CEA/INAC/SP2M/LEMMA, France, <sup>2</sup>Institut Neel CNRS, France, <sup>3</sup>CEA/LETI, France, <sup>4</sup>Institute of Materials Science, Japan

ZnTe/CdSe superlattices employed for photovoltaic application and (Cd,Cr)Te diluted magnetic semiconductor are both II-VI hetero-structures with physical properties strongly related to their atomic scale structures. Interface chemistry, defects formation or clustering are interesting features worth studying to properly grow and design the devices with the expected properties. Laser assisted atom probe tomography (APT) combined with scanning transmission electron microscopy (STEM) with energy dispersive spectroscopy (EDX) measurements brings powerful tools capable of performing 3D imaging and chemical composition measurements at the atomic scale and are employed for the study of ZnTe/CdSe and (Cd,Cr)Te hetero-structures.

- First, we performed APT and HAADF-STEM to investigate the chemical nature of the ZnTe/CdSe interfaces in super-lattices grown by molecular beam epitaxy. Interface chemical composition observations highlight the formation of a ZnSe interfacial layer between CdSe and ZnTe, which is known to affect the optical properties of the super-lattice and then might weakened device efficiency. A physical model related to chemical affinities between atoms is proposed to explain such an interface formation.
- (Cd,Cr)Te is predicted to be ferromagnetic for high content of Cr. The solubility of Cr in CdTe is quite low and STEM-EDX and APT are employed to check the homogeneity in composition and crystallographic phase in the sample. TEM and ATP are used on (Cd,Cr)Te layers with Cr compositions varying from 3.4% to 8.3%. We bring out the formation of Cr rich nano-clusters at 3.4% evolving in shape when the sample composed of 8.3% of Cr is imaged.

APT and TEM have proven to be valuable and complementary instruments to get structural and chemical information on II-VI hetero-structures at the nano-scale.

## Atom probe analysis of sub-surface phosphorus implantation profiles in single crystal silicon

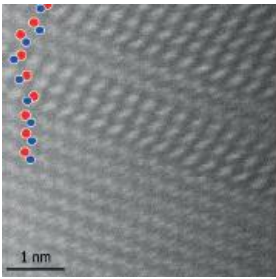
J Douglas, P Bagot and M Moody

University of Oxford, UK

Modern silicon integrated circuit (IC) devices have features and interfaces that are measured in hundreds of atoms and the position of individual dopant atoms has been shown to cause a measurable effect on device behavior. To further decrease device sizes and progress towards single atom components, atomic scale control of dopants is now becoming necessary.

Ion implantation is a common method of doping semiconductor materials and devices and enables a high level of control over dopant distribution and concentration within sub-micron volumes. Advanced implantation techniques have been demonstrated to reliably implant single phosphorus atoms into silicon photodiode devices through nanostencil masked regions of 20 nm<sup>2</sup> into known volumes of 100s of nm<sup>3</sup> [1]. To precisely map dopant distributions within such volumes and better inform implantation models, 3D atomic scale characterization is required.

Atom Probe Tomography (APT) is a atomic scale material characterization technique for typical analysis volumes of tens of millions of atoms (80 nm x 80 nm x 250 nm) with a chemical sensitivity up to tens of ppm and 3D spatial



# Microscopy of Semiconducting Materials (MSM-XIX)

resolution of individual atoms up to 0.1 nm in the analysis direction. APT has shown promise in analyzing dopant profiles from implanted silicon substrates using Focused Ion Beam (FIB) lift-out techniques [2] but there are difficulties in analyzing low concentrations in localized, near-surface volumes. These regions are easily damaged during sample preparation and are often in the initial calibration period of an APT analysis.

In this work the optimization of APT sample preparation, analysis conditions and reconstruction methodologies for near-surface implanted phosphorus (14 keV  $P^+$  with predicted 0.1 at.% to 0.2 at.% peak concentration at a  $\sim 20$  nm range) in single crystal silicon substrates will be presented.

- [1] Jamieson, D. N., et al., *Applied Physics Letters*, 86 202101 (2005)
- [2] Prosa, T.J., et al., *Ultramicroscopy*, 132 (2013) 179-185

## Session 5b: Lattice defects in bulk materials

### (Invited) Structural characterization of semipolar GaN grown on Si(001)

L Sorokin, A Kalmykov, A Myasoedov, V Bessolov and S Kukushkin

Ioffe Physical Technical Institute of the Russian Academy of Sciences, St Petersburg, Russia

Nowadays freestanding GaN substrates for homoepitaxy are very expensive. That is why foreign wafers such as sapphire and SiC substrates are usually used.

*Silicon wafers* are a low-cost alternative for GaN growth. Today the growth is usually performed on Si(111) plane. On the other hand growth on Si(001) plane has a possibility to integration of GaN-based devices in the well-established Si electronics.

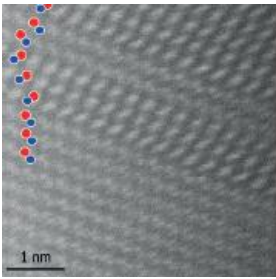
The luminous efficiency of existing LEDs is still low, owing to the presence of electrostatic fields within the active layers. These fields are generated by the spontaneous and piezoelectric polarization along the [0001] axis of hexagonal group-III nitrides. One way of the field reduction is to grow GaN layers on semi-polar planes.

In our work we report on the TEM study of epitaxial growth of thick semi-polar GaN mono-crystalline layer on SiC/Si(001) substrate by HVPE. The 100 nm 3C-SiC buffer layer was formed on off-cut Si(001) substrate using an original solid-phase epitaxy method. GaN growth by HVPE was initiated by deposition of 2  $\mu\text{m}$  AlN buffer layer followed by deposition of thick (about 15  $\mu\text{m}$ ) GaN.

It's revealed that the main structural defects of GaN epitaxial layer are mixed dislocations and basal stacking faults (BSF) bounded by partial dislocations. It will be shown the influence of asymmetry associated with off-cut substrate

on defect structure of GaN epitaxial layer: i) mixed dislocations (Burgers vector  $b=1/3\langle 11-23 \rangle$ ) with line direction inclined at the least angle to the substrate normal constitute the majority of threading dislocations; ii) only small fraction (less than 10%) of BSFs is characterized by fault vector belonging to the plane which is perpendicular to the substrate surface and containing the off-cut direction.

The epitaxial tilting of GaN grown on the Si(001) substrate has been revealed using analysis of selected area electron diffraction patterns and HRTEM images of GaN/AlN interface.



# Microscopy of Semiconducting Materials (MSM-XIX)

## Epitaxial growth of GaN on polycrystalline diamond substrates

R Webster<sup>1</sup>, D Cherns<sup>1</sup>, M Kuball<sup>2</sup>, Q Jiang<sup>2</sup> and D Allsopp<sup>2</sup>

<sup>1</sup>University of Bristol, UK, <sup>2</sup>University of Bath, UK

Diamond is an attractive material for electronic applications as it has one of the highest known thermal conductivity of any material. Using Diamond as a substrate for high electron mobility transistors (HEMTs), or light emitting diodes (LEDs) could improve the lifetime of such devices by allowing them to operate at a lower temperature than they would on conventional substrates such as sapphire or silicon. Single crystal diamond however is expensive so is not currently a realistic substrate to grow on. However, polycrystalline diamond retains a high thermal conductivity, albeit less than single crystal diamond, whilst also being more affordable.

This paper explores the growth of GaN on polycrystalline diamond substrates by MOVPE with an AlN buffer layer. These films grow in (0001) orientation on the substrate with no cracking observed in the GaN or detachment from the substrate, but do, however, have high dislocation densities  $\sim 8 \times 10^9 \text{ cm}^{-2}$ . An epitaxial layer overgrowth (ELOG) technique was used in an attempt to reduce the dislocation densities of these films. This was achieved by depositing silicon nitride stripes on the surface of a deposited GaN layer, and etching the unmasked regions down to the diamond substrate. Growth was then performed on the side walls of the original GaN growth resulting in a massive reduction in dislocation density in the overgrown regions. This paper will further explore the nature and development of the dislocations and grain structure in the GaN in both the original and the ELOG growths.

## STEM optical sectioning for imaging screw displacements in dislocation core structures

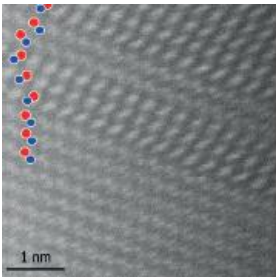
H Yang<sup>1</sup>, J Lozano<sup>1</sup>, T Pennycook<sup>2</sup>, P Hirsch<sup>1</sup> and P Nellist<sup>1</sup>

<sup>1</sup>University of Oxford, UK, <sup>2</sup>University of Vienna, Austria

Aberration corrected (scanning) transmission electron microscopes (STEM) with sub-angstrom resolution have advanced our knowledge of the atomic structure of edge dislocations, which are viewed end-on with the tensile or compressive strain normal to the dislocation being clearly visible. Atomic displacements associated with screw dislocations however cannot be observed in end-on images because the helical screw displacements are parallel to the viewing direction. We show that the helical displacements around a screw can be imaged with the dislocation lying transverse to the electron beam by “optical sectioning” in high-angle annular dark-field (HAADF) imaging in STEM. In optical sectioning the few nanometer depth of focus of aberration corrected microscopes is utilized to extract information along the beam direction by focusing the electron probe at specific depths within the sample.

This novel technique is applied to the study of the c-component in the dissociation reaction of a mixed  $[\mathbf{c}+\mathbf{a}]$  dislocation in GaN. A focal series of experimental images were recorded using a Nion UltraSTEM100 aberration-corrected STEM operating at 100 kV. A  $1 \mu\text{m}$  thick sample of GaN, grown by metalorganic vapour phase epitaxy on a sapphire substrate, was thinned to be viewed along the a-axis. A dislocation was found lying in the plane of the

sample, and characterized using weak-beam imaging to be of a mixed  $[\mathbf{c}+\mathbf{a}]$  type along  $[0001]$ . As the electron beam is focused closer to the dislocation, the shearing of the (0002) planes becomes more localized in the image, and a more detailed observation of the screw displacements shows that the shearing occurs equally along two distinct lines along  $[0001]$ . It is therefore apparent that the screw component of the dislocation has dissociated according to the reaction  $\mathbf{c} = [\frac{1}{2}\mathbf{c} + \frac{1}{2}\mathbf{c}]$  confirming the assumption made in previous end-on observations [1].



# Microscopy of Semiconducting Materials (MSM-XIX)

## Session 5c: Device studies

### (Invited) The microstructure characterization of nitride laser diodes

P Perlin, J Smalc-Koziorowska and L Marona

Institute of High Pressure Physics “Unipress”, Warsaw, Poland

Nitrides laser diodes are challenging structures for growers because in contrast to their arsenide cousins they are built out of the stack of layers of quite dissimilar materials. This mention dissimilarity includes the lattice constant mismatch and huge differences in the optimum growth conditions. The mechanical, biaxial strain combined with susceptibility of the active layer to temperature-induced decomposition may lead to generation of various types of defects. This happens for instance in the case of high-indium content blue and green light laser diodes. The strategies of the epitaxial growth of such structures are designed accordingly to the results of microscopic studies (scanning electron microscopy including cathodoluminescence and tunneling electron microscopy). Within my presentation I will discuss the typical defects observed in blue/green laser diode structures and also the problem of InGaN homogeneity as seen by cathodoluminescence.

Microstructural studies are also an indispensable part of post-degradation characterization. I will show the examples of the use of TEM and SEM techniques for identification of degradation mechanism in the stressed InGaN laser diodes.

### 3D imaging of Si FinFET devices by combined HAADF-STEM and EDS tomography

Y Qiu<sup>1</sup>, P Van Marcke<sup>2</sup>, O Richard<sup>2</sup>, H Bender<sup>2</sup> and W Vandervorst<sup>2</sup>

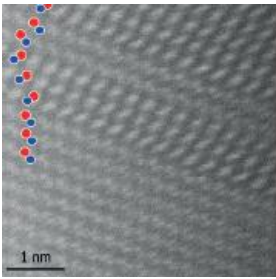
<sup>1</sup>imec, FPS MCA, Belgium <sup>2</sup>IMEC, Belgium

In last few decades electron tomography is intensively studied to investigate the 3D shape of a wide range of nano-scale materials. High angle annular dark-field scanning transmission electron microscopy (HAADF-STEM) tomography attracts also increasing attention to study the morphology of semiconductor nano-devices with dimensions below 10 nm scale. The 3D reconstruction allows to obtain morphological information also along the beam direction which is lost in standard 2D projection images. Recent advances of TEM systems with high brightness field emission gun (FEG) coupled with high count rate energy dispersive X-ray spectrometers opens the possibility to analyze the 3D volume both in imaging and chemical analysis modes.

Samples after different major process steps of FinFET devices are explored: 1) dense Si fins (45 nm pitch) after Si etch, oxide fill and recess and thin epi-Si growth, 2) similar fin structure with poly gate lines across and thicker epi-Si growth, and 3) similar fin structure with replacement metal gate (RMG) lines across. Cylindrical or square-shaped pillar specimens are prepared and deposited on top of either standard TEM grid to maximize the tilt range ( $\pm 80^\circ$ ) or copper post specially designed for  $360^\circ$  tilted holder.

Alignment procedures for images and chemical maps will be discussed. We show that the alignment can be done without marker tracking. Effects of reduced image sets (variation of angular interval or angular ranges limited to major directions of the structures) compared to results with full  $180/360^\circ$  data set are investigated. Shape effects of the pillars are compared.

The reconstructed volume based on HAADF images and EDS maps can bring useful fully interpretable information in composition and morphology and reveals morphological information of the device structures that cannot be deduced from the 2D images.



# Microscopy of Semiconducting Materials (MSM-XIX)

## Multi-microscopy analysis of inhomogeneous electroluminescence in InGaN/GaN quantum well LED structures

C Ren<sup>1</sup>, M Wallace<sup>2</sup>, P Edwards<sup>1</sup>, R Martin<sup>2</sup>, B Rouet-Leduc<sup>1</sup> and R Oliver<sup>1</sup>

<sup>1</sup>University of Cambridge, UK, <sup>2</sup>University of Strathclyde, UK

The most commonly grown type of LED structure, c-plane InGaN/GaN quantum wells (QW), faces many obstacles in terms of optimisation of device performance [1]. A recently reported issue present is an acute inhomogeneity in the electroluminescence, resulting in the appearance of bright spots in the emission over the area of the device [2].

In this study, multi-microscopy has led to the isolation and characterisation of structural features which are believed to cause the inhomogeneities in the electroluminescence of c-plane LEDs.

The LED devices examined consist of an undoped GaN layer grown on a sapphire substrate, followed by n-type GaN, a series of InGaN wells of 4.5 nominal thickness and a 20 nm AlGaIn electron blocking layer (EBL) followed by a p-GaN capping layer.

We have analysed the same inhomogeneities using electroluminescence (EL), cathodoluminescence (CL) and electron beam induced current (EBIC) hyperspectral imaging. Simultaneous scanning electron microscopy (SEM) and CL revealed a hexagonal pit at the centre of the inhomogeneities. By preparing a transmission electron microscope (TEM) lamella from an area of interest using focussed ion beam milling (FIB) and using scanning transmission electron microscopy with a high angle annular dark-field detector (STEM-HAADF) and energy-dispersive X-ray spectroscopy (STEM-EDX) we have identified the presence of aluminium from the EBL in the active region, suggesting this may be the cause of the inhomogeneities.

[1] C.J. Humphreys. (2008) *MRS Bulletin*. 33, 459

[2] Lin *et al.* (2012) *Appl.Phys.Let.* 101, 252103

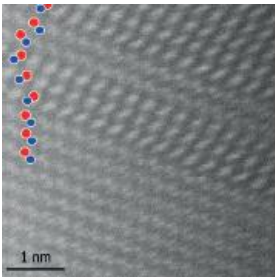
## Spatial inhomogeneities in structural and optical properties of Al<sub>x</sub>Ga<sub>1-x</sub>N quantum wells induced by surface morphology of AlN/sapphire templates

U Zeimer<sup>1</sup>, J Jeschke<sup>1</sup>, A Mogilatenko<sup>1</sup>, A Knauer<sup>1</sup>, V Kueller<sup>1</sup>, V Hoffman<sup>1</sup>, C Kuhn<sup>2</sup>, M Martens<sup>1</sup>, M Kneissl<sup>1</sup> and M Weyers<sup>1</sup>

<sup>1</sup>Ferdinand-Braun-Institut, Leibniz-Institut für Höchstfrequenztechnik, Germany, <sup>2</sup>Technical University Berlin, Germany

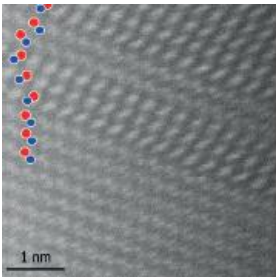
Al<sub>x</sub>Ga<sub>1-x</sub>N quantum wells (QWs) with a high Al content ( $x > 0.6$ ) are required for fabrication of high-efficiency light emitting diodes (LEDs) and laser diodes (LDs) operating in the UV-C spectral range. Structural and optical properties of these QWs are determined by the structural quality of AlN/sapphire templates, i.e the optical properties are strongly degraded by the high threading dislocation densities (TDDs) in the AlN templates. To overcome this problem we applied epitaxial lateral overgrowth (ELO) of patterned sapphire substrates with different offcut directions. ELO AlN layers with a reduced TDD in the range of  $10^8 \text{ cm}^{-2}$  have been obtained. The impact of the surface morphology of AlN/sapphire templates on the structural and optical properties of subsequently grown AlGaIn quantum wells has been investigated. For this study atomic force microscopy, cathodoluminescence (CL) spectroscopy, X-ray diffraction and transmission electron microscopy have been used.

A significant lateral wavelength variation has been observed by CL mapping in the AlGaIn QWs grown on ELO-AlN templates. This wavelength modulation correlates with the macrosteps on the surface of the ELO-AlN. It will be shown, that the Ga adatom diffusion to the surface macrosteps results not only in a local Ga enrichment within the



## Microscopy of Semiconducting Materials (MSM-XIX)

QWs, but also in a spatial variation of the QW thickness. In contrast, the QWs deposited onto planar AlN/sapphire templates with an atomically smooth surface morphology show a more uniform wavelength distribution as well as a homogeneous thickness. Thus, a reduction of step height is required to improve the QW homogeneity. In spite of the inhomogeneity of AlGaIn QWs on ELO-AlN/sapphire, these structures are promising for enhancing the light output of UV-C devices. Laser structures grown on ELO-AlN exhibit laser operation near 240 nm under optical pumping, whereas laser structures grown on planar AlN/templates do not show any laser operation.



# Microscopy of Semiconducting Materials (MSM-XIX)

## Poster Session 1

### P.1.1 - In situ UHVEM study of {113}-defect formation in Si nanowires

J Vanhellemont<sup>1</sup>, S Anada<sup>2</sup>, H Yasuda<sup>3</sup>, H Bender<sup>3</sup>, R Rooyackers<sup>3</sup> and A Vandooren<sup>3</sup>

<sup>1</sup>Ghent University, Belgium, <sup>2</sup>Osaka University, Japan, <sup>3</sup>IMEC, Belgium

High fluxes of electrons with energies above 200 keV can create self-interstitial clusters in thin Si and Ge foils. In TEM, these clusters are observed as so called {113}-defects with {113}-habit planes and elongated along <110>-directions. Previous studies on bulk material showed that dopants, capping layers and local stress fields influence the defect formation kinetics and stability.

Results are presented on in situ {113}-defect formation during UHVEM irradiation of Si nanowires with diameters between 40 and 500 nm. The Si nanowires are part of TFET structures and their top is p<sup>+</sup>-type ( $> 5 \times 10^{19} \text{ B cm}^{-3}$ ) either by epitaxy or by ion implantation. The nanowires are embedded in SiO<sub>2</sub> covered with other capping layers and are etched into a stack consisting of an n<sup>-</sup>-type ( $10^{17} \text{ As cm}^{-3}$ ) epitaxial layer grown on a n<sup>+</sup>-type substrate ( $2 \times 10^{19} \text{ As cm}^{-3}$ ).

The UHVEM of Osaka university is equipped with an ion trap and is using an oil-free vacuum system so that both the e-beam and the vacuum in the specimen chamber (about  $7 \times 10^{-6} \text{ Pa}$ ) are very pure and possible contamination related influences on intrinsic point defect cluster nucleation and growth are reduced to a minimum. This allows in situ study of the formation of self-interstitial clusters while varying the e-beam flux and irradiation temperature over a wide range.

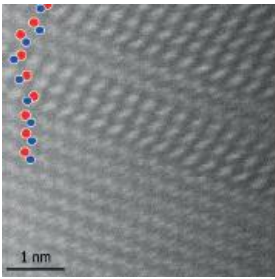
In situ irradiations are performed on cross-section samples with thicknesses ranging from 50 to 400 nm prepared by FIB. Samples are irradiated with different fluxes of 2 MeV electrons at temperatures between room temperature and 375 °C. A strong dependence of {113}-defect formation on nanowire radius and dopant concentration and type is observed as well as on specimen thickness. The observations are compared with simulations based on quasi-chemical reaction rate theory and with results from scanning spreading resistance microscopy and from earlier work on bulk material.

### P.1.2 -Influence of post-growth thermal annealing on InGaAs/GaAs quantum dot structures monolithically grown on silicon

W Lei<sup>1</sup>, S Chen<sup>2</sup>, J Wu<sup>2</sup>, Q Jiang<sup>2</sup>, H Liu<sup>2</sup>, R Hogg<sup>1</sup> and I Ross<sup>1</sup>

<sup>1</sup>University of Sheffield, UK, <sup>2</sup>University College London, UK

Thermal annealing is a widely applied process to tune and enhance the optical properties of photonic devices. In recent years, significant attention has been dedicated to the influence of post-growth rapid thermal annealing (RTA) on InAs/InGaAs quantum dot (QD) structures grown on GaAs substrates however the influence of such treatment on QD's grown monolithically on silicon has been less well documented. Interest in the development of III-V growth on silicon is motivated by the drive to integrate III-V technology with mature silicon processing however it is not without its drawbacks. Complications arise from the high defect density generated in the buffer layers due to the large lattice misfit between III-V compounds and Si and the residual stress induced by the mismatch of the relative thermal expansion coefficients.



# Microscopy of Semiconducting Materials (MSM-XIX)

In this study, we investigate the effect of post-growth RTA between 650-800 °C on the optical and microstructural characteristics of a series of InAs/InGaAs Dot in Well layers grown on a Si (100) substrate with a 4° offcut. Photoluminescence data indicates a significant spectral blue shift in the peak emission above 700 °C attributed to an intermixing effect during the RTA treatment. Subsequently, cross sectional TEM and aberration corrected STEM has been performed for each annealing temperature. The relationship between the microstructure revealed and the spectral response will be discussed.

## P.1.3 - Automated background subtraction for electron energy-loss spectroscopy and application to spectral imaging of semiconductor layers

V C Angadi, T Walther and C Abhayaratne

University of Sheffield, UK

A novel approach for automated background subtraction of core-loss edge is proposed. In conventional methods, prior knowledge of the pre-edge region is inevitable. We exploit the fact that core-loss edge is superimposed on an almost exponentially decaying background. Principle component analysis (PCA) is used to detect clusters of positive slope angle between the spectral points. A moving average filter is adopted to minimise the false positive detection of core-loss edges due to shot noise.

We choose the threshold for the PCA as  $0^\circ$  for the slope angles. The cluster of points is detected by sliding a window across the energy loss axis. If two thirds of the size of the window contain positive slope angle then the window contains a cluster. If a cluster isn't detected then the window slides to next position and the previous step is repeated throughout the spectrum.

Background subtraction by a curve fit through all pre-edge regions is used. The background in the spectrum from zero-loss peak to first core-loss edge is modelled using simple interpolation algorithms like spline. This is to reduce large statistical errors after background subtraction. Small pre-edges regions are selected for all the detected core-loss edges. An inverse power-law is used to fit these pre-edge regions separately, beginning at the higher energy loss edge and progressing to smaller energies. The background fitting of these points is modelled individually. The modelled background is an ensemble of spline fit and an inverse power-law fit. If the background is subtracted from the spectrum we get difference spectra for each individual core-loss edge.

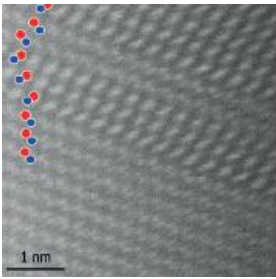
## P.1.4 - Cross-sectional cathodoluminescence investigations of GaN epitaxial grown on Si-based substrates

L Piot<sup>1</sup>, N Mante<sup>1</sup>, N Rochat<sup>1</sup>, G Feuillet<sup>1</sup>, P Vennéguès<sup>2</sup>, F Semond<sup>2</sup> and E Frayssinet<sup>2</sup>

<sup>1</sup>CEA - LETI, France, <sup>2</sup>CRHEA-CNRS, France

Gallium nitride is a widely used material in optoelectronic devices like LEDs. The LED structures are mostly grown by epitaxy onto sapphire substrates, but, for cost reasons, silicon is a possible contender. Nevertheless, the large misfit and the difference in coefficient of thermal expansion between silicon and the nitrides lead to numerous dislocations and possible cracks during cooling down from the growth temperature, both being detrimental for LED applications.

The cathodoluminescence (CL) technique constitutes a fast and highly relevant way to investigate the above material properties. Indeed, besides the distribution of dislocations can be visualized due to their higher rate of non-



# Microscopy of Semiconducting Materials (MSM-XIX)

radiative recombination, emission lines give us an access to several punctual defects identification as well as variation of strain, doping, growth direction and carrier concentrations.

In this work, we performed high spatial resolution cathodoluminescence by hyperspectral imaging on cross section GaN layers obtained through several growth conditions. The cross-sectional imaging gives us an insight into the thickness of the samples and provides direct information on interfaces roles as the growth proceeds. Development of an innovative cryogenic sample holder compatible with both CL and TEM equipment allowed us, by coupling of these techniques, to get a good comparison of different growth processes aiming to improve nitride layers quality for LED applications.

The samples were grown by MOVPE and MBE on Si-based substrate in CRHEA-CNRS. The structural properties were determined from TEM diffraction contrast analysis together with nano-diffraction for strain analysis. The optical properties were assessed by low temperature (down to 10K) cathodoluminescence.

Acknowledgments: this work was supported by the National Research Agency (ANR) through the French "Recherche Technologique de Base" Program. CL experiments were performed in the frame of the joint development program with Attolight and the Nanocharacterisation platform (PFNC) at MINATEC.

## P.1.5 -Facetted growth of Fe<sub>3</sub>Si shells around GaAs nanowires on Si(111)

B Jenichen, M Hilse, J Herfort and A Trampert

PDI, Germany

GaAs nanowires and GaAs/Fe<sub>3</sub>Si core/shell nanowire structures were grown by molecular-beam-epitaxy on oxidized Si(111) substrates and characterized by scanning and transmission electron microscopy (TEM). The surfaces of the original GaAs NWs are completely covered by magnetic Fe<sub>3</sub>Si exhibiting an enhanced surface roughness compared to the bare GaAs NWs, due to formation of nanofacets. Growth of the shells at the substrate temperature of T(S) = 200 °C leads to a regular nanofacetted growth of the Fe<sub>3</sub>Si shell. The resulting facets of the shells were analyzed by combined selected area diffraction and high resolution TEM. Twins are formed at the grain boundaries. The facets lead to thickness inhomogeneities of the shells. They consist mainly of well pronounced Fe<sub>3</sub>Si(111) planes. The crystallographic orientations of core and shell coincide. The nanofacetted Fe<sub>3</sub>Si shells found in the present work are probably the result of the Vollmer-Weber growth mode of Fe<sub>3</sub>Si on the (110) side facets of the GaAs NWs.

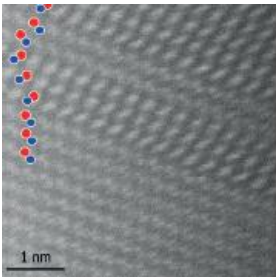
## P.1.6 -A nanoscale cathodoluminescence study of nitride semiconductor nanowires

D Stowe<sup>1</sup>, R Williams<sup>2</sup>, S Carnevale<sup>2</sup>, T Kent<sup>2</sup>, R Myers<sup>2</sup> and D McComb<sup>2</sup>

<sup>1</sup>Gatan UK, UK, <sup>2</sup>Ohio State University, USA

III-nitride semiconductors are an important class of materials being the foundation of energy efficient LED lighting. Currently, state of the art white LEDs are made up of thin films of GaN and InGaN grown on sapphire or silicon substrates. It is known that LED devices based on self-assembled semiconductor nanorods offer many potential benefits including lower costs and increased efficiencies and lifetimes. However, attempts to realize nanorod-based devices have, so far, failed to deliver the expected benefits and there is recognition that much basic science research is still required.

The correlation between a material's luminescence properties and its morphology, microstructure and local chemistry offers great benefit in developing the fundamental understanding of semiconductor nanorods including



# Microscopy of Semiconducting Materials (MSM-XIX)

band gap analysis, identifying defect centers and carrier mobility. This has encouraged a growing interest in performing cathodoluminescence (CL) microscopy at high spatial resolution. Here, we use spectroscopic CL in a (S)TEM to analyze individual and assemblies of III-nitride nanorods and to correlate the micro- or nanoscale luminescence with the nanorod's microstructure. CL experiments in the SEM were performed using the Gatan MonoCL4 system whilst experiments in the STEM were performed using the Gatan Vulcan system.

Test nanowire structures were grown by MBE. HAADF imaging reveals multiple  $(\text{In}_x)\text{Ga}_{1-x}\text{N}/\text{AlN}$  quantum discs (QDs) 30-50nm diameter and 2-3nm thickness separated by 3nm thick AlN barrier. CL hyperspectral imaging using the Gatan Vulcan system was used to measure the luminescence emission from each quantum disc. Analysis of the CL spectra reveal a blue shift in the CL emission energy for QDs <2.6nm thick. This study analyses a variety of nanowire structures to identify how the nanowire morphology and microstructure impacts luminescence quantum efficiency.

## P.1.7 - Epitaxial growth of wurtzite silicon on diamond silicon

Y Qiu<sup>1</sup>, O Richard<sup>2</sup>, H Bender<sup>2</sup>, M S Kim<sup>2</sup>, I Vos<sup>2</sup>, M de Potter<sup>2</sup>, E Van Besien<sup>2</sup>, D Mocuta<sup>2</sup> and W Vandervorst<sup>2</sup>

<sup>1</sup>IMEC FPS MCA, Belgium, <sup>2</sup>IMEC, Belgium

Hexagonal silicon with wurtzite structure (also referred to as diamond-hexagonal Si or Si IV) is a metastable phase that can be formed e.g. during indentation experiments or growth of silicon nanowires. It is recently shown that wurtzite silicon can emit visible and near-infrared light and therefore has potential for application in optoelectronic devices.

In this work a new method to form wurtzite silicon is discussed and the phase is characterized in detail with high resolution scanning transmission electron microscopy and chemical analysis. The growth procedure is based on finFET device processing for sub 14 nanometer technology. After the etch step of the fins the spacings are filled with  $\text{SiO}_2$ . By applying the appropriate conditions during the subsequent low temperature anneal hexagonal, silicon can form at the base of the fins. The phase transition generally results in an outward shift of the fin which however maintains its crystal alignment relative to the substrate. The hexagonal silicon is stable during further high temperature processing.

The hexagonal wurtzite silicon slabs observed are 5-8 nm thick and generally extend over the full width and length of the fins. The hexagonal phase grows epitaxially on the (001) Si mainly with (001)- diamond cubic (dc)-Si and (115)-dc-Si interfaces. The phase and interface characterization and formation mechanism leading to this phase transition will be discussed in detail.

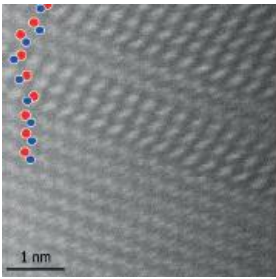
## P.1.8 - CL investigation of ZnO nanorods grown by ultra-fast hydrothermal process

B Witkowski, L Wachnicki, S Gieraltowska, A Reszka, A Pieniazek, B Kowalski and M Godlewski

Institute of Physics PAS, Poland

Zinc oxide is a II-VI semiconductor material that focused a growing interest in various fields such as biology, medicine or electronics. This semiconductor reveals very special physical and optical properties, which imply many applications including a transparent electrode in solar cells or LED diodes.

In this work we present results of cathodoluminescence (CL) investigations of high quality zinc oxide nanorods obtained by extremely fast hydrothermal method (developed in Institute of Physics PAS) on silicon substrate.



# Microscopy of Semiconducting Materials (MSM-XIX)

Scanning Electron Microscopy (SEM) system equipped with CL allows direct comparison of SEM images and CL maps, taken from exactly the same areas of samples. Investigations are performed at a temperature of 5K. An inter-link between samples microstructure and emission properties is investigated. We also present comparison of optical properties between ZnO nanorods and ZnO layers grown by Atomic Layer Deposition. CL confirms a very high quality of ZnO nanorods produced by our method.

In addition, the CL intensity collected from single isolated nanorod is orders of magnitude lower than for one excited nanorod inside nanorods array. We believe this is an evidence for presence of super radiation effects in ZnO nanorods arrays. Detail information about experiments will be presented.

The research was financially supported by the National Science Centre through grant (DEC-2012/07/N/ST3/03144).

## P.1.9 - Quantitative characterization of composition and interface roughness of (GaIn)As quantum wells

H Han, A Beyer, K I Gries, W Stolz and K Volz

Philipps University Marburg, Germany

The physical properties of semiconductors, like (GaIn)As, are significantly influenced by the chemical composition and the interface morphology. In the present work, high angle annular dark field (HAADF) imaging in scanning transmission electron microscopy (STEM), in combination with STEMsim simulation, is used to estimate both at atomic resolution. To obtain the composition information, a quantitative way to measure the TEM sample thickness is also in need.

The (GaIn)As quantum wells were grown with metal organic vapor phase epitaxy (MOVPE) on GaAs (001) substrate at temperatures of 525 °C and 625 °C with different growth interruption times (0s, 20s, 40s, 120s) on the quantum well to modify the interface morphology. High resolution HAADF STEM images were obtained in a double-aberration-corrected JEOL 2200 FS. The thickness of the TEM samples was derived from the intensity maps of the group V atomic columns, where no alloying takes place. Afterwards, quantitative evaluation of the group III atomic column contrast was possible by comparing experiment with simulation. The composition maps show that the chemical composition distribution across the quantum well is not completely homogeneous and that there are nanoscale composition fluctuations by almost a factor of two. Besides, the growth temperature of the quantum well can greatly influence the composition fluctuations and the interface morphology, whereas the growth interruptions only exert minor effects on that the interface morphology.

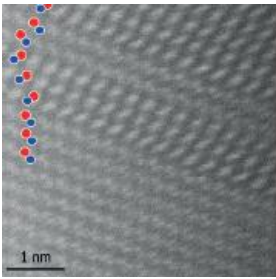
The present contribution will correlate quantitative information on composition homogeneity and interface morphology of (GaIn)As quantum wells derived from STEM to MOVPE growth conditions.

## P.1.10 - Morphological and Compositional STEM Analysis of Organic-Inorganic Hybrid Perovskites

F Wisnivesky Rocca Rivarola, G Divitini and C Ducati

University of Cambridge, UK

Recent advances in photovoltaic devices and light emitting diodes (LEDs) have focused in developing materials that are cost effective and that provide high efficiencies while being easily processable. Devices based on hybrid organic-inorganic materials have attracted a lot of interest in recent years, and special attention has been given to an emerging generation of hybrid organic-inorganic halide perovskite materials. Perovskite-based solar cells and LEDs offer promising prospects both in terms of their low processing cost and of their increasingly high conversion



# Microscopy of Semiconducting Materials (MSM-XIX)

efficiency, which can be tuned by tailoring the composition of the perovskite and the structure of the device. The morphology of the hybrid material as well as the deposition techniques used are known to affect the electrical properties of these devices, however a more detailed understanding of their direct effects on the charge transport is still lacking.

This work studied the morphology of hybrid organic-inorganic semiconductors using complementary microscopy and analytical microscopy techniques to characterise the chemical composition and morphology of hybrid organic-inorganic halide perovskites.

The samples analysed were probed by combining scanning transmission electron microscopy (STEM) and analytical spectroscopy techniques with focused ion beam (FIB) milling for preparation of cross-sectional specimens. This approach revealed the structure of the different components at length scales of 1-100 nm. Furthermore, the effect of temperature on the perovskite layer's morphology and composition is currently being investigated, and correlated with the expected working mechanisms of the photovoltaic device.

## P.1.11 - Construction and test of an annular aperture for novel Z-contrast imaging

T Mehrtens, T Händel, K Müller and A Rosenauer

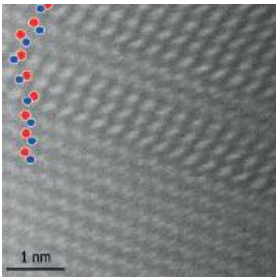
University of Bremen, Germany

In this study, annular apertures for transmission electron microscopy (TEM) are fabricated by focused ion beam (FIB). These apertures are inserted into the back focal plane of the objective lens and work as a central beam stop [1,2]. Thus, only electrons scattered into higher angles contribute to the image formation and the influence of Bragg-scattering is strongly reduced. Therefore, the main part of the image intensity stems from thermal diffuse scattering and contrast in annular dark-field TEM (ADF-TEM) images strongly depends on the chemical composition of the specimen, which is similar to the "Z-Contrast" in high-angle annular dark-field scanning TEM (HAADF-STEM).

The two fabricated apertures tested in this study differ by their geometry (inner radius and width of the annulus). The influence of these parameters on the resulting ADF-TEM images was studied for sphalerite GaAs/InGaAs and wurtzite GaN/InGaN. For the aperture with the higher inner radius (43.9mrad) a well pronounced Z-Contrast was found, while for the second aperture (inner radius of 16.6mrad) the contrast was dominated by Bragg-scattering for a specimen orientation close to zone-axis. Nevertheless, tilting away from zone-axis also resulted in a more pronounced Z-Contrast.

Furthermore, for GaN/InGaN the experimental data were compared to multislice simulations in the Frozen Lattice approach. The simulations were carried out with the STEMsim program [3]. Qualitatively the dependence of contrast on the aperture parameters and the chemical composition (indium concentration) could be reproduced.

- [1] S. Bals et al., Sol. Stat. Com. 130 (2004), pp. 675-680
- [2] S. Bals et al., Ultramicroscopy 104 (2005), pp. 281-289
- [3] A. Rosenauer and M. Schowalter, Springer Netherlands (2008)



# Microscopy of Semiconducting Materials (MSM-XIX)

## P.1.12 - Analysis of Sb and In distribution in GaAsSb-capped InAs quantum dots by advance transmission electron microscopy

D Fernández<sup>1</sup>, J M Ulloa<sup>2</sup>, A Guzman<sup>2</sup>, A Hierro<sup>2</sup>, D L Sales<sup>1</sup>, R Beanland<sup>3</sup>, A M Sanchez<sup>3</sup> and D Gonzalez<sup>1</sup>

<sup>1</sup>Universidad de Cádiz, Spain, <sup>2</sup>Institute for Systems based on Optoelectronics and Microtechnology, Spain,

<sup>3</sup>University of Warwick, UK

A promising alternative to design semiconductor laser devices in the near infrared is the use of GaAsSb strain reduction layers (SRL) over InAs quantum dots (QDs). However, the incorporation of high Sb contents has been less explored due to the resulting indirect radiative transitions (type-II), where holes are located outside the QD. Nevertheless, type-II QD lasers might have advantages, such as wavelength, gain tunability and a reduced threshold current due to the possible inhibition of spontaneous emission and Auger recombination. However, the spatial separation of electrons and holes also produces a reduction of emission efficiency. Thus, the resulting optical properties are sensitive to the exact potential distribution, and consequently to the local QD-SRL structure. Therefore, determination of the atomic distribution is essential to fully exploit their advantages in device applications.

The present work analyses the effect of rapid thermal annealing (RTA) on InAs-QDs embedded in a GaAsSb-SRL grown by molecular beam epitaxy, and studied by advanced transmission electron microscopy (TEM) and photoluminescence techniques. In particular, atomic-scale distribution and the strain-state of the nanostructures were obtained using high resolution aberration-corrected scanning-TEM (HRSTEM) and conventional HRTEM.

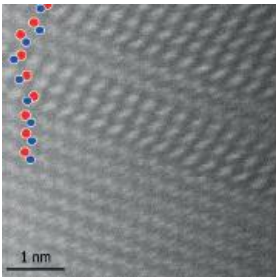
The photoluminescence efficiency was greatly enhanced by RTA, preserving the type-II emission, and showing a better luminescence than the type-I reference. The integrated intensities and strain analysis from HRSTEM and HRTEM images reveal the preservation of Sb content in the SRL far from QDs after annealing, while it is not the case around the QDs. Then, RTA activates both Sb segregation over the QDs as well as the In-Ga intermixing between QDs and SRL, changing the size of QDs and reducing the In content. All this leads to an accumulation of In and Sb over the QD. The huge changes in the atomic distribution around the QDs by RTA and its effect on the photoluminescence are discussed.

## P.1.13- Composition analysis in SEM and STEM

M Falke

Bruker Nano GmbH, Germany

Successful design and development of nanoscale semiconductor structures requires suitable quantitative analysis methods. Electron microscopy combined with spectroscopy techniques, such as energy dispersive X-ray spectroscopy (EDS) is one option to characterize material compositions with spatial resolution ranging from the mm to the atomic scale. Using standard EDS in an aberration corrected cold FEG transmission electron microscope even the identification of single Si and Pt atoms on graphene is possible [1]. The smaller the scale, the more complex become sample preparation and instrumentation issues though. It is worth facing those, because modern silicon drift detector EDS offers high solid angles for signal detection at good take-off angles not just in STEM but also in SEM. The resulting highly sensitive and fast EDS data acquisition can be used for the nanoscale but also for beam sensitive samples or 3D analysis. Additionally, EDS can be combined with other complementary analysis techniques used in electron microscopy, such as EBSD and X-ray fluorescence (micro-XRF) in case of bulk samples and EELS, quantitative imaging and Kikuchi diffraction in transmission. Micro-XRF offers the detection of trace



# Microscopy of Semiconducting Materials (MSM-XIX)

elements and the analysis at higher penetration depth than EDS. Diffraction techniques allow crystallographic characterization.

In this contribution, examples of spatially resolved chemical composition analysis of various semiconductor structures will be shown. Those include the comparative micro-XRF and EDS characterization of semiconductor devices in SEM, quantitative EDS of layered CMOS structures in SEM and TEM-EDS of silicon-silicide interfaces and III-V-based thin films, quantum wells and nanowires.

Furthermore, we discuss advantages and drawbacks of the Cliff-Lorimer and Zeta-factor methods as options for quantitative TEM-EDS analysis of light and heavy element mixtures, for which absorption effects are relevant.

[1] T. C. Lovejoy et al., Appl. Phys. Lett. 100, 154101 (2012)

## P.1.14 -Structural properties of Si Nanowires

M J Lo Faro<sup>1</sup>, C D'Andrea<sup>2</sup>, B Fazio<sup>1</sup>, G Franzò<sup>2</sup>, F Iacona<sup>2</sup>, P Musumeci<sup>2</sup>, F Priolo<sup>2</sup> and A Irrera<sup>1</sup>

<sup>1</sup>IPCF CNR Messina, Italy, <sup>2</sup>Matis IMM CNR Catania, Italy

Silicon Nanowires (Si NWs) are playing a leading/key role in the development of new and innovative Si technology, attracting the interest of the research community. In this work we propose a cheap and maskless method for the synthesis of Si NWs based on chemical etching assisted by the presence of thin discontinuous metal layer, realized by electron beam evaporation. We performed a detailed study on the dependence of mean radius of NWs from the morphology and the type of the metallic layer, we are able to vary the radii of NWs as desired in the range of few nanometers. We report and discuss the structural properties of the metallic layer and its influence on the NWs characteristics. Thus with this method we can synthesize ultrathin Si NWs that emit light at room temperature due to quantum confinement effect. Moreover this technique guarantees a high control on the doping of Si NWs determined by the starting Si substrate and we can also vary the length of the wires from a few hundreds of nanometers to tens of microns. Besides this method allows to realize a high density array of vertically aligned Si NWs that has interesting optical properties, such as light trapping. This technique can realize with good reproducibility a forest of Si NWs with a controlled and periodic structure that shows raman enhancement phenomena. This template Si NWs forest is also a promising material for further applications, such as photovoltaics and sensing.

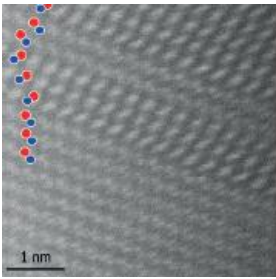
## P.1.15 - Strained heterostructures in III-Nitride nanowires

T Karakostas<sup>1</sup>, T Pavloudis<sup>1</sup>, T Koukoulas<sup>1</sup>, J Kioseoglou, T H Karakostas<sup>1</sup>, T H Kehagias<sup>1</sup>, C D Latham<sup>2</sup>, P R Briddon<sup>3</sup>, M J Rayson<sup>2</sup>, M Eickhoff<sup>4</sup> and P H Komninou<sup>1</sup>

<sup>1</sup>Aristotle University of Thessaloniki, Greece, <sup>2</sup>University of Surrey, UK, <sup>3</sup>University of Newcastle upon Tyne, UK,

<sup>4</sup>Justus-Liebig-University Giessen, Germany

III-Nitride Nanowires (NWs) consisting of a GaN base part incorporate usually a superlattice part of successive thin  $\text{In}_x\text{Ga}_{1-x}\text{N}/\text{GaN}$  strained heterostructures with the  $\text{InGaN}$  being in the form of nanodiscs (NDs) or embedded dot like structures. In this work we report on the structure and the effect of strain on their energetics and their electronic properties. The structure and the strain state of the heterostructures are investigated by quantitative high resolution transmission electron microscopy using Geometric Phase Analysis and the corresponding models are built and simulated using Molecular Dynamics and Density Functional Theory calculations. Three possible types of strain, i.e. biaxial, hydrostatic and uniaxial, are considered and the energetics and electronic properties of the modeled



# Microscopy of Semiconducting Materials (MSM-XIX)

structures are compared. For homogeneous composition of the ternary alloys, the biaxial strained model is attributed to the  $\text{In}_x\text{Ga}_{1-x}\text{N}/\text{GaN}$  NDs superlattice while the hydrostatic model can be attributed to the dot-like  $\text{In}_x\text{Ga}_{1-x}\text{N}/\text{GaN}$ . Concerning the optoelectronic properties of such strained nanostructures, independent of the In content up to  $x=0.25$ , they do not induce states in the bandgap of the NWs.

Acknowledgment: Work supported by EC under the FP7 STREP Project “DOTSENSE” (Grant Agreement 224212)

## P.1.16 - Alloying variations in self-assembled InAs/GaAs (211)B quantum dot heterostructures

N Florini<sup>1</sup>, J Kioseoglou<sup>1</sup>, G P Dimitrakopoulos<sup>1</sup>, S Germanis<sup>2</sup>, Z Hatzopoulos<sup>2</sup>, N T Pelekanos<sup>2</sup> and T H Kehagias<sup>1</sup>

<sup>1</sup>Aristotle University of Thessaloniki, Greece, <sup>2</sup>University of Crete and IESL/FORTH, Greece

InAs quantum dots (QDs) single photon sources are of particular interest since they can provide optical stability and at the same time high efficiency emissions. Additionally, using a high index substrate, increased control over the spatial ordering of QDs at room temperature can be achieved, due to the piezoelectric effect.

InAs QDs were spontaneously grown by molecular beam epitaxy (MBE) on GaAs (211)B substrate and subsequently were buried under a GaAs layer. Nanostructural analysis was performed by high-resolution transmission electron microscopy (HRTEM). InAs QDs tend to acquire an anisotropic pyramidal shape, elongated along the  $\langle 111 \rangle$  direction, while their length and height ranged from 5 to 10 nm and from 3 to 4 nm, respectively. Geometrical phase analysis (GPA) was used to investigate the strain state of the InAs QDs, along both the in-plane and growth directions. The strain analysis showed a full in-plane registration of the two lattices and in the absence of any dislocations associated with the QDs a fully strained heterostructure is anticipated. However, along the growth direction an anisotropic allocation of strain inside the various QDs was observed, with lattice strain values ranging from 14% to 5%, using the GaAs lattice as reference. Assuming the biaxial formulation and the validity of Vegard's law, these values correspond to QDs of different alloying, from pure InAs to a variety of ternary InGaAs alloys. The observed tendency of a gradual increase of the In content towards the apex of the QDs, implies that Ga segregation mainly occurred in the initial stages of QD growth.

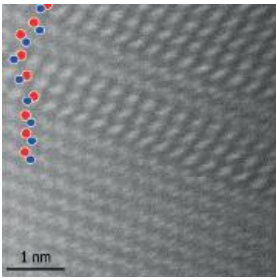
Acknowledgement: research co-financed by the European Union (European Social Fund-ESF) and Greek national funds - Research Funding Program: THALES, project NANOPHOS.

## P.1.17 - Nanostructure and strain properties of core-shell GaAs/AlGaAs nanowires

P Komninou<sup>1</sup>, T H Kehagias<sup>1</sup>, N Florini<sup>1</sup>, J Kioseoglou<sup>1</sup>, T H Pavludis<sup>1</sup>, P H Komninou<sup>1</sup>, T Walther<sup>2</sup>, K Moratis<sup>3</sup>, Z Hatzopoulos<sup>3</sup> and N T Pelekanos<sup>3</sup>

<sup>1</sup>Aristotle University of Thessaloniki, Greece, <sup>2</sup>University of Sheffield, UK, <sup>3</sup>University of Crete and IESL/FORTH, Greece

III-V compound semiconductors based solar cells present high efficiencies, due to their increased light absorption and charge mobility. Integrating the photovoltaic properties of III-V semiconductors into one-dimensional nanostructures such as nanowires (NWs), further enhancement of the efficiency is anticipated, due to their high surface-to-volume ratio and defect-free crystal structure. Furthermore, in NWs with a core-shell configuration, owing to the vertical heterointerfaces, light absorption is separated from carrier collection pathways and hence, excellent optical quality and longer carrier lifetimes can be achieved.



# Microscopy of Semiconducting Materials (MSM-XIX)

GaAs/AlGaAs core-shell NWs were grown on Si (111) by molecular beam epitaxy (MBE) via the vapour-liquid-solid mechanism, using Ga as catalyst. Their nanostructure was explored by high-resolution and scanning transmission electron microscopy (HRTEM-STEM). NWs are zinc-blende (ZB) single crystals that emerge directly from the Si surface despite the presence of the amorphous native oxide. Then, NW growth advances by a continuous sequence of (111) mirror twins. Wurtzite structure NW pockets are occasionally observed within the ZB overall structure. Diffraction contrast TEM and annular dark-field (ADF) STEM imaging revealed the core-shell structure, showing that the AlGaAs shell occupies at least half of the projected diameter (80 nm to 200 nm) of the NWs. The Al content of the shell was estimated at ~35% by energy dispersive X-ray (EDX) analysis. Moreover, molecular dynamics (MD) simulations of plan-view NW slices were applied to calculate the variation of the energy, the stress tensors, the displacement field and the strain components of the core-shell heterostructure.

Acknowledgement: research co-financed by the European Union (European Social Fund-ESF) and Greek national funds - Research Funding Program: ARISTEIA II, project NILES.

## P.1.18 -Local optical properties of GaN/Al<sub>x</sub>Ga<sub>1-x</sub>N nanowires studied by cathodoluminescence

A Reszka<sup>1</sup>, U Zeimer<sup>2</sup>, U Jahn<sup>3</sup>, KP Korona<sup>4</sup>, A Pieniżek<sup>1</sup>, M Sobanska<sup>1</sup>, K Klošek<sup>1</sup>, G Tchutchulashvili<sup>1</sup>, Z R Zytkiewicz<sup>1</sup> and B J Kowalski<sup>1</sup>

<sup>1</sup>Polish Academy of Science, Poland, <sup>2</sup>Ferdinand-Braun-Institut, Germany, <sup>3</sup>Paul Drude Institut für Festkörperelektronik, Germany, <sup>4</sup>Warsaw University, Poland

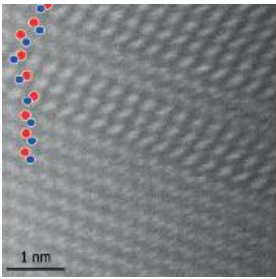
In this work we present the nano-scale correlation of morphology, structural and optical properties of GaN/Al<sub>x</sub>Ga<sub>1-x</sub>N based nanowires with the use of scanning electron microscopy and cathodoluminescence spectroscopy (CL).

III-N family nanowires (NWs) grown on Si substrates have attracted a lot of attention due to their promising applications in optoelectronic nano-devices. Their main advantage over planar layers is high surface-to-volume ratio. Small contact area of GaN with Si substrate allows easy elastic accommodation of misfit strain and reduction of related extended defects.

GaN nanowires (~1 μm long) with AlN and Al<sub>x</sub>Ga<sub>1-x</sub>N insets were grown on *in-situ* nitridized Si(111) substrates without catalyst by plasma-assisted molecular-beam epitaxy. Aluminium content within Al<sub>x</sub>Ga<sub>1-x</sub>N inset as well as the thickness of the inset was varied in subsequent samples. CL measurements were performed at room and low temperatures. CL spectra and maps were recorded for NW ensembles as well for individual NWs dispersed onto silicon substrates.

For the NW ensembles, an ultra violet region of the spectrum was analysed. At temperature of 5 K, the NWs spectrum consists of donor-bound-exciton in GaN peak (3.47 eV) with surface-related luminescence shoulder (3.45 eV), ultra-violet-luminescence band (with the maximum at 3.28 eV) (UVL) and near band-gap emission from Al<sub>x</sub>Ga<sub>1-x</sub>N insets. UVL contribution increases with the increase of Al content in the inset.

Individual NW spectra exhibit the strong blueshifted excitonic emission (3.51-3.54 eV), only in the region below the GaN-AlN/Al<sub>x</sub>Ga<sub>1-x</sub>N interface without detectable evidence of 3.47 eV emission present in NW ensembles spectra. The blue-shifted emission can be related to compressive strain existing on the GaN base/inset interface and in the part of the GaN base of the NW unintentionally overgrown by AlN/Al<sub>x</sub>Ga<sub>1-x</sub>N shell. Spectral features characteristic of ensembles and individual NWs, as well as the differences between them are discussed.



# Microscopy of Semiconducting Materials (MSM-XIX)

## P.1.19 - Green luminescence band in ZnO microrods – a cathodoluminescence study

A Pieniążek<sup>1</sup>, B S Witkowski<sup>1</sup>, A Reszka<sup>1</sup>, Ł Wachnicki<sup>1</sup>, S Gierałtowska<sup>1</sup>, G Godlewski<sup>1,2</sup> and B K Kowalski<sup>1</sup>

<sup>1</sup>Polish Academy of Science, Poland, <sup>2</sup>Cardinal S. Wyszyński University, Poland

ZnO nanostructures are considered as an effective light emitting medium acting simultaneously as an ensemble of optical resonators with the Fabry-Perot (FP) and whispering gallery (WG) modes.

The light emission properties of ZnO microrods with hexagonal cross-section prepared by a microwave hydrothermal method were investigated by spatially resolved cathodoluminescence (CL). The measurements were performed at the liquid-helium temperature.

The CL spectra of ZnO microrods are dominated by an emission band at 2.2 eV, called the green band (GB). This band includes a fine structure, which consists of separated peaks, repeated with energy spacing varying from 39 meV at the high energy side of the spectra to 65 meV at the low energy side. The monochromatic CL maps of GB showed green luminescence locally concentrated near the facets of the hexagonal microstructures.

The shape of the emission spectra and luminescence inhomogeneity in ZnO microrods could be related to the FP or the WG modes. We analyzed the mode spacing using classical plane wave model. The calculated spacing for WG modes changes in the range of spectra from 120 meV to 171 meV. For FP modes the calculated mode spacing is from 65 meV to 81 meV, which is in better agreement with the experimentally observed mode spacing than in the case of WG modes [1].

An alternative explanation based on a vibronic model of transitions from shallow donor to deep acceptor [2] would lead to a broad emission band with the series of possible D-A transitions with the same periodicity (close to the longitudinal optical phonon energy of ZnO).

[1] S. Choi et al., Applied Physics Letters, 103, 171102 (2013)

[2] D. C. Reynolds et al., Journal of Applied Physics, 89, 6189 (2001).

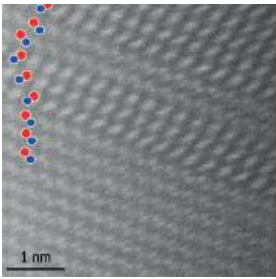
## P.1.20 - Polarity-driven compositional segregation in core-shell GaAsP nanowires

A M Sanchez<sup>1</sup>, Y Zhang<sup>2</sup>, J Wu<sup>2</sup>, R Beanland<sup>3</sup>, T Ward<sup>3</sup> and H Liu<sup>2</sup>

<sup>1</sup>University of Warwick, UK, <sup>2</sup>University College London, UK, <sup>3</sup>University of Warwick, UK

GaAsP semiconductor nanowires provide large composition tenability and have potential as materials for water splitting and solar energy conversion. The lack of lateral constraints on a nanowire far from the substrate allows it to readily adopt a dislocation-free unstrained lattice parameter. Additionally, radial-core shell geometries open new possibilities for band structure engineering.

Our research is based on self-catalysed GaAsP core-shell nanowires to create a p-n nanodiode that greatly enhances light absorption and charge-separation efficiency[1] while suppressing carrier recombination and enhancing charge transport. GaAsP NWs were grown on Be-doped silicon (111) substrates with a thin layer of native oxide by a solid-source MBE. The core NWs were grown by Ga-catalyzed vapor-liquid-solid (VLS) growth [2]. Subsequent shell growth was carried out by reopening the Ga flux at the substrate temperatures between 460 and 470 °C, resulting in hexagonal [111] NWs with {110} side facets and a diameter of 100-300nm. Focused ion beam lift-out was employed to prepare cross-section specimens that were subsequently examined using transmission electron microscopy.



# Microscopy of Semiconducting Materials (MSM-XIX)

The NWs showed compositional phase segregation in the GaAsP shell, in the form of phosphorus-rich sheets on radial {110} planes with a quasi-3-fold symmetry. The alternating arrangement of six P-rich bands (with higher and lower P content) is polarity-driven. This phenomenon is explained by the chemical potential at small {112} facets between the {110} faces that drives As adatoms away more efficiently than P adatoms in combination with a difference in adatom bonding energy at {112}A and B facets. The three bands with higher P content are along  $\langle 112 \rangle_A$  directions and those with a lower P content are along  $\langle 112 \rangle_B$ . [3]

- [1] Lauhon, L. J. et al. *Nature* 2002, 420, 57.
- [2] Wagner, R. S. et al. *Appl. Phys. Lett.* 1964, 4, 89
- [3] Zhang, Y. et al. *Nano Letters* 2015 (submitted)

## P.1.21 - Approaches for quantifying X-ray spectra from thick semiconductor specimens in a transmission electron microscope

T Walther

University of Sheffield, UK

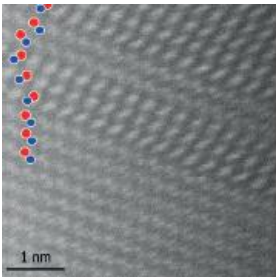
Energy-dispersive X-ray spectroscopy is a routine method to perform local chemical analysis of cross-sectioned samples in a transmission electron microscope. For thin specimens, absorption and fluorescence effects may be ignored and the standard Cliff-Lorimer k-factor approach can be used to determine the chemical composition in cross-section. This raises two questions:

1. When can a specimen be considered sufficiently thin?
2. Will surface effects influence the results for very thin specimens?

The answer to question 1 will depend on the accuracy needed, which itself may be difficult to estimate. The answer to question 2 is obvious for semiconductors which tend to oxidise rapidly on the surface.

For thicker specimens, the thin film approach does no longer work, and quantification typically relies on a number of approximations to model absorption and fluorescence.

Here, theoretical and experimental results from elemental (SiGe) and compound (InGaAs) semiconductor specimens are compared, and a self-consistent scheme is described whereby a thickness-dependent, effective k-factor can be directly determined from the K/L intensity ratio of at least one of the constituting elements. This makes thickness or density estimates for absorption and fluorescence correction no longer necessary and provides a self-calibrating quantification that is consistent for K and L lines.



# Microscopy of Semiconducting Materials (MSM-XIX)

## Poster Session 2

### P.2.1 - Homogeneity and composition of MOVPE-grown AlInGaN: A multiprobe nanostructure study

F F Krause<sup>1</sup>, M Schowalter<sup>1</sup>, J-P Ahl<sup>2</sup>, J Hertkorn<sup>2</sup>, R Egoavil<sup>3</sup>, D Tytko<sup>4</sup>, P-P Choi<sup>4</sup>, T Mehrtens<sup>1</sup>, K Müller<sup>1</sup>, D Raabe<sup>4</sup>, J Verbeeck<sup>3</sup>, K Engl<sup>2</sup>, and R Andreas<sup>1</sup>

<sup>1</sup>Institut für Festkörperphysik, Universität Bremen, Germany, <sup>2</sup>OSRAM Opto Semiconductors GmbH, Germany, <sup>3</sup>EMAT, Univeriteit Antwerpen, Belgium, <sup>4</sup>Max-Planck-Institut für Eisenforschung GmbH, Germany

The material system of quaternary AlInGaN has recently attracted attention for the construction of electronic and optoelectronic devices, benefiting from its additional compositional degree of freedom opposed to ternary materials. Electronic properties of AlInGaN-devices significantly depend not only on the composition but also on the homogeneity of the alloy. The identification or exclusion of compositional fluctuations is hence of large interest, especially as indium-rich clusters have been reported for this system [Phys. Rev. B **70**, 073202 (2004)].

A comprehensive multiprobe study of homogeneity and composition is presented. Five AlInGaN layers with indium concentrations from 0 to 17 at.% and aluminum concentrations between 0 and 39 at.% grown by metal-organic vapor phase epitaxy (MOVPE) were investigated. Energy dispersive X-ray spectroscopy (EDX), high-angle annular dark field scanning transmission electron microscopy (HAADF STEM) and atom probe tomography (APT) were employed. EDX mappings reveal distributions of local concentrations which are in good agreement with random atomic distributions. This is further investigated with HAADF STEM by quantifying the agreement of measured intensities and frozen-lattice multislice simulations of an ideal random alloy employing various statistical tests. By comparison to additional simulations for the case of indium-rich clusters with nanometer dimensions the power of these tests is validated. The investigated samples are found to be fully homogeneous on this scale with high significance. Statistical analyses of APT reconstructions, whose power is demonstrated with a sample containing known composition fluctuations, support these results. A broadening of the AlInGaN emission peak observed in photoluminescence spectroscopy (PL) thus can be attributed solely to random alloy fluctuations.

Though HAADF STEM evaluation only allows for reduction of possible combinations of indium and aluminum concentrations to proximity of isolines in the two-dimensional composition space, the found ranges of composition are in good agreement with the EDX and APT results within the respective precisions.

### P.2.2 - 3D investigation of gallium containing structures within silicon

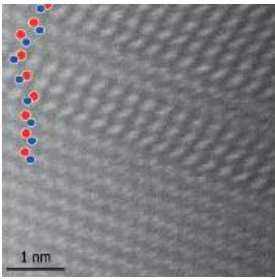
K Gries, K Werner, A Beyer, W Stolz and K Volz

Philipps-Universität Marburg, Germany

To get deeper insight into composition and shape of nanostructures not just the investigation of cross sectional samples but also of plan-view samples as well as the creation of electron tomographic data is of great importance.

In our work Ga deposited on Si (001) substrates via metalorganic chemical vapor phase deposition (MOCVD) was analyzed to obtain information on the fundamentals of the growth process.

Scanning transmission electron microscopic (STEM) investigations in combination with energy dispersive X-ray (EDX) spectroscopy of cross sectional samples revealed gallium containing structures reaching into the silicon [1].



# Microscopy of Semiconducting Materials (MSM-XIX)

These structures seem to exhibit a pyramidal structure forming facets on the Si {111} planes. To receive more knowledge on the three-dimensional shape of these gallium containing structures, electron tomography measurements of cross sectional samples have been performed. In addition plan-view samples have been analyzed. However the conventional plan-view sample preparation including mechanical grinding followed by ion polishing is not suitable for this material since the gallium containing structures are sensitive to chemicals normally used during these preparation steps. For this reason focused ion beam (FIB) samples based on the H-bar method [2] have been created avoiding any treatment with chemicals.

By means of this preparation procedure and in combination with the electron tomographic data the pyramidal shape of the gallium containing structures could be confirmed.

- [1] K. Werner et al., Journal of Crystal Growth 405 (2014) 102
- [2] K. J. O'Shea et al., Micron 66 (2014) 9

## P.2.3 - InGaN/GaN multiple quantum wells grown on *m*-plane bulk GaN

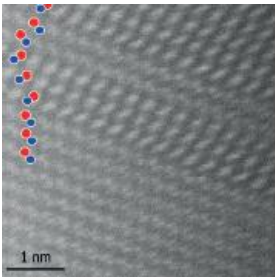
F Tang, T Zhu, J Barnard, F Oehler, J Griffiths, M Kappers, R Oliver, T Martin, P Bagot and M Moody

<sup>1</sup>University of Cambridge, UK, <sup>2</sup>University of Oxford, UK

Non-polar *m*-plane InGaN/GaN quantum well (QW) structures grown on bulk GaN substrates are of great interest, despite the high costs of these native substrates, because non-polar *m*-plane QW structure has the potential of achieving high internal quantum efficiency compared to its *c*-plane counterpart. In addition, the epitaxial growth on bulk GaN results in QW structures with low densities of threading dislocations (TDs) and basal-plane stacking faults (BSFs), both of which could reduce the radiative recombination efficiency.

We have studied the microstructure and indium distribution of a structure containing five  $\text{In}_x\text{Ga}_{1-x}\text{N}/\text{GaN}$  QWs grown on ammonothermal bulk *m*-plane GaN with a  $2^\circ$  misorientation towards [000-1]. The sample was grown by metal-organic vapor-phase epitaxy, and has an indium content  $x \approx 25\%$ . Step bunches were observed at the surface, accommodating the global miscut of substrate. Correlated scanning electron microscopy - cathodoluminescence (SEM-CL) and transmission electron microscopy analysis has revealed that nano-steps have a longer emission wavelength than the surrounding materials.  $I_1$ -type BSFs were occasionally identified on the main *m*-plane facets, while the large nano-steps are frequently associated with BSFs, and BSF arrays are sometimes observed. High-

angle annular dark-field imaging and energy dispersive x-ray spectroscopy shows that the InGaN active layers deposited on the large inclined steps have higher In contents than those on the adjacent *m*-plane facets. The sample displays not only a longer emission wavelength but also a significantly wider full width at half maximum (FWHM) of the CL spectrum in contrast to another sample with  $\sim 15\%$  In content grown using the same method. Atom probe tomography showed a non-random In distribution in the QWs with 25% indium, but a random distribution in the QWs with 15% indium. The In clustering in the sample might be a contributor to the increase in FWHM.



# Microscopy of Semiconducting Materials (MSM-XIX)

## P.2.4 - Electron energy-loss spectroscopy and energy dispersive X-ray spectroscopy studies of indium concentration in InGaN thin film structures

X Wang<sup>1</sup>, T Walther<sup>1</sup>, P Ruterana<sup>2</sup> and MP Chauvat<sup>2</sup>

<sup>1</sup>University of Sheffield, UK, <sup>2</sup>CNRS, France

We demonstrate a method to determine the indium concentration of InGaN thin film by combining the study of plasmon excitation in electron energy-loss spectroscopy (EELS) and the intensity of X-ray line in energy dispersive x-ray spectroscopy (EDXS). The plasmon peak in EELS is broad and noisy, leading to an unreliable determination of the plasmon peak position. In this paper we applied Lorentz fitting for the main plasmon peak to suppress noise and the influence from the Ga 3d transition in the spectrum, in order to improve the precision of plasmon peak position evaluation. It is shown and explained clearly below. The  $\text{In}_x\text{Ga}_{1-x}\text{N}$  samples were grown by metalorganic chemical vapour deposition (MOCVD) or molecular beam epitaxy (MBE) techniques. As the indium concentration is difficult to control due to a variety of reasons, the nominal indium concentrations were not reliable enough. The indium concentration obtained from Oxford Instrument ISIS 300 X-ray quantification often did not agree with the nominal indium concentration. We have therefore applied a self-consistent iterative procedure to determine it from thickness-dependent k-factors using the In(L), Ga(L) and Ga(K) lines. When the corrected indium concentration is plotted versus plasmon peak position we obtain a linear relation, and the error bar calculated from EDXS shows that the indium concentration can be determined from the plasmon peak position to within 6% relative error, which implies an uncertainty in  $x_{\text{In}}$  of  $\Delta x = \pm 0.03$ .

## P.2.5 - STEM strain measurement from a stream of diffraction patterns recorded on a pixel-free delay-line detector

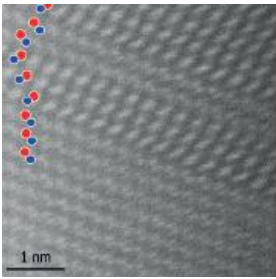
K Müller-Caspar<sup>1</sup>, A Oelsner<sup>2</sup>, A Rosenauer<sup>1</sup> and P Potapov<sup>3</sup>

<sup>1</sup>Universität Bremen, Germany, <sup>2</sup>SurfaceConcept GmbH, Germany, <sup>3</sup>Globalfounders, Germany

Recent progress in nano-beam electron diffraction (NBED), ptychography or differential phase contrast microscopy is based on the acquisition of a four-dimensional data set  $I(x,y,p,q)$  with  $(x,y)$  the position of the electron probe in scanning transmission electron microscopy (STEM),  $(p,q)$  a coordinate in the diffraction pattern and intensity  $I$ . Since the speed of conventional charge-coupled devices is limited, a major challenge is the development of fast detectors.

Here we present pilot experiments with a delay-line detector (DLD) mounted on an FEI Titan facility. The top of the DLD consists of a microchannel plate (MCP) stack that causes a cascade of secondary electrons for each 300keV electron impinging on the detector. The heart of the DLD is a meandering wire in which each cascade causes electrical pulses travelling towards the end of the wire. Depending on the incident position of the electron a characteristic time delay between the arrivals of the 2 conjunct pulses at the wire ends is measured with high accuracy, giving the coordinate of incidence perpendicular to the meander. By crossing two such delay-lines coupled to a time-to-digital converter the incident point  $(p,q)$  and time is measured for each detected electron, with a time precision in the picosecond range.

To characterise the DLD, we determined the quantum efficiency as a function of the incident intensity to be between 50% for  $0.5 \times 10^6$  and 22% for  $17 \times 10^6$  electrons/second for uniform illumination of the detector. Moreover, the modulation transfer function was determined to 0.1 at Nyquist frequency. Finally, we present strain measurements in a GeSi/Si MOSFET for the [001] and [110] direction at a STEM raster of  $100 \times 100$  pixels by recording the 004



# Microscopy of Semiconducting Materials (MSM-XIX)

and 220 CBED discs on the DLD. Dwell times between 40 and 5ms have been used, corresponding to an acquisition of 10,000 diffraction patterns in 6.5 and 0.8min, respectively.

## P.2.6 - Artifacts due to accidental single electrons in atom counting - Two different techniques for atom counting from HAADF-STEM imaging

M Schowalter, F Krause, T Grieb, K Müller, T Mehrtens and A Rosenauer

Universität Bremen, Germany

Two different techniques for atom counting from HAADF-STEM images have been introduced in recent years [1, 2]. Van Aert et al. [1] apply model fitting to experimental images and a subsequent statistical analysis of derived scattering cross sections. LeBeau et al. [2] count the number of atoms by a comparison of measured normalized intensities with simulations. For that the incoming beam intensity as well as the background intensity of the amplifier of the HAADF detector is determined from a detector scan.

Recently Ishikawa et al. [3] found that accidental single electrons impinge on the detector during scanning the electron beam in vacuum. In this contribution we shall show how these electrons influence the result of atom counting: the artificial electrons affect the background level in the normalization of the HAADF intensity. Measurements showed that the angle distribution of these electrons is not homogenous, but exhibits a decrease with detection angle. Furthermore, an apparent cut-off was revealed that turned out to be a reversal point for the scattered electrons in further investigations.

The single electron response of the detector was measured by reducing the beam current as much as possible and taking many detector scans using this setting. For each pixel histograms were built over the series of detector scans and the single electron signals were evaluated.

We will discuss the influence of these effects on results of atom counting from normalized intensities and statistical method.

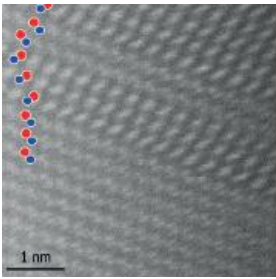
- [1] S. Van Aert, K. J. Batenburg, M.D. Rosell, R. Erni and G. Van Tendeloo, Nature 470 (2011), 374.
- [2] J. LeBeau, S. D. Findlay, L. J. Allen and S. Stemmer, Nanoletters 10 (2010), 4405.
- [3] R. Ishikawa, A.R. Lupini, S.D. Findlay and S.J. Pennycook, Microscopy and Microanalysis 20 ( 2014), 99.

## P.2.7 - Hydrogen etching of InGaN/GaN quantum wells and epilayers

A Bao, M Kappers, SL Sahonta, M Frentrup and R Oliver

University of Cambridge, UK

InGaN/GaN quantum wells grown by a 2-temperature (2T) process [1] can achieve high radiative efficiencies but with relatively large linewidths, because the InGaN layers have gross well width fluctuations (GWWFs). An alternative, quasi-2-temperature (Q2T) growth method, in which each InGaN layer is capped with a thin protective GaN layer, results in QW structures with narrow photoluminescence (PL) linewidths but a reduced radiative efficiency [1]. The aim of this study is to obtain high-efficiency quantum wells with a narrow emission line, which is desirable for laser applications. The growth process follows the Q2T method but includes a growth interruption of 30s after the InGaN QW but prior to the GaN protective layer deposition at the same temperature. Various amounts of hydrogen (0-250-500 sccm) were introduced during the growth interruption. InGaN epilayers without a GaN cap were grown under the same conditions as the quantum well samples with the temperature quenched after the



# Microscopy of Semiconducting Materials (MSM-XIX)

growth interruption/etching step. In this way, the InGaN epilayer is analogous with the InGaN layers within the quantum well structures. The topography and surface roughness of the InGaN layers was investigated using atomic force microscopy (AFM). The average In contents and repeat period of the MQW structures were determined by X-ray diffraction (XRD). Transmission electron microscopy (TEM) was used to measure GWWFs and gaps within the quantum wells. It seems that annealing under  $H_2$  flow leads to nonuniform quantum wells and thus narrow linewidths are difficult to achieve. However, the growth interruption without hydrogen lead to a much narrower 300K-PL peak compared to the reference sample grown using the standard Q2T method.

[1] R.A. Oliver, et al. Appl. Phys. Lett. 103, 141114, (2013)

## P.2.8 - Non-polar (11-20) InGaN nanostructures grown by modified droplet epitaxy

H Springbett, J Griffiths, T Zhu and R Oliver

University of Cambridge, UK

Nitride-based quantum dots (QDs) show promise as sources for single photon emission, enabling comparably high temperature emission and access to the blue and green spectral region. The wurtzite structure of gallium nitride (GaN) results in significant electric fields across strained QDs grown in the c-plane orientation due to the very large piezoelectric constants. This reduces the radiative recombination efficiency due to the spatial separation of the electron and hole via the quantum confined Stark effect (QCSE). Thus, non-polar structures are of interest as this internal electric field can be largely eliminated. In this study we will report on non-polar a-plane (11-20) InGaN QDs grown by modified droplet epitaxy.

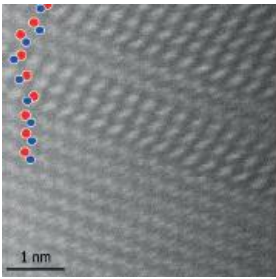
During modified droplet epitaxy (MDE), a thin InGaN layer is grown on a GaN pseudo-substrate and annealed in  $N_2$ , resulting in partial decomposition of the InGaN. Nanoscale metallic droplets remain on the sample surface. It has been hypothesised that these droplets re-react with ammonia during capping to form InGaN quantum dots. However, in MDE growth on the a-plane, ring-like structures have been observed to be associated with the larger droplets, and thus a local droplet etching mechanism has been hypothesised. The ring structures are being investigated in relation to possible formation mechanisms of QDs, and as potential 'quantum rings'. AFM data reveals raised ring structures, enclosing a region of lowered material. Some rings are observed to consist of discrete hillocks adjoining one another in a ring-like formation, rather than a single continuous toroid. Large droplets are often seen to sit on top of these rings in a consistently asymmetric position. Following etching in HCl to remove the droplets, smaller rings were seen to lie within the larger rings. The structural properties were studied by Scanning Transmission Electron Microscopy (STEM) and the chemical composition analysed by energy dispersive x-ray analysis (EDX).

## P.2.9 - Investigation of defect formation during thermal annealing of Ga(NAs) and Ga(NP) using aberration corrected STEM

L Duschek, A Beyer, E Sterzer, P Sträßer, T Wegele, K Volz and W Stolz

Philipps-Universität Marburg, Germany

The quaternary material system Ga(NAsP) shows great potential for realizing optical light sources on Si substrates. A thermal annealing procedure after growth, which was performed by metal organic vapour phase epitaxy, can remove certain crystal defects and thus increase the efficiency of active regions of the devices<sup>1</sup>. As a result of the annealing procedure of Ga(NAsP) multiple quantum wells, a gradual exchange of arsenic and phosphorous atoms between the quantum wells and the barriers could be found<sup>2</sup>. With high angle annular dark field (HAADF) data from a scanning



# Microscopy of Semiconducting Materials (MSM-XIX)

transmission electron microscope (STEM), several defects in the quantum well structures annealed at temperatures up to 1000°C, could be visualized.

For gathering a detailed view in the formation mechanisms of defects on an atomic scale and to get insight into the driving forces for element exchange at interfaces, the ternary material systems Ga(NAs) and Ga(NP) were also investigated. The two ternary material systems were annealed at different temperatures and analyzed in a double Cs-corrected Jeol JEM-2200FS STEM, operating in scanning mode. Aside from the rather big difference in the atomic number between the elements in the samples, it is known that alloying cubic III/V semiconductors with Nitrogen results in static atomic displacements which can influence the ADF contrast significantly<sup>3</sup>. Therefore, we varied the camera length, i.e. the annular acceptance range of the detector, systematically to visualize light atoms as well as heavier atoms appropriately.

This work shows the influence of thermal annealing on defect formation and on element redistribution for the metastable materials under investigation.

- [1] Liebich, S. *et al. Appl. Phys. Lett.* 99, 071109 (2011).
- [2] Gies, S. *et al. J. Cryst. Growth* 402, 169–174 (2014).
- [3] Grillo, V. *et al. J. Phys. Conf. Ser.* 326, 012006 (2011).

## P.2.10 - Compositional analysis of non-polar (11-20) InGaN/GaN quantum well structures and the relation to the emission wavelength

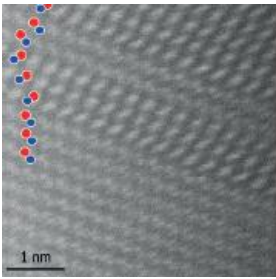
J Griffiths<sup>1</sup>, F Oehler<sup>1</sup>, F Tang<sup>1</sup>, S Zhang<sup>1</sup>, WY Fu<sup>1</sup>, T Zhu<sup>1</sup>, F Massabuau<sup>1</sup>, S Findlay<sup>2</sup>, C Zheng<sup>2</sup>, J Etheridge<sup>2</sup>, T Martin<sup>3</sup>, P Bagot<sup>3</sup>, M Moody<sup>3</sup>, D Sutherland<sup>4</sup>, P Dawson<sup>4</sup>, M Kappers<sup>1</sup>, C Humphreys<sup>1</sup> and R Oliver<sup>1</sup>

<sup>1</sup>University of Cambridge, UK, <sup>2</sup>Monash University, Australia, <sup>3</sup>University of Oxford, UK, <sup>4</sup>University of Manchester, UK

We report on analysis of the composition and Indium distribution in non-polar (11-20) InGaN quantum wells (QWs) by quantitative scanning transmission electron microscopy (Q-STEM), atom probe tomography (APT) and X-Ray Diffraction (XRD). Samples for compositional analysis were grown by metal-organic vapour phase epitaxy (MOVPE) on free-standing ammonothermal GaN substrates with five InGaN/GaN QWs. The expansion of the lattice due to the larger covalent radius of In relative to Ga was studied using the LAMMPS molecular dynamics code (MD) [1] and confirmed by density functional theory (DFT). The In distribution was quantified from high resolution HAADF-STEM images obtained on an FEI Titan<sup>3</sup> FEG-TEM fitted with both probe and image aberration correctors by comparison with image intensities of theoretical specimens simulated using a frozen phonon multislice model [2] [3]. The distribution of In was also studied by APT and the mean In content was found to agree quantitatively within the stated errors. Compositional measurements by XRD were also found to agree with both techniques where the expansion of the lattice was modelled by MD values.

XRD was applied to measure the average In content of a further three non-polar (11-20) samples and study the relationship between the In content and the emission wavelength. Compared to equivalent polar samples, the non-polar samples emit at longer or comparable wavelengths despite the influence of an internal electric field in the polar samples which is predicted to reduce the emission bandgap [4, 5]. Non-polar (11-20) optoelectronic devices may therefore be relevant to bridging the green gap with faster recombination rates than comparable polar structures.

- [1] Plimpton, J. *Comput. Phys.* 117, 1 (1995)
- [2] D. Findlay, J.M. LeBeau, *Ultramicroscopy* 124, 52 (2013)



# Microscopy of Semiconducting Materials (MSM-XIX)

- [3] Rosenauer et al., Ultramicroscopy 109, 1171 (2009)
- [4] A.B. Miller et. al. Phys. Rev. Letts. 53, 2173 (1984)
- [5] Akasaki, H. Amano, Jpn. J. Appl. Phys. 36, 5393 (1997)

## P.2.11 - Atomic structure of the GaN on Ge(111) interface

S Zhang<sup>1</sup>, Y Zhang<sup>2</sup>, Y Cui<sup>3</sup>, C Freysoldt<sup>3</sup>, J Neugebauer<sup>3</sup>, R Lieten<sup>4</sup> and C Humphreys<sup>1</sup>

<sup>1</sup>University of Cambridge, UK, <sup>2</sup>EMPA, Switzerland, <sup>3</sup>MPIE Düsseldorf, Germany, <sup>4</sup>Entegris Inc., Belgium

The structure and chemistry of the interface between a Ge(111) substrate and a GaN thin film has been studied by aberration-corrected scanning transmission electron microscopy (STEM), electron energy loss spectroscopy (EELS), and density functional theory (DFT).

GaN-based semiconductors have been widely applied in optoelectronic and electronic devices. The conventional substrates for GaN growth, sapphire, SiC and Si have a large lattice mismatch and thermal expansion mismatch with respect to GaN, while Ge has a low thermal expansion mismatch (-5.5%) and four of Ge [110] distances are almost matched (+0.4%) to five of GaN [11-20]. High quality GaN films were directly grown on a Ge(111) substrate by plasma-assisted molecular beam epitaxy.

From atomically resolved STEM high-angle-annular-dark-field (HAADF) and annular-bright-field (ABF) images, the epitaxial relationships GaN (0001) parallel to Ge (111), and GaN [11-20] parallel to Ge [110] were observed and a N-polarity of GaN was determined. The interface was found to be crystalline and sharp, with a matching between 4 Ge [110] and 5 GaN [11-20] distances. A novel interfacial structure with a 5:4 closely spaced atomic bilayer is resolved between the Ga-N and Ge-Ge dumb-bells, and EELS suggests they are composed of Ga and Ge.

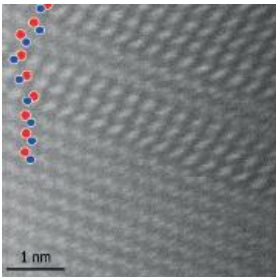
To understand the structure and chemistry of the observed interface, DFT based total energy calculations were performed for various atomic configurations. The bilayer is shown to be composed of Ge atoms, plus a number of Ga atoms depending on the growth conditions, and to be free of N atoms. Having the bilayer in between GaN and Ge(111) not only lowers the interfacial energy, but also enables lattice-matched GaN growth. The flat, crystalline and 5:4 domain matched interface is suitable for applications in semiconductor heterostructures.

## P.2.12 - InN/GaN Superlattices – Resolving the Discrepancies between Theory and Experiment

T Markurt<sup>1</sup>, T Schulz<sup>1</sup>, XQ Wang<sup>2</sup>, XT Zheng<sup>2</sup>, DY Ma<sup>2</sup>, T Suski<sup>3</sup>, I Gorczyca<sup>3</sup>, A Svane<sup>4</sup>, N Christensen<sup>4</sup> and M Albrecht<sup>1</sup>

<sup>1</sup>Leibniz Institute for Crystal Growth, Germany, <sup>2</sup>Peking University, China, <sup>3</sup>Institute of High Pressure Physics UNIPRESS, Poland, <sup>4</sup>Aarhus University, Denmark

m-InN/n-GaN short period superlattices (SPSL), with m, n being integer numbers of monolayers, have attracted great interest because of the possibility for band gap engineering in optoelectronic devices or as a novel opportunity to form topological insulator states. A major advantage of such m-InN/n-GaN SPSLs compared to conventional  $\text{In}_x\text{Ga}_{1-x}\text{N}$  alloys is the absence of compositional fluctuations, which occur on a nanometer-scale even in random alloys. However, recent experimental work uncovered a stunning discrepancy between the calculated band gap of m-InN/n-GaN SPSLs and the observed luminescence emission peak energy. E.g. for single InN monolayers embedded in 4nm thick GaNUNIPRESS barriers the experimentally observed emission typically occurs at around 3eV instead of the theoretically expected range around 2eV.



# Microscopy of Semiconducting Materials (MSM-XIX)

This motivated us to perform quantitative analyses of several nominal 1-InN/n-GaN SPSs by means of aberration corrected high resolution transmission electron microscopy (HRTEM) and scanning transmission electron microscopy (STEM) Z-contrast imaging. Although latter technique is nowadays commonly applied to determine the composition of thick layers, our frozen phonon simulations reveal a crucial influence of the local neighborhood (composition and strain) on the Z-contrast in  $\text{In}_x\text{Ga}_{1-x}\text{N}$  monolayers. Even vanishing contrast between pure Ga and In columns is observed. However, combining STEM and HRTEM we find that (i) the In content of nominal InN monolayers never exceeded values above 35% and (ii) certain growth conditions promote a laterally ordered and periodic monolayer structure, which we identified as a  $\sqrt{3}\times\sqrt{3}R30^\circ$  reconstruction having a stoichiometry of  $\text{In}_{0.33}\text{Ga}_{0.67}\text{N}$ . With this new compositional information at hand the re-calculated band gaps are in very good agreement with the measured photoluminescence data. Though from our result we may infer on strong limitations in the In incorporation, the observed ordered  $\text{In}_{0.33}\text{Ga}_{0.67}\text{N}$  monolayers, however, open the perspective for ordered  $\text{In}_x\text{Ga}_{1-x}\text{N}$  alloys with vanishing lateral compositional fluctuations and possibly unknown optical and physical properties.

## P.2.13 - Determination of ion beam induced artifacts in TEM sample preparation of strained semiconductor heterostructures by means of FIB target preparation

J Münzner, A Beyer and K Volz

Philipps-Universität Marburg, Germany

Transmission electron microscopy (TEM) offers the possibility of imaging atomically resolved structures. In the last decade true quantitative atomic resolution became easily feasible due to aberration correction. However, correct image interpretation requires samples of only a few nanometer thickness, because of dynamical diffraction in crystalline materials. It is clear that for truly quantitative interpretation of HRTEM (as well as HRSTEM) contrast, artifacts arising during conventional ion thinning should be considered.

Strained semiconductor heterostructures were prepared in standard cross-section geometry and thinned down to electron transparency by conventional argon broad ion thinning (BIB). These samples are usually wedge shaped and provide suitable regions for TEM analysis on both sides of the epoxy adhesive. A modern dual beam focused ion beam (FIB)/SEM (JEOL4601F) is utilized to acquire profiles of the electron transparent regions from the original BIB prepared samples. Owing to this approach it is possible to investigate the profile of real TEM samples with atomic resolution using a double-aberration-corrected scanning TEM (JEOL 2200FS) in the high angle annular darkfield mode. This enables a direct correlation between TEM sample preparation conditions and sample quality.

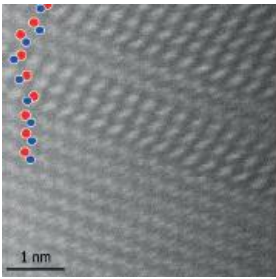
Because of the elastic relaxation of the strained semiconductor material and varying sputtering rates the quantum well structures show selective etching at interfaces under inappropriate thinning conditions. Additional amorphization of nearly constant magnitude on the upper and lower surface can be detected. The geometry is in agreement with finite elements simulations of the elastic relaxation geometry expected by strained wedge structures due to the additional free surfaces. It can be concluded that selective etching of strained layers is presumably enhanced by the local bulging which increasing local sputtering angles during ion beam thinning.

## P.2.14 - Automated defect analysis with EBIC

M Hiscock<sup>1</sup>, G Moldovan<sup>1</sup>, S Lotharukpong<sup>2</sup> and P Wilshaw<sup>2</sup>

<sup>1</sup>Oxford Instruments NanoAnalysis, UK, <sup>2</sup>University of Oxford, UK

Electron Beam Induced Current (EBIC) characterization is unique in its ability to provide quantitative high-resolution imaging of electrical defects in solar cells. In particular, EBIC makes it possible to image electrical activity of single



# Microscopy of Semiconducting Materials (MSM-XIX)

dislocations in a Dual-Beam Focused Ion Beam (FIB) Scanning Electron Microscope (SEM), to cut and lift out a micro-specimen containing a particular dislocation, and then transfer it for further structural or chemical analysis. As typical solar cell material presents a complex array of defects, it is important to observe statistical variations within a sample and select key sites for analysis.

This work describes a method for automated defect identification and characterization, and shows an application to multi-crystalline silicon (mc-Si) solar cell wafers selected from different heights along a manufactured ingot. Information presented here includes the experimental setup for data acquisition, as well as the analysis algorithms used for identification and extraction of dislocation contrast.

Application to this solar cell material revealed that the average contrast of dislocations is shifting from 0.12 at the bottom of the ingot to 0.08 at the top of the ingot. This shift may be assigned to the different total times available for collecting impurities, where dislocations at the bottom of the ingot have more time compared with those at the top, or to the different densities of dislocations along the height of the ingot, where impurities at the bottom are spread between a reduced number of dislocations, as compared with those at the top.

## P.2.15 - Structural and chemical studies of the GaN(0001)/GaAs (111)B Interface

S-L Sahonta<sup>1</sup>, R Oliver<sup>1</sup>, C Humphreys<sup>1</sup>, T Foxon<sup>2</sup> and S Novikov<sup>2</sup>

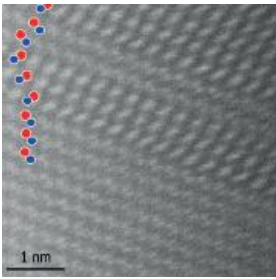
<sup>1</sup>University of Cambridge, UK, <sup>2</sup>University of Nottingham, UK

Commercial III-nitride optoelectronic devices are typically grown heteroepitaxially on foreign substrates, resulting in structural defects in the GaN film which may inhibit the emission properties of the device. Bulk GaN substrates, with surface areas about 1 cm<sup>2</sup>, grown by hydride vapour phase epitaxy, ammonothermal and high-pressure techniques are now available, but large-area free-standing GaN substrates are still a problem for commercial device growth.

Molecular beam epitaxy (MBE) is not considered to be a bulk growth process due to its slow growth rate. However, a newly-developed plasma-assisted molecular beam epitaxy (PA-MBE) process for the growth of bulk zinc blende GaN layers has been shown to achieve 100 μm-thick free-standing wurtzite GaN wafers [1]. In this work we study the crystallographic structure of the substrate-film interface of wurtzite GaN layers grown on 2-inch (111)B GaAs wafers by PA-MBE, with the potential goal of growing thick free-standing 2-inch wurtzite GaN wafers.

Three MBE-grown 500 nm-thick wurtzite GaN films on GaAs (111)B substrates with different growth initiation procedures are investigated by high-resolution transmission electron microscopy. Zinc blende crystallites bounded by prismatic stacking faults are observed at the GaN/GaAs interface, which extend tens of nanometres into the wurtzite film, before being terminated at (0001) basal plane stacking faults. It appears that optimisation of the nucleation process results in smaller cubic crystallites at the GaN/GaAs interface, and a conversion to wurtzite at an earlier stage in the growth. The interface is rough with a high density of structural defects in the lower tens of nanometres of deposition, with periodic depressions in the GaAs substrate, suggestive of GaN/GaAs intermixing. The film morphology will be discussed, and the implications for the growth of large-scale bulk nitride films on GaAs (111) will be considered.

[1] SV Novikov, CT Foxon, AJ Kent, Phys. Stat. Sol. C 8 (2011) 1439.



# Microscopy of Semiconducting Materials (MSM-XIX)

## P.2.16 - Microstructural analysis of cubic InGaN/GaN multiple quantum well structures grown on large-area 3C-SiC/Si (001)

S-L Sahonta<sup>1</sup>, M Kappers<sup>1</sup>, D Wallis<sup>1</sup>, I Guiney<sup>1</sup>, C Humphreys<sup>1</sup>, J Shaw<sup>2</sup> and P Ward<sup>2</sup>

<sup>1</sup>University of Cambridge, UK, <sup>2</sup>Anvil Semiconductors Ltd., UK

Highly efficient blue light-emitting diodes for white lighting are based on polar wurtzite InGaN/GaN multiple quantum wells (MQWs), however increasing the indium content to achieve green emission results in reduced quantum efficiencies due to higher defect densities. Additionally, the internal electric field present in polar nitrides limits efficient carrier recombination. Non-polar cubic nitride films do not have this electric field, are suitable for silicon (001) electronics integration, and can have a narrower bandgap and higher p-type conductivity [1] than wurtzite GaN, resulting in the need for less indium in the MQWs and improved diode characteristics respectively. However, cubic nitrides are metastable, requiring careful control of metal-organic vapour phase epitaxy (MOVPE) growth parameters.

In this work we demonstrate the MOVPE growth of 250 nm-thick single phase cubic nitride films on thick 3C-SiC (001) epilayers which have been grown separately on 4-inch silicon (001) wafers by Anvil Semiconductors Ltd., with cubic blue- and green-emitting InGaN/GaN MQW structures deposited onto the GaN epilayers.

Transmission electron microscopy reveals a single phase cubic GaN film with an abrupt GaN/SiC interface with {111}-stacking faults (SFs) forming at the SiC surface, which reduce in density to  $\sim 5 \times 10^5 \text{ cm}^{-1}$  at the transition between the low-temperature GaN buffer and high-temperature GaN epilayer proper, possibly due to annihilation of oppositely-oriented faulted {111} planes bounded by  $\langle 110 \rangle$  dislocations *via* the formation of SF tetrahedra. SFs are likely to have formed by the dissociation of  $60^\circ$  and screw dislocations into partial dislocations separated by an intrinsic SF in the {111} slip plane by the reaction  $a/2[1-10] \rightarrow a/6[1-21] + a/6[2-1-1]$ . The effect of SFs on the nanostructure and optical properties of blue and green light-emitting MQW structures will be discussed.

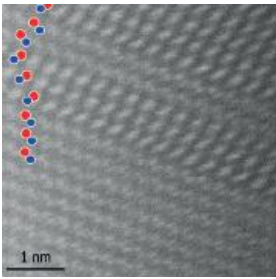
[1] DJ As, D Schikora, A Greiner, M Lubbers, J Mimkes, K Lischka, Phys. Rev. A 54(16) (1996), R11118-R11121.

## P.2.17 - Strain accommodation and indium incorporation in $\text{In}_x\text{Ga}_{1-x}\text{N}$ epilayers grown by molecular beam epitaxy

C Bazioti<sup>1</sup>, E Papadomanolaki<sup>2</sup>, T Kehagias<sup>1</sup>, T Walther<sup>3</sup>, J Smalc-Koziorowska<sup>4</sup>, P Komninou<sup>1</sup>, E Iliopoulos<sup>2</sup> and G Dimitrakopoulos<sup>1</sup>

<sup>1</sup>Aristotle University of Thessaloniki, Greece, <sup>2</sup>University of Crete & IESL FORTH, Greece, <sup>3</sup>University of Sheffield, UK, <sup>4</sup>Polish Academy of Sciences, Poland

InGaN epilayers with increased InN molar fractions promise high efficiency photovoltaic applications. However, a complex interplay exists between compositional homogeneity, misfit strain relaxation, and the phenomena of phase separation, indium segregation, compositional pulling, and interfacial sequestration. We have investigated the structural properties of a range of  $\text{In}_x\text{Ga}_{1-x}\text{N}$  samples ( $x = 0.1-0.6$ ) with thicknesses up to 500 nm. The samples were deposited by plasma-assisted molecular beam epitaxy (PAMBE) on (0001) GaN/sapphire templates over a range of growth temperatures, in order to assess the influence of attained growth conditions on the indium incorporation, phase separation, strain relaxation, and the resulting defect microstructure. To this end, we have employed (scanning) transmission electron microscopy [(S)TEM] methods were used, including high resolution TEM (HRTEM), geometrical phase analysis (GPA), and energy dispersive x-ray spectroscopy, in conjunction with high resolution X-



# Microscopy of Semiconducting Materials (MSM-XIX)

ray diffraction (HRXRD). The transition from strain relaxation through V-pits to sequestration layering with increasing indium content was recorded. Abrupt film sequestration was correlated to a critical thickness for the transition from elastic to the plastic strain relaxation. An indium concentration gradient with increasing thickness was observed. Basal stacking faults served to relieve the strain through their delimiting partial dislocations, leading to emanation of a-type threading dislocations. The stacking faults were invariably correlated to the sequestration phenomenon, and were suppressed together with it upon further increasing the indium content.

Acknowledgement: Research co-financed by the EU (ESF) and Greek national funds - Research Funding Program: THALES, project NITPHOTO.

## P.2.18 - Microstructure of $\text{In}_x\text{Ga}_{1-x}\text{N}$ ( $x = 0.22$ to $0.67$ ) films grown by metal-modulated epitaxy

Y O Wei<sup>1</sup>, A M Fischer<sup>1</sup>, F A Ponce<sup>1</sup>, M Moseley<sup>2</sup>, B Gunning<sup>2</sup> and W A Doolittle<sup>2</sup>

<sup>1</sup>Arizona State University, USA, <sup>2</sup>Georgia Institute of Technology, USA

The microstructure of  $\text{In}_x\text{Ga}_{1-x}\text{N}$  films, with indium composition  $x$  in the range from 0.22 to 0.67, has been investigated. The films were grown by metal-modulated epitaxy at low temperatures ( $\sim 400^\circ\text{C}$ ) to facilitate indium incorporation, and with precursor modulation to enhance surface morphology and metal adlayer diffusion. A high density of crystalline defects consisting mainly of stacking faults associated with island growth is observed in the lower composition range  $x = 0.22$ . The microstructure evolves into fine columnar domains devoid of stacking faults in the middle range ( $x = 0.46$ ). A significant improvement in the crystalline quality and optical properties is observed for  $x \geq 0.60$ , with strain relaxation at the interface evidenced by the presence of moiré fringes. High luminescence intensity, low defect density, and near-complete uniform misfit strain relaxation are observed for  $x = 0.67$ . The strain relaxation can be explained by a critical thickness value of the order of a monolayer. This behavior is reproducible in variations of the growth technique, and provides an approach for growth under high lattice mismatch conditions

## P.2.19 - High quality FIB lamella preparation for wide area atomic resolution TEM investigations

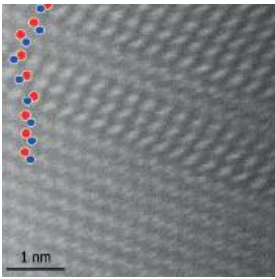
R Staubinger<sup>1</sup>, A Beyer<sup>1</sup>, K I Gries<sup>1</sup>, C Schneider<sup>2</sup>, M Rohnke<sup>2</sup>, B Mogwitz<sup>2</sup>, J Janek<sup>2</sup> and K Volz<sup>1</sup>

<sup>1</sup>Philipps-University Marburg, Germany, <sup>2</sup>Justus-Liebig-Universität Gießen, Germany

A large increase in research efforts on thermoelectric power generation is currently occurring because of the improved properties of various nano structured thermoelectric materials.  $\text{Na}_x\text{CoO}_2$  is a thermoelectric material which for example makes the recovery of the waste heat emitted by vehicles and factories possible. In addition it can be used in electronic processors. The single phase  $\text{Na}_x\text{CoO}_2$  crystals we are working with are grown by pulsed laser deposition on  $\text{Al}_2\text{O}_3$  (001) or  $\text{LaAlO}_3$  (111). To improve this material transmission electron microscopy (TEM) investigations are indispensable. Especially for structures that reveal a lot of inhomogeneity it is necessary to have high quality focussed ion beam (FIB) TEM lamellas for wide area atomic resolution.

During our research we continuously improve the FIB preparation process. Because of the hardness of the sapphire substrate it is necessary to thin the lamella from the substrate side (bottom-top). Especially when working with very ion beam sensitive structures this preparation technique is also very interesting for other materials, like even organic material.

It became clear during this work, that FIB preparation is a useful method to obtain thin samples over a wide range. This enables in combination with (S)TEM the characterization of samples containing a lot of inhomogeneities. This presentation will summarize the necessary steps to optimize the FIB preparation to obtain optimal samples.



# Microscopy of Semiconducting Materials (MSM-XIX)

## Poster Session 3

### P.3.1 - The effects of Si-doping on dislocation core structures in GaN

S K Rhode<sup>1,2</sup>, S L Sahonta<sup>1</sup>, T J Pennycook<sup>3</sup>, M J Kappers<sup>1</sup>, C J Humphreys<sup>1</sup>, R O Dusane<sup>4</sup>, and M A Moram<sup>2</sup>

<sup>1</sup>University of Cambridge, UK <sup>2</sup>Imperial College London, UK <sup>3</sup>STFC, UK, <sup>4</sup>Indian Institute of Technology Bombay, India

Lattice mismatch between GaN and sapphire produces a high density of threading dislocations in hexagonal GaN films grown on sapphire. These dislocations act as non-radiative recombination centers when they propagate into the active regions of GaN-based light-emitting devices and can reduce device efficiencies and lifetimes. We currently lack a clear understanding of how growth conditions affect dislocation core-structures, in particular, the effects of technologically important Si-doping (n-type) on dislocation core-structures in GaN are unknown.

Here, we present a statistically valid study comparing the dislocation core-structures found in undoped GaN and Si-doped GaN with Si concentrations similar to those used in devices, to determine the effect of Si-doping on dislocation core-structures by high-angle annular dark-field imaging in an aberration-corrected scanning transmission electron microscope.

In both undoped and Si-doped GaN, *a*-type cores formed 5/7-ring structures and half the (*a*+*c*)-type cores dissociated into variable lengths, while the other half remained undissociated. A new core-structure, a 4-atom core, which has never been observed for an (*a*+*c*)-core in GaN-based alloys, was observed for Si-doped GaN sample. Tensile stresses introduced by Si-doping initiates glide in TDs, thus forming a 4-atom core. Moreover, a local decrease in the *a*-lattice parameter caused by the substitution of Ga with Si atoms at the core was shown to result in slightly lower dissociation lengths for extended (*a*+*c*)-type dislocations in Si doped GaN samples.

### P.3.2 - Multi-microscopy investigation of the optical properties of dislocations in InGaN

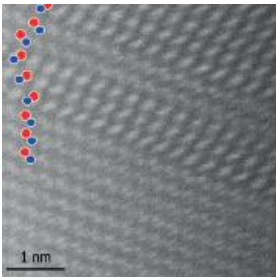
F Massabuau<sup>1</sup>, P Chen<sup>1</sup>, T O'Hanlon<sup>1</sup>, C Ren<sup>1</sup>, S Rhode<sup>1</sup>, A Kovacs<sup>2</sup>, M Kappers<sup>1</sup>, C Humphreys<sup>1</sup>, R Dunin-Borkowski<sup>2</sup> and R Oliver<sup>1</sup>

<sup>1</sup>University of Cambridge, UK, <sup>2</sup>Forschungszentrum Jülich, Germany

InGaN alloys are widely used as the active material in GaN-based light emitting diodes. However, this material contains a high density of threading dislocations, which are thought to act as non-radiative recombination centres [1]. Conversely, in InGaN/GaN quantum well structures, dislocations have been observed to open as V-pits which are believed to prevent carrier recombination at dislocation cores [2]. The impact of dislocations is therefore twofold and is still poorly understood. In this study we employ a multi-microscopy analysis study of dislocations in InGaN to correlate the emission and structural properties of the same defect.

A 150 nm In<sub>0.09</sub>Ga<sub>0.91</sub>N layer was grown by metal-organic vapour phase epitaxy. We conducted a multi-microscopy analysis, by performing atomic force microscopy, scanning electron microscopy with cathodoluminescence and transmission electron microscopy on exactly the same dislocations. In this study we were interested in investigating the correlation between the dislocation type, the light emitted by different parts of the V-pit forming at the dislocation apex, and the structure of the dislocation core.

We show that irrespectively of the dislocation type, a V-pit can emit more intense light than its surrounding material. This observation challenges our current thinking about the behaviour of dislocations in semiconductors. We also reveal that the light is emitted at a longer wavelength than that of the surrounding material. This result suggests that



# Microscopy of Semiconducting Materials (MSM-XIX)

indium may segregate around the dislocation. Finally we highlight a correlation between the wavelength shift of the emission from the facets of a V-pit and the intensity of light emitted from the centre of the V-pit. This correlation suggests that different core structures may be at the origin of the various optical properties of dislocations in InGaN.

- [1] Sugahara et al., *Jap. J. Appl. Phys.* 37, 398 (1998)
- [2] Hangleiter et al., *Phys. Rev. Lett.* 95, 127402 (2005)

### P.3.3 - TEM Characterization of Perfluoropentacene grown on graphene

R Felix Angel, KI Gries, T Breuer, G Witte and K Volz

Philipps-Universität Marburg, Germany

Organic semiconductors (OSC) are up-and-coming in research and industry, due to their potential applications in electronic devices such as organic field-effect transistors (OFETs) and light-emitting diodes (OLEDs). Perfluoropentacene (PFP,  $C_{22}F_{14}$ ) [1] is the perfluorinated of the well-known OSC pentacene (PEN,  $C_{22}H_{14}$ ). PFP adopts a triclinic arrangement with the P1 space group and it exhibits high hole mobilities. Using Transmission Electron Microscopy (TEM) characterization, PFP has been widely studied on different substrates such as halides [2] or  $SiO_2$  [3] with optimal imaging conditions which minimize the radiation damage that destroys the PFP [3].

It is known that molecular orientation and ordering of different organic semiconductors depends on substrate interaction and substrate roughness. Until now, characterization of Pi-Stacked PFP on graphene-coated quartz was carried out by combining X-ray diffraction with theoretical structure modeling [4], but with this work, we use TEM techniques to study the crystal phase and orientation of PFP grown on graphene. Thereby, we use Conventional TEM, Bright Field and Dark Field, as well as Electron Diffraction (ED) and Energy-Dispersive X-Ray Spectroscopy (EDX) to report on characteristic growth of PFP in islands with distinct faceting where the orientation is induced by the suspended monolayer of graphene. In this way, the edges of these islands are created by specific planes which are the most favorable places where bonds between the molecules should be broken and they keep a relationship with the substrate orientation.

Summarizing, for the first time, with this study we provide an evidence for the epitaxial relation of PFP grown on graphene by using different TEM techniques.

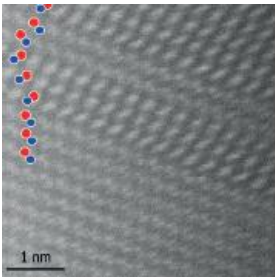
- [1] Y. Sakamoto et al., *J. Am. Chem. Soc.*, 126, 8138 (2004)
- [2] T. Breuer et al., *Phys. Rev. B* 83, 155428 (2011)
- [3] B. Haas et al., *J. Appl. Phys.* 110, 073514 (2011)
- [4] Salzmann et al., *ACS Nano* 6, 112, 10874–10883 (2012)

### P.3.4 - Multi-microscopy analysis of GaN-based microdisk lasers

T Puchtler<sup>1</sup>, C Ren<sup>1</sup>, A Woolf<sup>2</sup>, D Gachet<sup>3</sup>, T Zhu<sup>1</sup>, E Hu<sup>2</sup> and R Oliver<sup>1</sup>

<sup>1</sup>University of Cambridge, UK, <sup>2</sup>Harvard University, USA

Whilst materials for microelectronics are becoming increasingly mature, our understanding of the factors limiting the performance of micro- and nanoscale optoelectronic devices remains more rudimentary. In this study, we demonstrate how, by applying multiple microscopy techniques to the same micro-device, it is possible to achieve a greatly enhanced understanding of the limitations of the materials comprising the device. The devices we focus on



# Microscopy of Semiconducting Materials (MSM-XIX)

are GaN-based microdisk lasers in which a microdisk membrane (diameter: 1 micron; thickness: 200 nm) has been formed by etching a sacrificial layer. For each specific device studied, we have measured the quality factor ( $Q$ ) of the microdisk cavity by micro-photoluminescence and then observed exactly the same device in scanning electron microscopy (SEM) and cathodoluminescence (CL). Side-view SEM images reveal whiskers extending from the underside of the undercut microdisk, whilst plan-view CL images reveal dark spots, arising from non-radiative recombination at dislocations. A direct correlation between the number of dislocations observed for each device and the number of whiskers confirms that the whiskers arise because of a reduced etching rate around dislocations. Analysing the dependence of the device  $Q$  on the number of dislocations and their position within the device shows that it is only dislocations in the periphery of the disk which affect  $Q$ ; the highest- $Q$  whispering gallery modes reside at the periphery. Using finite difference time domain simulations, we show that whiskers create a radiative pathway for light to couple to the substrate, thus degrading  $Q$ . Our multi-microscopy approach thus allows us to identify a route to improved devices: the elimination of whisker formation during fabrication, rather than elimination of the dislocations themselves. Furthermore, we have developed a focussed ion beam micromachining method to extract individual devices for analysis in the transmission electron microscope, allowing further insights into the structure and formation of whiskers.

## P.3.5 - Structure and morphology of para-sexiphenyl on polar and mixed-polar ZnO surfaces

H Kirmse, M Sparenberg, S Blumstengel and F Hennberger

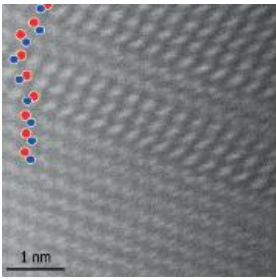
Humboldt University of Berlin, Germany

The combination of inorganic and organic materials (here ZnO and para-sexiphenyl - 6P) for semiconductor applications is a rather new field of fundamental research. The mechanisms of organic crystal growth on an

inorganic substrate are poorly understood. In order to gain some understanding of the formation of hybrid inorganic/organic interfaces, high-resolution transmission electron microscopy (HRTEM) and corresponding image contrast simulations were performed. From this combination, parameters like, e.g., molecule alignment and interface separation will be derived.

In particular, two interface setups were studied. The first setup comprises 6P on (000-1)ZnO and the second one 6P on (10-10)ZnO. 6P is found to be crystalline in both cases as concluded from (100) lattice fringes visualized by zero-loss energy filtered HRTEM imaging. Although weak interaction between 6P and ZnO is expected, a decisive influence of the substrate on the alignment of molecules is observed. For the deposition of 6P on the oxygen-polar (000-1) surface the 6P molecules form extended islands and align upright as indicated by (100) lattice fringes running parallel to the interface. On the contrary, flat lying 6P molecules are concluded for the deposition on mixed-polar (10-10)ZnO. Here, (100) lattice fringes are inclined with respect to the 6P/ZnO interface. 6P forms needles exhibiting a cross section of about 50nm in width, about 10nm in height, and extending up to several micrometers in length. These striking different structural properties will be explained by the strong polarity of ZnO.

Image contrast simulations support the interpretation of the experimental HRTEM images. In particular, the monoclinic bulk structure of 6P holds for the nanostructure as well. Moreover, the alignment of the 6P molecules on (10-10)ZnO is found to be perpendicular to the in-plane [00.1] direction of the (10-10)ZnO substrate surface being in good agreement with calculations of the electrostatic field of ZnO done earlier.



# Microscopy of Semiconducting Materials (MSM-XIX)

## P.3.6 - Magnetic and magneto-optical properties of doped and co-doped CdTe

A R Abderrahim, S Younes, B Abdelilah and B Lahoucine

Med V University, Morocco

On the basis of ab-initio calculations, the magnetic properties of CdTe doped with transition metals Mn, Fe and co-doped with both, which make this material a possible candidate for spintronic applications, have been investigated. Moreover, the density of state DOS for different dopant concentrations have been calculated and plotted with the energy diagram, we studied the experimental results of the doping of CdTe and determined which one is responsible of the magnetism appearing, Mn or Fe, then we observed the effect of the codoping with Mn and Fe. We found that the iron Fe does not contribute strongly in the magnetism but affects the optical properties of the DMS, so in experimental work we find that a low concentration of Fe improves well the magneto-optical properties such as the Faraday rotation. We also investigate the microscopic behavior of electrons by studying its electronic structure and density of states.

## P.3.7 - Synthesis and some surface features of laminated ZnO/TiO<sub>2</sub> transparent bilayer by two growth techniques

B Taleatu<sup>1</sup>, E Arbab<sup>2</sup> and G Mola<sup>2</sup>

Obafemi Awolowo University, Nigeria, <sup>2</sup>University of KwaZulu-Natal, South Africa

In this laminated bilayer, a titanium dioxide (TiO<sub>2</sub>) nanostructure with high surface area was first deposited on transparent conductive glass substrate by electrochemical deposition. Top layer consisting of zinc oxide (ZnO) thin film was later grown on the TiO<sub>2</sub> after brief heat treatment. Morphological study indicated that average particle sizes of the TiO<sub>2</sub> underlayer were between 110 and 138 nm. Scanning electron microscopic (SEM) images of the bilayer (ZnO/TiO<sub>2</sub>) revealed that the ZnO overlayer was formed without any major chemical interaction with the proximate

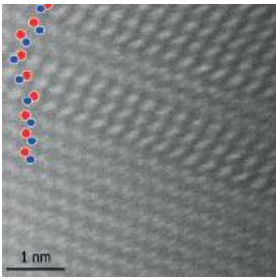
surface. Cross-sectional FESEM image gave the estimated values of thickness below 55  $\mu\text{m}$ . Optical studies showed that all the films exhibited strong absorption edge at  $\lambda \approx 330 \text{ nm}$ . In the bilayer, slight shift in absorption edge was observed towards visible spectrum. Values of energy band gap estimated from Tauc's plots ranged between 3.24 and 3.43 eV.

## P.3.8 - Effects of deposition period on the optical properties of nano-crystallised Al/Pb-oxide and -sulphide films

M E Ojo and S S Oluyamo

Federal University of Technology, Nigeria

Oxides and Sulphides of Al/Pb at deposition periods of 2.5, 3.5, 4.5 and 5.5 hours were prepared using the Chemical Bath Deposition (CBD) technique. Nano crystalline films of thickness 100-470 nm were produced in the study. Optical characterisation of the films was carried out using the Jenway 6405 UV-VIS model spectrometer. The absorbance decreases with increase in wavelength and has relatively low values in the InfraRed (IR) region of the electromagnetic spectrum. Highest absorbance was observed at a period of 3.5 hours for PbO, 3.5 hours and 5.5 hours for PbS, 2.5 hours for Al<sub>2</sub>O<sub>3</sub> and 5.5 hours for Al<sub>2</sub>S<sub>3</sub> at wavelength range between 275-400 nm, hence, the films possess potential applications within this region. The transmission increases as the wavelength increases, values greater than 85% were obtained for transmittance spectra of PbO, while the PbS gives transmittance in the range 10-35%. The high transmission in the visible region suggests the suitability of the films for solar energy collector and aesthetic window glaze materials. On the other hand, the low reflectance values of the thin films reveal their importance as material for anti-reflectance coating. These results show that, thin films of Al/Pb oxide and



# Microscopy of Semiconducting Materials (MSM-XIX)

sulphide can also be used as optical sensors. The direct band gap energy of the films deposited ranges between 1.8-3.4 eV. The result of the study also revealed that optimum performance of the materials could be achieved by varying the period of deposition.

Key Words: Al/Pb oxide and sulphide, period of deposition, optical properties.

## P.3.9 - Characterisation of vacancy-related point defects in Zn-doped CdTe

D Keeble<sup>1</sup>, M Elsharkawy<sup>1</sup>, G Kanda<sup>1</sup> and E Abel-Hady<sup>2</sup>

<sup>1</sup>University of Dundee, UK, <sup>2</sup>Minia University

Point defect detection and identification remain formidable challenges. Aberration corrected electron microscopy and electron energy loss spectroscopy provides atomic resolution and can observe point defects, for example vacancies, when the local concentration is sufficiently high, typically in the percent range. However, for the majority of semiconducting materials defect concentrations are more typically in the parts per million (ppm) range. Advances in positron annihilation techniques, in particular the ability of density functional theory to calculate positron lifetimes and momenta, make these methods ideally suited to the sensitive detection and identification of vacancy-related defects. This can be in bulk materials, or by using positron beam technology also in thin films. In this work positron annihilation lifetime spectroscopy is applied to study vacancy related defects in lightly Zn-doped CdTe single crystals.

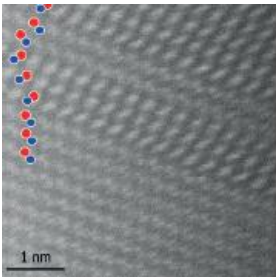
The positron lifetime spectra clearly identify the Cd-vacancy. Density function theory calculations supporting the assignment are also detailed. The temperature dependence of positron trapping to the vacancy defects is also investigated in the range 300 K to 10 K, and shows unusual behaviour. Positrons de-trap from vacancies at lower temperatures. This provides direct evidence for the presence additional defect centres that act as shallow traps, and are not vacancy defects. Negatively charged acceptor-type impurities are likely candidates.

## P.3.10 - Microscopical characterization of 2D-film selenide heterostructures deposited on polar wurtzite AlN by molecular beam epitaxy

C Bazioti<sup>1</sup>, GP Dimitrakopoulos<sup>1</sup>, P Komninou<sup>1</sup>, K Aretouli<sup>2</sup>, P Tsipas<sup>2</sup>, D Tsoutsou<sup>2</sup>, E Xenogiannopoulou<sup>2</sup> and A Dimoulas<sup>2</sup>

<sup>1</sup>Aristotle University of Thessaloniki, Greece, <sup>2</sup>NCSR Demokritos, Greece

We have employed high resolution transmission electron microscopy (HRTEM) in order to study the structural and interfacial properties of a range of selenide heterostructures comprising two-dimensional (2D) films that were grown on (0001)AlN/(111)Si templates by molecular beam epitaxy (MBE). Bi<sub>2</sub>Se<sub>3</sub> is a topological insulator that is promising for novel spintronics and quantum computing. Device performance can be greatly benefited by depositing ultrathin films on wide band gap substrates such as wurtzite AlN [1], whereas silicon wafers offer device integration. HRTEM, combined with geometrical phase analysis, showed an epitaxial heterostructure with AlN, for 2D films with controlled thickness in terms of quintuple layers (3 and 5 QLs), and a well-ordered crystalline interface with the substrate. The observed defects were vertical and in-plane 180° rotational domain boundaries. Similar interfacial quality was not achievable when Bi<sub>2</sub>Se<sub>3</sub> was deposited directly on silicon. Additionally to Bi<sub>2</sub>Se<sub>3</sub>, 2D films comprising a few monolayers (MLs) of MoSe<sub>2</sub> semiconductor were deposited either directly on (0001)AlN or on the Bi<sub>2</sub>Se<sub>3</sub> layers. Such heterostructures and multilayers were found to be of high crystalline quality over an extended scale, thus offering advanced device possibilities mediated by the van der Waals bonding. HRTEM image simulation was employed in order to characterize and verify the crystalline structure of interfaces between dissimilar materials.



# Microscopy of Semiconducting Materials (MSM-XIX)

Cross sectional observations revealed a high quality crystalline structure with no extended defects inside the MoSe<sub>2</sub> films. These structural observations were corroborated from the angle-resolved photoelectron spectroscopy measurements.

[1] P. Tsipas *et al.*, ACS Nano **8**, 6614 (2014).

Acknowledgement: Work is supported by the ERC Advanced Grant SMARTGATE-291260- and the National program of excellence (ARISTEIA-745) through the project TOP-ELECTRONICS.

## P.3.11 - Origin of surface defects in RP-CVD grown Si<sub>1-y</sub>C<sub>y</sub> epilayers by the oversaturation of Carbon

G Colston, M Myronov, S Rhead and D Leadley

University of Warwick, UK

Silicon Carbon (Si<sub>1-y</sub>C<sub>y</sub>) is an alloy formed from the substitutional incorporation of C in the Si lattice. Due to the huge lattice mismatch between Si and diamond, the incorporation of relatively low levels of C in Si<sub>1-y</sub>C<sub>y</sub> alloys can reduce the lattice constant quite significantly. The main applications of Si<sub>1-y</sub>C<sub>y</sub> are within strain engineering such as inducing strain within MOSFET channels to enhance mobility or compensating for strain in Si<sub>1-x-y</sub>Ge<sub>x</sub>C<sub>y</sub> ternary alloys.

Strained Si<sub>1-y</sub>C<sub>y</sub> epilayers have been grown on Si(001) substrates by RP-CVD. Analysis of the crystal structure and surface of the Si<sub>1-y</sub>C<sub>y</sub> layers has been carried out by TEM, SEM and AFM techniques. Layers with C composition of approximately 1.5% were found to form amorphous surface hillocks. The size of these defects increases with layer thickness and the density dramatically increases in layers with greater C incorporation. Beyond a critical thickness of Si<sub>1-y</sub>C<sub>y</sub> the hillocks fuse and form an amorphous region that caps the epilayers. This critical thickness significantly decreases with higher C incorporation during the growth process. The hillocks also increase the surface roughness of samples which may be a huge limitation during the incorporation of Si<sub>1-y</sub>C<sub>y</sub> into electronic devices. After the fusion of the hillocks the surface roughness significantly reduces.

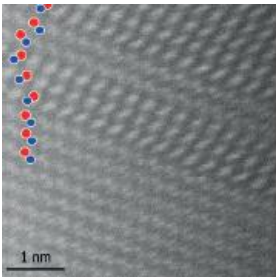
The presence of the hillocks is attributed to the precipitation of C atoms from the Si<sub>1-y</sub>C<sub>y</sub> epilayers forming point defects which subsequently cause accelerated polycrystalline growth. The increase in hillock density with C incorporation could be being affected by changes in surface energy due to the strain induced by the epilayers or as a result of the higher C content within the layers increasing precipitation directly.

## P.3.12 - Examination of polycrystalline growth caused by contaminations in epilayers by electron microscopy

P Allred, M Myronov, S Rhead and D Leadley

University of Warwick, UK

With the ever increasing development into research of Group IV semiconductors for a plethora of different applications, the overall quality of these heterostructures becomes ever more important for device performance. Various epitaxial methods are utilised for growth of these layers. With the high level of tunability and throughput, chemical vapour deposition (CVD) is a prevalent choice, often referred to as the ultimate industrial tool for epitaxy. Clean substrates and high purity precursor gases are critical in maintaining smooth monocrystalline growth throughout the process. Many devices are to be produced on a mass scale, so must be reproducible in large quantities.



# Microscopy of Semiconducting Materials (MSM-XIX)

Contamination or leaks in the system prevent the growth of any high quality structures. Small levels of contaminants in the gases, or particles on the substrate can be particularly detrimental to the quality of epitaxy. Relatively low levels of oxygen present at the growth surface may form an oxide and create a nucleation site for polycrystalline growth. A common side effect of growing these layers under these circumstances is the formation of polycrystalline layers which are unsuitable for desired device performance.

Reduced pressure (RP) CVD grown samples have been imaged using cross sectional transmission electron microscopy (TEM) to understand the extent of these potential issues. Energy dispersive spectroscopy (EDS) was employed to identify which contaminants were present, providing an indication to the cause of the polycrystalline growth.

Very low levels of oxygen and moisture introduced into the epitaxial growth system have prevented crystalline growth, highlighting the importance of clean growth environment. The interface at the substrate has also been inspected to observe the nature of the initial growth on contaminated wafers. This has served as a key technique in rectifying any growth issues and minimise the systems down time.

## P.3.13 - Challenges of growth and sample preparation of GeSn for electron microscopy

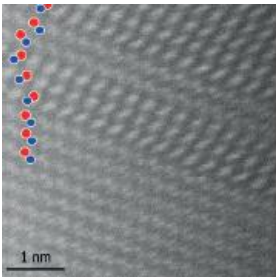
D Patchett, M Myronov, G Colston and S Rhead

University of Warwick, UK

Great research effort has recently been applied to the development of alloying Sn into Ge and SiGe. The major goal of this research is to advance the functionality of group IV semiconductors for photonic and optoelectronic applications, but additionally towards the creation of high mobility strained layers. For effective use of this research effort appropriate protocols must be developed for obtaining quality data from electron microscopy. The metastable nature of high Sn fraction (<1%) semiconducting alloys makes growth challenging, and the ability to distinguish between defects from sample preparation and defects intrinsic to the as-grown sample are paramount.

GeSn is a mechanically soft material and great care must be taken in preparing samples for electron microscopy. High Sn fractions are desirable for many device applications; however increasing Sn fraction increases the alloy sensitivity to mechanical damage. This is of particular concern for samples prepared by FIB-SEM, but is also a challenge for standard preparation techniques using a combination of mechanical and ion beam polishing.

A range of GeSn samples, grown by RP-CVD with Sn fractions from 2 to 11%, were prepared by both FIB-SEM and standard preparation methods for TEM and have been examined to definitively understand the effect of these preparation methods on thin GeSn epitaxial layers. Ion bombardment from FIB milling is recognized to damage thin GeSn layers. However, ion beam polishing steps in standard techniques also cause defects, with significant damage to GeSn layers in parts the observable regions of the sample. The development of GeSn devices requires FIB-SEM, thus methods to reduce ion implantation, which is detrimental to crystal quality, need further investigation. While neither sample preparation method produces pristine samples, appropriate standard preparation methods produce optimal image quality.



# Microscopy of Semiconducting Materials (MSM-XIX)

## P.3.14 - Atom probe tomography analysis of defects in nitride semiconductors

R Oliver<sup>1</sup>, SE Bennett<sup>1</sup>, MJ Kappers<sup>1</sup>, JS Barnard<sup>1</sup>, CJ Humphreys<sup>1</sup>, RM Ulfing<sup>2</sup>, PH Clifton<sup>2</sup>, DW Saxey<sup>3</sup> and GDW Smith<sup>4</sup>

<sup>1</sup>University of Cambridge, UK, <sup>2</sup> Cameca Instruments Inc., UK, <sup>3</sup>University of Western Australia, Australia, <sup>4</sup>University of Oxford, UK

Whilst atom probe tomography (APT) has been extensively applied to the study of defects in metals, it has only recently been used to address defects in semiconductors. In this context, nitride semiconductors provide a rich field for the application of APT, due to the high densities of defects found in device quality material. Nitride light emitting diodes (LEDs) are typically grown on layers of GaN deposited onto unlike substrates. The lattice mismatch between the GaN and the substrate is usually large, and results in a density of threading dislocations typically in excess of  $10^8 \text{ cm}^{-2}$ . In the growth of the  $\text{In}_x\text{Ga}_{1-x}\text{N}$  quantum wells (QWs) which form the active region of an LED, V-shaped pits open up at the threading dislocation, leading to regions where the QWs are inclined to the overall growth direction and show a different thickness and composition to the surrounding material. Surprisingly, these changes to the quantum wells have been suggested to *improve* LED efficiency.

We have used APT to study a dislocation-related V-defect and to assess the changes in indium content and composition occurring in the QWs on the walls of the V-defect. Our results suggest that both the QW thickness and the indium content are reduced on the sidewalls of the V-defect, consistent with the suggestion that the V-defect can impede carrier diffusion to dislocations. We have also assessed another common defect, which is usually

found in the Mg-doped p-type region of LEDs: pyramidal inversion domains. Our studies of such inversion domains in an Mg-doped AlGaIn/GaN superlattice allow us to quantify the Mg content in structures only a few nanometres in extent; it may be as high as 8%. For both the V-defect and the inversion domains, we compare APT data to TEM and demonstrate how they can be employed in a complementary fashion.

## P.3.15 - Dislocation filters in GaAs on Si

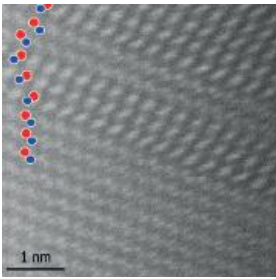
R Beanland<sup>1</sup>, F Becagli<sup>1</sup>, I George<sup>1</sup>, T Ward<sup>1</sup>, AM Sanchez<sup>1</sup>, M Tang<sup>2</sup>, J Wu<sup>2</sup> and H Liu<sup>2</sup>

<sup>1</sup>University of Warwick, UK, <sup>2</sup>University College London, UK

Growth of high quality GaAs on Si has been attempted for well over twenty years, with each effort eventually abandoned in the face of two apparently insuperable problems: (a) a high threading dislocation density and (b) cracking in the GaAs layer, induced by thermal expansion mismatch. To some extent the two problems are linked, since a way to reduce the threading dislocation density is to grow a thick GaAs layer (which is more prone to cracking).

Strained layer superlattices have also been used for some time as 'dislocation filters' to reduce the threading dislocation density more rapidly than simple thick layer growth. [1] Nevertheless, there is no detailed study that relates their efficacy to their structure, and hence no way to optimise their design. The possibility remains that an understanding of dislocation structure will allow them to be optimised, reducing their thickness sufficiently to overcome the problems mentioned above. Significant technological gains would result.

Here, we use conventional TEM methods to measure and count hundreds, or thousands, of dislocations that interact with dislocation filters across a range of samples, using the data to test the predictions of numerical models of dislocation reactions and annihilation. [2]



# Microscopy of Semiconducting Materials (MSM-XIX)

- [1] R. Fischer et al, Journal of Applied Physics 60, 1640 (1986).
- [2] T. Ward et al, Journal of Applied Physics 116, 063508 (2014).

## P.3.16 - Structural characterisation of N-type SiGe/Ge superlattice structures for Terahertz emission

J Halpin, M Myronov, S Rhead and D Leadley

University of Warwick, UK

Terahertz radiation lies in the  $3 \times 10^{11} > 3 \times 10^{12}$  Hz ( $\lambda = 0.1$  mm to 1 mm) region of the electromagnetic (EM) spectrum and has many applications. However, the uptake of THz applications is currently limited by the lack of a cheap, practical source.

Terahertz quantum cascade lasers (QCL's) have been constructed from group III-V semiconductors, where polar optical phonon scattering reduces the non-radiative lifetimes above 35 K and so they only operate at cryogenic temperatures. A Si and Ge based QCL can be grown on higher thermally conductive Si substrates and have active regions which should be more tolerant to higher temperatures, making room temperature lasing of Si and Ge based QCLs a possibility. III-V QCLs are also limited by their Reststrahlen band in which lasing is prohibited; however, Ge and Si are non-polar and hence do not have this limitation. The realization of a Si based QCL requires very challenging epitaxial growth.

In this work we present reduced pressure chemical vapour deposition (RP-CVD) grown n-type QCL structures. The structures have complex active regions with a total active region thickness of 4  $\mu$ m. The thinnest epilayer is around 3 nm. The design uses a high Ge content structure grown on a relaxed virtual substrate, also with a high Ge composition. Extensive materials characterisation was required for high quality and accurate growth. Characterisation was performed by TEM, HR-TEM, STEM, XRD and other techniques and the relative merits of each technique are discussed.

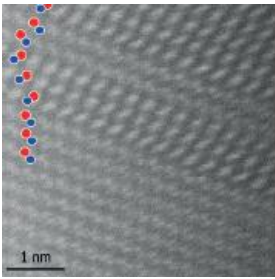
## P.3.17 - Image processing approaches towards optical microscopic analysis of monolayers to thin films

S Sanyal

University College Dublin, Ireland

Single-layered graphene crystallites are known to be visible on a certain thickness of SiO<sub>2</sub> on silicon wafers using optical microscopy at particular wavelength of incident light [1-4]. This opens up potential towards designing control systems for micro fabrication. The dependence of color on layer thickness, wavelength of incident light and thickness of spacer material is well understood analytically [5].

In this work we automate the process of separating individual layers for any given multi-layered two-dimensional nano-structure or thin films. This is done by first removing the high frequency dirt components from the image, followed by a normalization of non-uniform illumination and one dimensional K-means clustering [6] of the resultant image. This is followed by calculating the average color for each layer. By iteratively matching the analytically derived color with the average color, we can compute the thickness of each layer. Thus we can reconstruct the two-dimensional morphology of the surface with the correct scaling. Such reconstruction typically involves use of procedures like Atomic Force Microscopes.



# Microscopy of Semiconducting Materials (MSM-XIX)

In addition reflectance spectrum for each of this layers can be produced, and a complex refractive index for the thin film can be computed in cases of novel materials. The same techniques can also be used for real time measurement of changes in morphology and thickness of individual layers and hence predict reaction rates in real time.

We also provide a compiled stand--alone software to facilitate implementation, NITEE (Nano Imageprocessing Toolbox Engineering Efforts)

- [1] Blake. P., E. W. Hill, A. H. C. Neto, K. S. Novoselov, D. Jiang, R Yang, T. J. Booth, and A. K. Geim. Making graphene visible. 2007. *App Phys Lett.* 91(7): 063124.
- [2] Teo. G, H. Wang, Y. Wu, Z. Guo, J. Zhang, Z. Ni, and Z. Shen. Visibility of graphenemultilayer structures. 2008. *J Appl Phys.* 103: 12430
- [3] Ouyang, W., X. Z. Liu, Q. Li, Y. Zhang, J. Yang and Q. S. Zheng. Optical methods for determining thickness of few-layer graphene flakes. 2013. *Nanotechnology.* 24(13): 505701
- [4] Yang H., H. Hu, Y. Wang and T. Yu. Rapid and non-destructive identification of graphene oxide thickness using white light contrast spectroscopy. 2013. *Carbon.* 52(13): 528534
- [5] Jung J. S., J. Y. Son, R. S. Ruoff, and K. Y. Rhee. Colors of graphene and graphene oxide multilayers on various substrates. 2012. *Nanotechnology.* 23(12): 025708
- [6] A Hartigan. (1975) *Clustering algorithms.* John Wiley & Sons, Inc.

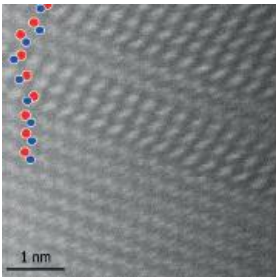
## P.3.18 - Correlating atom probe tomography with high-resolution scanning transmission electron microscopy and micro-photoluminescence spectroscopy: the case of III-Nitride heterostructures

L Rigutti<sup>1</sup>, L Mancini<sup>1</sup>, I Blum<sup>1</sup>, D Shinde<sup>1</sup>, F Vurpillot<sup>1</sup>, A Vella<sup>1</sup>, D Hernández-Maldonado<sup>1</sup>, W Lefebvre<sup>1</sup>, J Houard<sup>1</sup>, B Deconihout<sup>1</sup>, M Tchernycheva<sup>2</sup>, C Durand<sup>3</sup> and J. Eymery<sup>3</sup>

<sup>1</sup>University and INSA of Rouen, France, <sup>2</sup>University of Paris Sud 11, France, <sup>3</sup>CEA/CNRS/Université Joseph Fourier, France

In this contribution, we present several results of correlated studies of micro-photoluminescence ( $\mu$ -PL), high-resolution scanning transmission electron microscopy (HR-STEM) and laser-assisted atom probe tomography (APT) on single nano-objects containing AlGaInN quantum well and quantum dot systems. We will show how this approach can be applied to the study of heterostructure interface definition, presence of defects, carrier localization and optical emission in III-N quantum confined systems [1]. Furthermore, we will show how the use of complementary techniques may be extremely helpful for a correct interpretation of atom probe results [2]. The possible implementation of micro-photoluminescence as an in-situ technique within the atom probe itself will finally be discussed [3].

- [1] L. Rigutti et al., Nano letters (2014), 14, 107–114.
- [2] L. Mancini et al. J. Phys. Chem. C (2014) 118, 24136-24151.
- [3] L. Rigutti et al., Ultramicroscopy (2013), 132, 75-80.



# Microscopy of Semiconducting Materials (MSM-XIX)

## P.3.19 - Atom probe tomography visualizes elusive quantum dots in GaAs/AlGaAs core-multishell nanowires

L Rigutti<sup>1</sup>, L Mancini<sup>1</sup>, Y Fontana<sup>2</sup>, I Blum<sup>1</sup>, L Francaviglia<sup>2</sup>, F Vurpillot<sup>1</sup>, E Russo-Averchi<sup>2</sup>, M Heiss<sup>2</sup> and A Fontcuberta i Morral<sup>2</sup>

<sup>1</sup>University and INSA of Rouen, France, <sup>2</sup>École Polytechnique Fédérale de Lausanne, Switzerland

Core-shell nanowires are currently investigated as potential building blocks for solar cell and quantum cryptography applications. It has recently been shown that AlGaAs/GaAs core-multishell nanowires grown by molecular beam epitaxy (MBE) exhibit Al segregation mechanisms potentially leading to the self-assembly of quantum dots (QDs) yielding single photon emission [1]. Nanowires containing quantum structures are also particularly interesting as model systems for the study of correlated atom probe and optical spectroscopy measurements [2]. In this contribution the structure of a set of GaAs /Al-GaAs core-multishell nanowires was analyzed in 3D by atom probe tomography (APT). The study allowed us to confirm that Al atoms within the AlGaAs shells tend to segregate towards the planes crossing the vertices of the hexagons defining the nanowire cross section along the (121) crystal direction. We also assessed that strong alloy fluctuations take place in the AlGaAs shell, leading occasionally to the formation of quantum dots which would be hardly detectable by transmission electron microscopy. The PL emission energies predicted in the framework of a 3D effective mass model for a quantum dot analyzed by APT and the PL spectra measured on other nanowires from the same growth batch are consistent within the experimental uncertainties [3].

- [1] M. Heiss, et al.. Nature materials, (2013) 12(5), 439-444.
- [2] L. Rigutti et al., Nano letters (2014), 14, 107-114.
- [3] L. Mancini et al. Appl. Phys. Lett. (2014) 105, 243106

## P.3.20 - Continuous changing of 1D TbBr<sub>x</sub> stoichiometry inside the SWCNTs under the electron beam

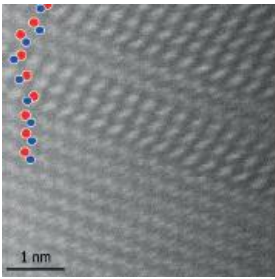
N Kiselev<sup>1</sup>, A Kumskov<sup>1</sup>, V Zhigalina<sup>1</sup>, A Eliseev<sup>2</sup>, A Vasiliev<sup>3</sup>, N Verbitskiy<sup>2</sup> and J Sloan<sup>4</sup>

<sup>1</sup>Russian Academy of Sciences, Russia, <sup>2</sup>Moscow State University, Russia, <sup>3</sup>National Research Centre, Russia, <sup>4</sup>University of Warwick, UK

The 1DTbBr<sub>x</sub>@SWCNT meta-nanotubes were obtained using capillary technique and investigated by HRTEM and HAADF STEM in JEOL ARM 200F at 80 kV. TbBr<sub>x</sub> crystals in SWCNT undergo structural transformation under electron beam irradiation, accompanied by bromine atoms drain from the nanotube channel. Four types of 1D TbBr<sub>x</sub> crystal structures have been proposed depending on the stoichiometry in TbBr<sub>x</sub>.

The first type of the structure (most complete) is characterized by rhombic unit cell with *Pmm* symmetry. The model corresponds to Br/Tb ratio of 3.25 which was confirmed by image simulation in (1-10) and (110) projections and local EDX analysis. Under irradiation it cumulates “rhomboid” defects in the (110) projection with Br/Tb ratio going down to 2.66. This corresponds to a bromine loss from the central position of the Br (Tb) tetrahedron in each unit cell, tentatively, accompanied by the loss of two peripheral Br atoms. Essentially Tb-Tb interatomic distance decreases with this phase transformation. The third type of structure is observed by HAADF STEM. In this case the “rhomboid” defect is observed in each unit cell and the Br/Tb ratio falls down to 2.5. The fourth type of structure resembles HRTEM images of the first type without outer bromide atoms. In this case the Br/Tb ratio equals to 2.0.

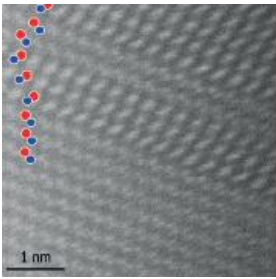
The existence of a structural variety for 1D TbBr<sub>x</sub> crystals with different Tb-Tb interatomic distances can be explained by possible intermetallic bonding between Tb atoms in one-dimensional crystal.



# Microscopy of Semiconducting Materials (MSM-XIX)

The electronic structure of  $1\text{TbBr}_x\text{@SWCNT}$  was investigated using X-ray photoelectron spectroscopy, Raman spectroscopy and optical absorption spectroscopy. It was shown that intercalation of terbium bromide into SWCNTs leads to acceptor doping, with Fermi level shift strongly dependent on Tb:Br stoichiometry in the intercalated crystal. The doping level varies under electron beam or X-ray irradiation.

The work is supported by Russian Science Foundation grant #14-13-00747.



# Microscopy of Semiconducting Materials (MSM-XIX)

The organisers would like to thank the following sponsors for their contribution to making this conference a success.

HREM Research Inc



European Microscopy Society (EMS)



Royal Microscopical Society (RMS)



# XHREM™

WinHEM™/MacHEM™  
**FFT-Multislice Simulation Suite**  
 STEM-HAADF

HREM image  
 Coherent CEED  
 STEM-HAADF

WinHEM (Mac/WinHEM) is a versatile simulation suite that generates HREM images, dynamical diffractions, coherent CEED patterns and STEM-HAADF images.  
 WinHEM is based on FFT-multislice dynamical calculation and wave-optics developed by Kazuo Ishizuka (Director of HREM Research).

# HoloDark

DigitalMicrograph Plugin  
**Dark-field holography for strain analysis**

Strained-silicon MOSFET transistor  
 Strain map,  $\epsilon_{xx}$   
 Fringe element model

HoloDark generates quantitative deformation and strain maps with high-accuracy (better than 0.1%) over wide fields of view from a pair of dark-field electron holograms of different diffraction vectors.  
 HoloDark is based on the patented technique and routines developed by Martin Hychal et al. (CNRS).

# DeConvHADF

DigitalMicrograph Plugin  
**STEM-HAADF Image Deconvolution**

HAADF image  
 JEMCO 2100F with CEOS Cs-sensor (20kV)  
 After deconvolution

DeConvHADF refines STEM-HAADF image by eliminating a spread of scan noise due to spherical aberration of the probe forming lens and/or a physical source size. DeConvHADF works well even on the STEM-HAADF image acquired with a Cs-corrected microscope by correcting a spread due to physical source size.

# MSA

DigitalMicrograph Plugin  
**Multivariate Statistical Analysis**

LAMOST/STO3 multilayer  
 No map from the based separability, with  
 100.0um, 100.0um, 1.0um, 2.5, 1.0

MSA finds statistically significant features from spectrum images (XEDS, EELS, EFTEM and cathodoluminescence) using PCA (Principal Component Analysis).  
 MSA plugin has originally been developed by Masashi Watanabe (Lough University).

# Quantitative Electron Microscopy

HREM Research Inc.  
 Specialized in Electron Microscopy

# GPA

DigitalMicrograph Plugin  
**Geometrical Phase Analysis**

High-resolution image  
 Rotation map  
 Stress map  
 Strain map

GPA generates fully quantitative deformation/rotation and strain maps from a single standard HREM image using geometric phase images.  
 GPA is based on geometric phase algorithms originally developed by M. Hychal (CNRS).

# DeCONVEELS

DigitalMicrograph Plugin  
**Electron Energy Loss Spectrum Deconvolution**

Before deconvolution  
 After deconvolution  
 C-K-edge (Diamond)  
 Exciton peak

DeCONVEELS refines an Electron Energy Loss Spectrum (EELS) by deconvoluting with a Dvornik or zero-loss spectrum using Maximum Entropy Method or Richardson-Lucy Algorithm.

# QED

DigitalMicrograph Plugin  
**Quantitative Electron Diffraction**  
 LARBED (Large Angle Backing Beam Electron Diffraction)  
 & PED (Precision Electron Diffraction)

LARBED pattern  
 PED pattern  
 Precision ON  
 Precision OFF

QED acquires LARBED and/or PED patterns from a small area by precisely controlling the nano-sized electron beam in your TEM. The QED calibrates detected coils, and measures aberrations of illumination system.  
 QED is based on the patented technique and routines developed by Christoph Koch at Max Planck Institute (now at Uln University).

# PPA

DigitalMicrograph Plugin  
**Peak-Pairs Analysis**

Strain maps  
 Moiré Detection

PPA locates atomic columns at sub-pixel resolution using 2D filtering or a small reference region (Moiré), and offers peak intensity analysis and local strain map calculation from high-resolution images.  
 PPA is based on Peak-Pairs algorithm originally developed by Pedro L. Galindo (University of Cadix).

# FTSR

DigitalMicrograph Plugin  
**Focal and Tilt Series Reconstruction**

Focal Series  
 Tilt Series  
 <1/2> silicon

FTSR works with a through focal series (FTSR) or tilt series (TFSR) of HREM images to reconstruct the complex wave function at the specimen exit surface.  
 FTSR uses a Wiener filter developed by Angus Kirkland et al. (University of Oxford)

# QPI

DigitalMicrograph Plugin  
**Quantitative Phase Technology**

Quantitative phase image  
 Under-focus image  
 Magnification vector map  
 Phase image  
 Symmetry in  $F_{xy}, G_{xy}$   
 Phase image reconstruction  
 (001) Si<sub>3</sub>N<sub>4</sub>

QPI generates a quantitative in-focus phase image over a wide range of magnifications only from three ordinary bright-field images.  
 QPI is based on Quantitative Phase Imaging (QPI) technology developed by Keith Nugent et al. (University of Melbourne).

# Jitterbug

DigitalMicrograph Plugin  
**Scan-noise and Drift Compensator**

Before  
 After  
 Frequency spectrum analysis of the residual scan

Jitterbug will correct STEM image scan-noise, and restore image resolution and SNR. It will rectify image drift and lattice distortion for a crystal sample.  
 Jitterbug plugin has originally been developed by Lewys Jones and Peter D. Nellist (University of Oxford).

# HREM-Filters

DigitalMicrograph Plugin  
**Optimal Noise Filters for HREM**

Original image  
 Normal Wiener filter  
 New Wiener filter  
 Residual  
 Residual

HREM-Filters are sophisticated Wiener and Dierckx filters that work even for nonideal crystals such as a nanocrystal of inorganic crystal.  
 New Wiener filter is based on the maximum likelihood estimation, while normal Wiener filter (routines) based on radial background does not work for non-ideal crystal.

# IWFR

DigitalMicrograph Plugin  
**Iterative Wave Function Reconstruction**

S/N, HREM image  
 Phase of exit wave  
 Phase of refined wave

IWFR works with a through focal series of HREM images to reconstruct a complex wave function at the specimen exit surface, and corrects spherical aberration. IWFR uses Gerchberg-Saxton-type iteration using only image intensities developed by Les Allen et al. (University of Melbourne).

# qHAADF

DigitalMicrograph Plugin  
**Quantitative HAADF Analysis**

Integrated intensities of InAs-GaAs  
 Bi content GaAs<sub>1-x</sub>Bi<sub>x</sub>

qHAADF performs column-to-column compositional analysis of materials from the integrated intensities of an atomic-column resolved HAADF-STEM image.  
 qHAADF is based on a method developed by Sergio I. Molina et al. (University of Cadix).

# FORTHCOMING INSTITUTE CONFERENCES

## MAY 2015 – JULY 2017

### 2015

**18–22 May**

**Nuclear Physics in Astrophysics VII: 28th EPS Nuclear Physics Divisional Conference**

The Royal York Hotel & Events Centre, York, UK

*Organised by the IOP Nuclear Physics Group*

**1–3 June**

**Theory Meets Experiment: Molecular Nanoscience and Applications**

University College London, London, UK

*Organised by the IOP Nanoscale Physics and Technology Group*

**9–10 July**

**Physics of Emergent Behaviour II**

Science Museum, London, UK

*Organised by the IOP Biological Physics Group*

**23–28 August**

**IPELS 2015**

Atholl Palace Hotel, Perthshire, UK

*Organised by the IOP Plasma Physics Group*

**26–28 August**

**Dynamic Behaviour of Structures and Materials, Interaction and Friction across the Strain - PETER 2015**

Institute of Physics, London, UK

*Organised by the IOP Shock Waves and Extreme Conditions Group*

**1–4 September**

**International Conference on Quantum, Atomic, Molecular and Plasma Physics (QuAMP 2015)**

University of Sussex, Brighton, UK

*Organised by the IOP Quantum Optics, Quantum Information and Quantum Control Group*

**6–9 September**

**Sensors & their Applications XVIII**

Kingston University, Surrey, UK

*Organised by the IOP Instrument Science and Technology Group*

**8–10 September**

**Physical Aspects of Polymer Science**

Manchester Institute of Biotechnology, Manchester, UK

*Organised by the IOP Polymer Physics Group*

**7–8 December**

**Quantitative Methods in Gene Regulation III**

Corpus Christi College, Cambridge, UK

*Organised by the IOP Biological Physics Group*

### 2016

**13–15 January**

**15th Anglo-French Physical Acoustics Conference**

Selsdon Park Hotel, Surrey, UK

*Organised by the IOP Physical Acoustics Group*

**7–8 April**

**EMAG 2016**

Durham University, Durham, UK

*Organised by the IOP Electron Microscopy and Analysis Group*

**3–6 July**

**EUFOAM 2016**

Trinity College Dublin, Dublin, Ireland

*Organised by the IOP Liquids and Complex Fluids Group*

**3–9 July**

**The XXVII International Conference on Neutrino Physics and Astrophysics**

Royal Geographical Society, London, UK

*Organised by the Institute of Physics*

**22–26 August**

**Joint European Magnetic Symposia (JEMS)**

SECC: Scottish Exhibition and Conference Centre, Glasgow, UK

*Organised by the IOP Magnetism Group*

**5–8 September**

**Photon16**

University of Leeds, Leeds, UK

*Organised by the IOP Computational Physics, Environmental Physics, Instrument Science and Technology, Optical, Quantum Electronics and Photonics and Quantum Optics, Quantum Information and Quantum Control Groups*

### 2017

**16–20 July**

**19th IUPAB Congress and 11th EBSA Congress**

Edinburgh International Conference Centre, Edinburgh, UK

*Organised by the Institute of Physics and British Biophysical Society*

See [www.iop.org/conferences](http://www.iop.org/conferences)

for a full list of IOP one-day meetings.

The conferences department provides a professional event-management service to IOP's subject groups and supports bids to bring international physics events to the UK.

**Institute of Physics**

76 Portland Place, London W1B 1NT, UK

Tel +44 (0)20 7470 4800

E-mail [conferences@iop.org](mailto:conferences@iop.org)

Web [www.iop.org/conferences](http://www.iop.org/conferences)







**Institute of Physics**

76 Portland Place, London W1B 1NT, UK

Telephone: +44 (0)20 7470 4800

Fax: +44 (0)20 7470 4848

**[www.iop.org/conferences](http://www.iop.org/conferences)**

Registered Charity Number: 293851